Effects of Substituents on the Photosensitizing and Electrocatalytic properties of Phthalocyanines

A thesis submitted in fulfilment of the requirements for the degree of

DOCTOR OF PHILOSOPHY

of

RHODES UNIVERSITY

by

SUZANNE ELIZABETH MAREE

November 2001

Contents

Acknowledgements

To say that this thesis was moulded from hard work only would be a truth half spoken. It is people like my supervisor, Prof. Nyokong, who nurtured me with personal interest, patience and enthusiasm. It is not often in one's life that you cross roads with such a respected and dedicated person like her.

I would also like to thank the following :

- The chemistry staff and students of Rhodes University for their unique contributions
- Henderson Scholarship program for financial support
- Imperial College through its International Office and EPSRC
- National Research Foundation of South Africa for financial support

My appreciation also extend to Diana, oom Pikkie and tannie Gretha for their continued interest and encouragement.

I dedicate this thesis to my parents Boeta and Rienie Greyling, my brother Heinie and especially, to my dear husband, David. Your love carries me through life and completes me.

But above all,

All glory to God, my Creator.

Creation

The God separated a spirit from Himself and fashioned it into beauty. He showered upon her all the blessings of gracefulness and kindness. He gave her the cup of happiness and said, "Drink not from this cup unless you forget the past and the future, for happiness is naught but the moment." And He also gave her a cup and you will understand the meaning of the fleeting instants of the joy of life, for sorrow ever abounds."

And the God bestowed upon her a love that would desert her forever upon her first sigh of earthly satisfaction, and a sweetness that would vanish with her first awareness of flattery.

And He gave her wisdom from heaven to lead her to the all-righteous path, and placed in the depth of her heart an eye that sees the unseen, and created in her affection and goodness toward all things. He dressed her with raiment of hopes spun by the angels of heaven from the sinews of the rainbow. And He cloaked her in the shadow of confusion, which is the dawn of life and light.

Then the God took consuming fire from the furnace of anger, and searing wind from the desert of ignorance, and sharp-cutting sands from the shore of selfishness, and coarse earth from under the feet of ages, and combined them all and fashioned Man. He gave to man a blind power that rages and drives him into a madness which extinguishes only before gratification of desire, and placed life in him which is the spectre of death.

And the God laughed and cried. He felt an overwhelming love and pity for Man, and sheltered him beneath His guidance. *-Kahlil Gibran-*

Abstract

In this work a selection of octasubstituted phthalocyaninato Zinc, Ge(IV) and Sn(IV) complexes were synthesized for possible use in photodynamic therapy and their photochemistry, photophysics and electrochemistry studied. Third-generation complexes containing steroids, e.g. cholesterol and estrone, were synthesized to improve tumour selectivity. The zinc phthalocyanine complexes (ZnPc) showed that complexes containing electron-donating groups have higher photostability. Germanium phthalocyanine complexes (GePc) undergo phototransformation rather than direct photobleaching and the tin phthalocyanine complexes (SnPc) undergo photobleaching mediated by photoreduction of the phthalocyanine ring.

Singlet oxygen production showed increased in the following order: GePc>SnPc>ZnPc. Triplet lifetimes of the GePc (168-340μs) are very similar to that of the ZnPc (197 - 366 μs), but the triplet lifetimes of the SnPc are ten fold shorter (10 - 32μs). Triplet quantum yields are higher for the GePc (0.20 - 0.50) and SnPc (0.08 - 0.45) than for the ZnPc (0.02 - 0.25). Fluorescence lifetimes of GePc (4.0 - 5.1 ns) are significantly longer than that of ZnPc (1.9 - 3.0 ns) and SnPc (0.2 - 0.4 ns). Fluorescence quantum yields decrease in the following order: GePc(0.21-0.31)>ZnPc(0.02-0.21)>SnPc(0.02 - 0.06).

Ring-substituted cobalt phthalocyanine complexes of the form $CoPc(R)_4$ (R= NH_2, NO_2, $C(CH_3)_3$, SO_3H and COOH) are compared for their catalytic activities towards the oxidation of cysteine. The potential for the electrocatalytic oxidation of cysteine is closely related to the Co^{III}/Co^{II} couple of the $CoPc(R)_4$ complexes in acidic media and to the Co^{II}/Co^{I} couple in basic media. The catalytic current and the oxidation potential for

cysteine are dependent on the pH of the solution, the potential becoming less positive and the currents increasing with increase in *pH*.

List of Figures

List of Schemes

List of Tables

List of Abbreviations

BEMP -	2-*tert*-butylimino-2-diethylamino-1,3-imethylperhydrodiazophophorin
BPD -	benzoporphyrin derivative
DABCO-	1,4-diazabicyclo[2.2.2]octane
DBN -	1,5-diazabicyclo[4.3.0]non-5-ene
DBU -	1,8-diazabicyclo[5.4.0]undec-7-ene
DMAE-	2-*N,N*-dimethylaminoethanol
DMF -	*N,N*-dimethylformamide
DMSO-	dimethylsulphoxide
DPBF -	1,3-diphenylisobenzofuran
FTIR -	Fourier transform infrared
HpD -	Haematoporphyrin derivative
HOMO-	highest occupied molecular orbital
LUMO-	lowest unoccupied molecular orbital
MeOH -	methanol
MPc -	Metallophthalocyanine
NMR -	nuclear magnetic resonance
OTTLE cell-	optically transparent thin-layer electrochemical cell
Pc -	Phthalocyanine
PDT -	Photodynamic therapy
Py -	pyridine
SCE -	saturated calomel electrode
TBD -	1,5,7-triazabicyclo[4.4.0]dec-5-ene
TEA -	triethylamine
THP -	1,2,3,6-tetrahydropyridine

TLC	-	thin layer chromatography
TPP	-	triphenylphosphine
UV/Vis-		ultraviolet/visible

List of symbols

Φ_Δ	-	singlet oxygen quantum yield
I_{abs}	-	amount of light absorbed by sensitizer
Φ_F	-	fluorescence quantum yield
Φ_D	-	photodegradation quantum yield
Φ_Δ	-	singlet oxygen quantum yield
τ_F	-	fluorescence lifetime
τ_t	-	triplet lifetime
Φ_T	-	triplet quantum yield
$^1O_2$	-	singlet oxygen
E_{pa}	-	anodic peak potential
E_{pc}	-	cathodic peak potential
$E_{½}$	-	half wave potential
I_{pa}	-	anodic peak current
I_{pc}	-	cathodic peak current
I_{abs}	-	amount of light absorbed by a photon
C_0	-	DPBF concentration at time 0
C_t	-	DPBF concentration at time t
I	-	light intensity
ps	-	picosecond
ns	-	nanosecond
A_s	-	area of the sample under an emission band
A_{std}	-	area of the standard under an emission band
η_s	-	refraction index of sample
η_{std}	-	refraction index of sample

Chapter 1

General introduction and aims

1.1 General introduction and aims

Porphyrins are vital compounds found in most living creatures. They behave like catalysts in biological processes for example chlorophyll in the photosynthesis of plants and haem in red blood cells in the respiratory system in animals. Phthalocyanines (formally known as tetrabenzo[5,10,15,20]-tetraazaporphyrins) are more stable derivatives of the porphyrins and are more commonly used in industry. Phthalocyanine (Pc) molecules have a conjugated system of 18 π electrons and posses very high thermal and chemical stability. The structure of the phthalocyanine ring resembles the naturally occurring porphyrins with the only basic difference being the aza groups instead of methine corner links (Figure 1.1).

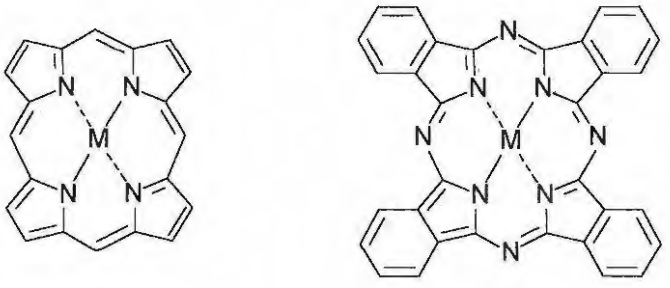

1 2

Figure 1.1 Structures of metalloporphyrin (**1**) and metallophthalocyanine (**2**).

Porphyrins in living creatures differ from one another according to their function and their biological environment. They may be required to harvest light and transfer it to the next molecule in the form of an electron or simply take part in reversible chemical reactions in the dark. In order for them to have these different properties they differ slightly in their chemical constitution, such as the central metal they contain or variation in the peripheral substituents.

Scientists have realized the potential hidden in phthalocyanine compounds and have been studying them intensely during the last few decades. The result of this has been overwhelming, with thousands of compounds being synthesized, patents being issued and a long list of applications being found. The original and most widely used application is that of dyes and pigments, but other uses include photovoltaic and solar cells,[1] molecular electronics,[2] gas sensors,[3] liquid crystals,[4] nonlinear optics,[5] semiconductors[6] and many more.

The stability of the Pc compounds during electron transfer or the generation of reactive species make these molecules particularly attractive as catalysts in the true definition of the word. The activation energy is harvested by the phthalocyanine in different ways ranging from light energy to energy supplied by an applied electrochemical potential, and then the Pc complexes efficiently transfer the energy to the system of interest. Hence, a study of two different catalytic processes (photosensitizing and electrocatalyses) have been undertaken in this work and the factors influencing them examined.

1.2 Photodynamic therapy

Photodynamic therapy (PDT) of cancer has been developed as an alternative to conventional treatments, such as chemotherapy and radiotherapy. These treatments tend to have well known harmful side-effects, for example toxicity to the kidneys and the bone marrow,[7,8] hair loss and nausea to name but a few. Increasing drug resistance with time also occurs. The advantage of PDT is based on the fact that the sensitizer is harmless until it is activated by light. Light can therefore selectively be shone on the tumour through an optical fibre, the sensitzer being activated and cell destruction is thus afforded in a predetermined area. Targets

included in PDT are mitochondria, lysosomes, plasma membrane, tumour vasculature and nuclei of tumor cells.[9] The photosensitiser is administered to the body and time is allowed for it to dissipate through the body (3-72 hours). Selectivity towards tumour cells in comparison to normal cells is often observed in very high ratios. There are many possible reasons for this, among which could be that tumours have a poor lymphatic draining system,[10] the interstitial space difference between cancer and normal cells, as well as higher vascular permeability due to the expression of a protein by the tumour to increase tumour growth.[11] The size, charge and binding characteristics of these sensitizers may also contribute to this phenomena.

The photosensitizer may be used in two ways in cancer treatment. Firstly, its ability to fluoresce may be used to image the tumour by fluorescence detection and hence its biodistribution can be followed. Fluorescence of these compounds is measured by exciting the long wavelength absorption bands. Secondly, the same molecule may be used to destroy the cancerous cells by generating a cytotoxic species. Fluorescence and the production of cytotoxic species for cell destruction are both a result of irradiation with light.

The history of PDT dates back a century and is summarized in Table 1.1.

Table 1.1 Brief history of photodynamic therapy.

1900	Oscar Raab observed that fluorescing compounds (paramecium) are able to transform light energy into chemical energy and could destroy living organisms.[12]
1901	Jessionek and von Tappeiner used dyes (eosin and fluoresceine) to treat skin carcinomas.[13]
1924	Policard studied red fluorescence from different animal sarcomas exposed to light and observed that this fluorescence is due to accumulation of porphyrins in tumours.[14]
1943	Auler and Banzer treated different animal tumours to observe fluorescence.[15]
1945	Figge et al.[16,17,18] and Rasmussen-Taxdal[19] administered porphyrins to patients and animals to study tumour detection through fluorescence.
1961	Lipson opened a new route in the medical field by synthesizing a new and efficient porphyrin called haematophorphyrin[20].
1972	Experiments similar those of Lipson were done by Diamond.[21]
1976	Thomas Dougherty started to treat animals with fluorescein and light.[22]

First clinical studies started thereafter at Rosewell Park Memorial Institute and ever since then more than 10 000 patients have been treated more or less successfully in the United States, Canada, Netherlands, Japan, France and Italy.[23,24] Photodynamic therapy has been used in treatment of lung, esophageal, bladder, brain, skin, colorectal, oral, head and neck cancers as well as breast metastases, gynecological and thoracic malignancies.

1.2.1 Photosensitizers in use and their requirements

1.2.1.1 First generation sensitizers

Haematoporphyrin derivative (HpD) has been the most commonly used clinical photosensitizer for PDT. HpD is a mixture of porphyrin monomers and oligomers derived from haematoporphyrin (**3**) (Figure 1.2). Haematoporphyrin itself is derived from blood by extracting the haem, reacting it with HBr and acetic acid, and then decomposing the HBr adduct with water. HpD is produced by reacting haematoporphyrin (**3**) with acetic and sulphuric acids, followed by an alkali work up.[25]

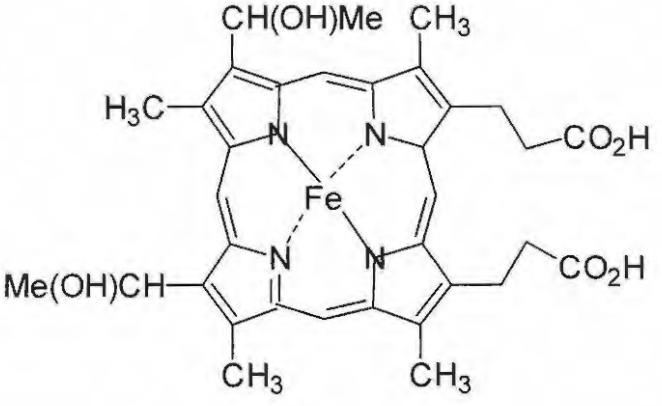

3

Figure 1.2 Structure of haematoporphyrin (**3**).

The reasons why there have been many attempts to improve on HpD are three fold. HpD is a mixture of compounds and therefore each batch would produce different photodynamic activity. Secondly, HpD is retained in the body for up to 6 weeks, rendering the patient

sensitive to light. The last reason is the fact that HpD has a strong absorption in the near-UV region instead of the near-IR region. The problem in the latter case is that the light exciting the sensitizer has to pass through living tissue, which effectively absorbs light in the near -UV region. Light at the red end of the spectrum (620-680nm) is much less attenuated by living tissues. HpD, and preparations derived from it are generally referred to as first-generation photosensitizers.

1.2.1.2 Second generation sensitizers

The second generation photosensitizers are in general intended to have the following desired characteristics:[26]

1. The synthesis must be simple, reproducible and yield a pure single product.
2. They must have strong absorption in the red region to ensure efficient tissue penetration and consequent activation by light.
3. Non-toxic in the absence of light thereby rendering better control over the treatment process.
4. The sensitizer must have a triplet excited state that is sufficiently long-lived to be able to photosensitize the production of singlet oxygen or other cytotoxic species.
5. Selective retention in tumours to optimize treatment of cancerous cells.
6. Rapid clearance from the body. However, if the clearance is too rapid, low selectivity may be a consequence because not enough time is given for selective accumulation.
7. Sufficient solubility in tissue fluids, or be capable of formulation, so that it can be injected and distributed to the tumour site.

Quite a few porphyrin-based compounds have been developed with these qualities in mind (Figure 1.3).

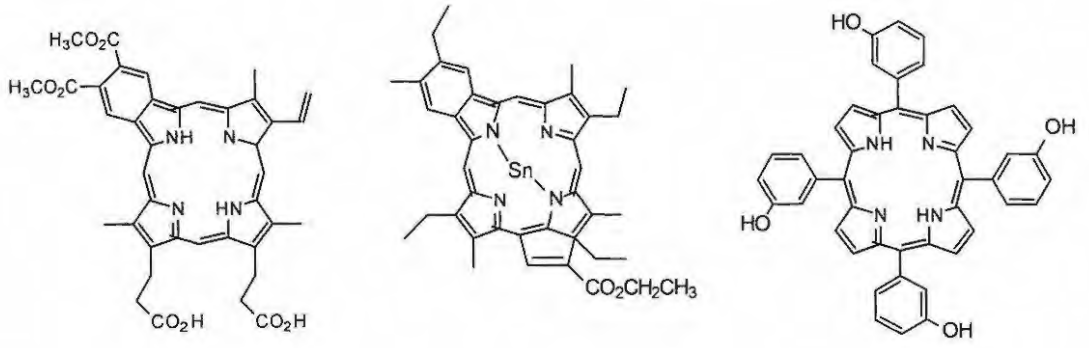

4 **5** **6**

Figure 1.3 Potential photosensitisers Benzoporphyrin derivative (**4**) (trade-name: Verteporfin), Tin etiopurpurin (**5**) (trade-name: Purlytin) and *meta*-tetrahydroxyphenyl chlorin (**6**) (trade-name: Foscan).

The benzoporphyrin derivative (**4**) (BPD) in Figure 1.3 has an absorption maximum at 690 nm. The disadvantage, however, is that it clears too rapidly from serum and tissues.[27] It has been found, however, that this compound is very useful in treating age-related macular degeneration. Tin etiopurpurin (**5**) (Figure 1.3), Purlytin as trade-name, is a chlorin photosensitiser with an absorption maximum at 650 nm. Purlytin has been evaluated for use against recurrent metastatic breast cancer[28] and is also being evaluated for the treatment of corneal neovascularization.[29] With Purlytin, the problem involves its localization in the skin resulting in skin photosensitivity for up to 14 days. The meta-tetrahydroxyphenyl chlorin (**6**) (Figure 1.3), trade-name Foscan, is highly phototoxic and only very low light doses are needed for treatment of esophageal, lung, laryngeal,[30]

thoracic[31] and skin[32] cancers. These are only a few of the sensitisers that are in clinical trials and additional porphyrin sensitizers are summerised in Table 1.2.

Table 1.2 Porphyrin sensitizers in clinical trials.

Sensitiser	Application	Characteristics and disadvantages
Monoaspartyl chlorin e6 (Npe6)	Adenocarcinoma of the breast, basal cell carsinoma, squamous cell carcinoma[33]	Rapid clearance
Lutetium texaphyrin (Lutex)	Malignant melanoma[34]	Absorbance at 732 nm
Δ_5-aminolevulinic acid (ALA)	Destruction of superficial deseases[35]	Precursor in biosynthesis of haem. Not effective for tumour tissues deeper than one millimeter.

The potential of phthalocyanines as photosensitizers for PDT was realized in the mid 1980's when it was discovered that they possess many, if not all, of the desired properties. Phthalocyanines may be modified peripherally as well as axially, therefore allowing fine-tuning of characteristics.

In Russia, the sodium salt of the tetrasulfonated aluminium phthalocyanine (**7**) (Figure 1.4) (Photosens) is already at the end of the second stage of clinical trials.[36] Silicon phthalocyanine containing an axially substituted monoaminosiloxy group (**8**) (Figure 1.4) is in advanced clinical trial stages, it has the desired absorption wavelength and is prepared in high purity.[37]

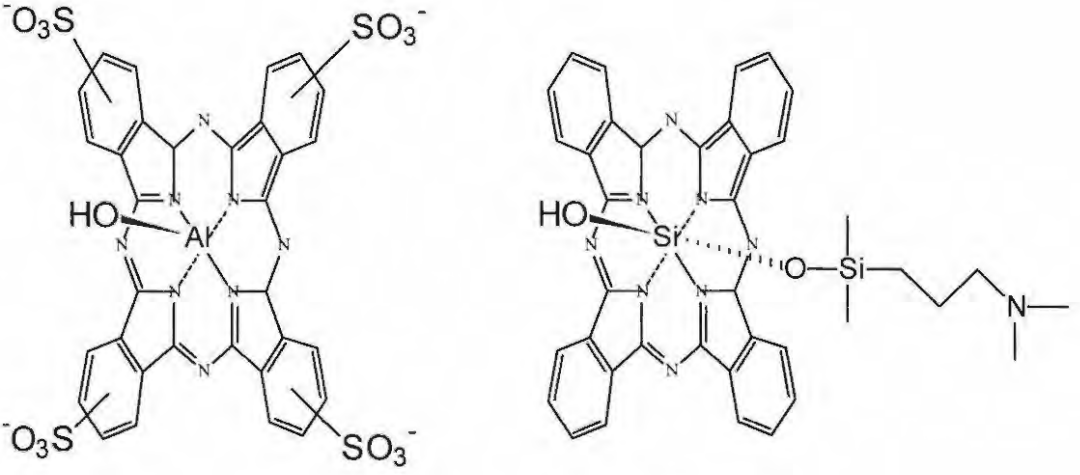

7 **8**

Figure 1.4 Phthalocyanine sensitizers currently in use.

Even though AlPc and SiPc have been extensively studied for PDT the other non-transition metal Pc's have received less attention. Ge(IV)Pc derivatives with cholesterol, cholestan and long fatty acids axially ligated have been tested and good therapeutic efficiency has been observed.[38] In this thesis it was decided to synthesize Sn(IV)Pc and Ge(IV)Pc with estrone (a steroid) attached to the ring as well as on the axial position on the Sn(IV)Pc.

Diamagnetic metals such as aluminium(III), zinc(II), tin(IV), germanium(IV) and silicon complexes are metals of choice for MPc's designed for PDT. The reason for this is that the intersystem crossing by the sensitizer from its excited singlet state to its triplet state, is increased. The choice of metal should not decrease the lifetime of the triplet state, which should be in excess of 100μs to ensure efficient $^1O_2$ generation. The triplet state of the sensitizer should also be higher than 94 kJ/mol since the energy of singlet oxygen is about 94 kJ/mol higher than that of triplet oxygen. This rules out paramagnetic transition metals, such as copper and iron.

Zinc phthalocyanine (ZnPc) complexes have also been explored for PDT, but even though they show excellent efficiency in the production of cytotoxic species in solvents like DMF [39] they have the tendency to aggregate and therefore advanced stages in PDT protocol have not been reached. In this thesis ZnPc complexes containing a series of substituents on the ring have been synthesized and their photophysical and photochemical properties examined. The presence of bulky groups on the ring often prevents aggregation. Substitution of the ring with steroids like cholesterol and estrone reported in this work is the first of its kind of ZnPc. Tin(IV)phthalocyanine (Sn(IV)Pc) complexes have not been explored for possible use in PDT. This work reports on the synthesis of ring substituted Sn(IV)Pc complexes. Sn(IV)Pc and Ge(IV)Pc complexes do not form aggregates due to the presence of axial ligands. Since Ge(IV)Pc with cholesterol on the axial position showed excellent potential for PDT, the synthesis and photocharacterization of Sn(IV)Pc complex directly ligated with the estrone steroid was explored. The biologically active steroids were considered of importance not only because of improved solubility due to the bulkiness of these substituents, but due to possible increase in selective retention in tumours.

1.3 Electrocatalyses

Electrochemistry is performed by applying a certain potential, forcing electrons to move between a working electrode and the compound under investigation. By modifying the working electrode this process may be enhanced or stimulated to occur at a lower potential. This is what electrocatalyses is about. It is a process whereby electron transfer between the working electrode and the active species is catalysed to occur at lower potential or with increased intensity where the concentration of the analyte is particularly low. It is often required that the catalyst should improve selectivity for a specific compound in a mixture of compounds having roughly the same potential or to increase stability by binding or coordinating with the active species.

Metallophthalocyanines (MPc) are well studied as homogeneous and heterogeneous catalysts. In particular, cobalt phthalocyanine (CoPc) and its derivatives have shown good electrocatalytic behaviour when adsorbed onto carbon electrodes. Many reactions are reported to be electrocatalysed by CoPc complexes. These include: (i) oxygen reduction[40 - 45] (ii) oxidation of cysteine and other thiols[40, 46 - 53] (iii) reduction of carbon dioxide, [40,54,55,56] (iv) reduction of thionylchloride,[40] (v) nitrite reduction[57,58,59] and (vi) oxidation of cysteine-containing proteins.[60,52] Selectivity of the CoPc complexes towards the analysis of species can be introduced by changes in the substituents attached to the phthalocyanine ring. For example, electrodes modified with 2,9,16,23-tetra-*tert*-butylphthalocyanine cobalt (CoTBPc) have been found to be selective to NO_2^- in the presence of SCN^-, I^-, ClO_4^-, Br^-, NO_3^- and Cl^-.[57] The catalytic behaviour of $Co^{II}Pc$ complexes is associated with the redox activity of the central metal. The potential at which catalytic currents are observed being closely related to Co^{III}/Co^{II}

or Co^{II}/Co^{I} couples in CoPc complexes.[40,61] The values of the oxidation or reduction potentials of the central metal in CoPc thus strongly influence the catalytic behaviour of the complexes.

Phthalocyanines as photosensitizers in photodynamic therapy of cancer and other diseases will be addressed in Chapters 2, 3 and 4 and the electrocatalytic properties of the versatile cobalt containing complexes will be discussed in the last chapter.

1.4 Aims of thesis

With all of the above mentioned in mind, the following aims were set:

a) To synthesize and characterize a series of substituted phthalocyanines containing different central metals as well as peripheral groups of different electronegativities in order to investigate the desired properties for application in PDT (Chapter 1).

b) To synthesize and characterize the so-called "third generation" PDT agents, which are targeted to specific tumours (Chapter 1).

c) To study the photochemistry, photophysics and electrochemistry of the synthesized compounds (Chapter 2 and 3).

d) To evaluate the electrocatalytic properties of peripherally substituted cobalt phthalocyanines in the presence of cysteine, a sulfur containing amino acid (Chapter 5).

1.5 References

1. C.W. Tang, *Appl. Phys. Lett.*, **60**, 1047 (1986)
2. B. Simic-Glavaski In *Phthalocyanine. Principles and Properties* C.C. Leznoff, A.B.P. Lever, Eds., VCH Publications: New York, **3**, 119-166 (1993)
3. A.W. Snow and W. R. Barger, In *Phthalocyanines, Principles and Properties* C.C. Leznoff and A.B.P. Lever Eds; VCH Publication New York, Vol. 1, Chapter 3, pp 341-392 (1986)
4. J.F. Van der Pol, E. Neeleman, J.W. Zwikker, R.J.M. Nolte, W. Drenth, J. Aerts, R.Visser and S. Picken, *J. Liq. Cryst.*, **6**, 577 (1989)
5. M.K. Casstevens, M. Samoc, J. Pfleger and P.M. Prasad, *J. Chem. Phys.*, **92**, 2019 (1990)
6. J. Simon and J.-J. Andre, *Molecular Semiconductors;* Springer: Berlin, Chapter 3 (1985)
7. M.F. Pera Jr., B.C. Zook and H.C. Harder, *Cancer Res.*, **37**, 1269 (1997)
8. J.M. Ward, M.E. Grabin, E. Berlin and D.M. Young, *Cancer Res.*, **37**, 1238 (1977)
9. T.J. Dougherty, C.J. Gomer, B.W. Henderson, G. Jori, D. Kessel, M. Korbelik, J. Moan and Q. Peng, *J. Natl. Cancer Inst.*, **90**, 889 (1998)
10. W.H. Henderson and T.J. Dougherty, *Photochem. Photobiol.*, **55**, 147 (1992)
11. W.S. Chan and W.F. Marshall, *Cancer Res.*, **48**, 3044 (1988)
12. O.Z. Raab, *Biol. (Munich)*, **39**, 524t, (1900)
13. A. Jessionek and H. Von Tappeiner, *Tisch. Ach. Klin. Med.*, **82**, 223 (1905)
14. A. Policard, *C.R. Soc. Biol.*, **91**, 1423 (1924)
15. H. Auler and G. Banzer, *Krebsforsch.*, **53**, 65 (1943)
16. F.H.J. Figge in *AAAS Research Conf. On Cancer*, F.R. Moulton (ed), 117 (1945)
17. F.H.J. Figge, *Ann. Int. Med.*, **24**, 143 (1947)
18. F.H.J. Figge, G.S. Weiland and L.O.J. Manganiello, *Proc. Soc. Exp. Biol. Med.*, **68**, 143 (1948)
19. D.S. Rasmussen-Taxdal, D.E. Ward and F.H.J. Figge, *Cancer*, **8**, 78 (1955)
20. R.B. Lipson, E.J. Balde and A.M. Olsen, *J. Natl. Cancer Inst.*, **26**, 1 (1961)
21. I. Diamond, S.G. Granell and A.F. McDonough, *Cancer*, **11**, 1175 (1972)
22. T.J. Dougherty, *J. Natl. Cancer Inst.*, **52**, 1336 (1974)
23. T.J. Dougherty, *Photochem. Photobiol.*, **58**, 395 (1993)
24. T.J. Dougherty and I.J. MacDonald, *J. Porphyrins Phthalocyanines*, **5**, 105 (2001)

25. R.K. Pandey, J.F. Majchrzycki, K.M. Smith and T.J. Dougherty, *Proc SPIE*, **1065**, 164 (1989)

26. D. Phillips, *Science Progress*, **77**, 295 (1993/1994)

27. A.M. Richter, S. Cerruti-Sola and E.D. Sternberg, *J. Photochem. Photobiol. B: Biol.*, **5**, 231 (1990)

28. T.S. Mang, R. Allison and G. Hewston, *Cancer J. Sci. Am.*,**4**, 378 (1998)

29. G.B. Primbs, R. Casey and K. Wamser, *Ophthalmic Surg. Lasers*, **29**, 832 (1998)

30. L.H.P. Murrer, J.P.A. Marijnissen and W.M. Star, *J. Cancer*, **88**, 744 (1999)

31. H.B. Ris, H.J. Altermatt and R. Inderbitzi, *Br. J. Cancer*, **64**, 1116 (1991)

32. A. Kuebler, T. Haase and C. Staff, *Lasers Surg. Med.*, **25**, 60 (1999)

33. S.W. Taber, V.H. Vingar, C.T. Coots and T.J. Wieman, *Clin. Cancer Res.*,**4**, 2741 (1998)

34. K.B.Woodburn, Q. Fan and D. Kessel, *J. Invest. Dermatol*, **110**, 746 (1998)

35. J.C. Kennedy, S.L. Marcus and R.H. Pottier, *J. Clin. Laser Med. Surg.*,**14**, 289 (1996)

36. E.A. Lukyanets, *J. Porphyrins Phthalocyanines*, **3**, 424 (1999)

37. C.Y. Anderson, K. Freye, K.A. Tubesing, Y-S Li, M. Kenney, H. Mukhtar and C.A. Elmets, *Photochem. Photobiol.*, **67**, 332 (1998)

38. K. Scheiweck, H-G. Capraro, U. Isele, E. Batt, M. Ochsner, P. van Hoogevest and W.A.. Love, *SPIE*, **2078**, 165

39. W. Spiller, H. Kliesch, D. Wöhrle, S. Hackbarth, B. Röder and G. Schnurpfeil, *J. Porphyrins Phthalocyanines*, **2**, 145 (1998)

40. J.H. Zagal, *Coord. Chem. Rev.*, **119**, 89 (1992)

41. S. Zecevic, B. Simic-Glavaski, E. Yeager, A.B.P. Lever and P.C. Minor, *J. Electroanal. Chem.*, **196**, 339 (1985)

42. P. Janda, N. Kobayashi, P.R. Auburn, H. Lam, C.C. Leznoff and A.B.P. Lever, *Can. J. Chem.*, **67**, 1109 (1989)

43. N. Kobayashi and W.A. Nevin, *Appl. Organomet. Chem.*, **10**, 579 (1996)

44. Y.-H. Tse, P. Janda, H. Lam and A.B.P. Lever, *Anal. Chem.*, **67**, 981 (1995)

45. Y.-H. Tse, P. Janda, H. Lam, J. Zang, W.J. Pietro and A.B.P. Lever, *J. Porphyrins Phthalocyanines*,**1**, 3 (1997)

46. X. Huang and W.Th. Kok, *Anal. Chim. Acta*, **273**, 245 (1993)

47. M.K. Halbert and R.P. Baldwin, *Anal. Chem.* **57**, 591 (1985)

48. A. Napier and J.P. Hart, *Electroanalysis,* **8**, 1006 (1996)
49. E. Kermann, D. Schlettwein and N.I. Jaeger, *J. Electroanal. Chem.*, **405**, 149 (1996)
50. T.J. O'Shea and S.M. Lunte, *Anal. Chem.* **66**, 307 (1994)
51. M. Sekota and T. Nyokong, *Polyhedron,* **16**, 3279 (1997)
52. J. Limson and T. Nyokong, *Electroanalysis,* **9**, 255 (1997)
53. F. Xu, H. Li, J. Cross and T.F. Guarr, *J. Electroanal. Chem.*, **368**, 221 (1994)
54. J. Premkumar and R. Ramaraj, *J. Photochem. Photobiol. A: Chem.,* **110**, 53 (1997)
55. T. Abe, T. Yoshida, S. Tokita, F. Taguchi, H. Imaya and M. Kaneo, *J. Electroanal. Chem.*, **412**, 125 (1996)
56. C.M. Lieber and N.S. Lewis, *J. Am, Chem. Soc.*, **106**, 5033 (1984)
57. J.-Z. Li, X.-Y. Pang and R.-Q. Yu, *Anal. Chim. Acta*, **297**, 437 (1994)
58. N. Chebotareva and T. Nyokong, *J. Appl. Electrochem.,* **27**, 975 (1997)
59. M.A. Thamae and T. Nyokong, *J. Appl. Electrochem.*, **470**, 126 (1999)
60. J. Limson and T. Nyokong, *Electroanalysis,* **10**, 988 (1998)
61. A. Napier and J.P. Hart, *Electroanalysis*, **8**, 1006 (1996)

Chapter 2
Synthesis and characterization

2.1 Introduction

In the design and synthesis of phototherapeutic drugs a strategy should be developed that will yield a product with an exact and known composition. Reactions with few or no by-products or with effective purification methods and yielding a single isomer, are desirable. Substituted phthalocyanines are prepared by cyclotetramerization of substituted phthalonitriles.[1] Monosubstituted phthalonitriles will yield tetrasubstituted phthalocyanines with the disadvantage of a mixture of regio isomers. If 4,5-disubstituted phthalonitriles are employed 2,3,9,10,16,17,23,24-octasubstituted phthalocyanines are formed with no isomers as a result. In this thesis a selection of 2,3,9,10,16,17,23,24-octasubstituted phthalocyanines were synthesized using Zn, Ge and Sn as central metals. An attempt was also made to synthesize a tetrasubstituted phthalocyanine, limiting the number of isomers to one through steric hindrance. These compounds all had to show strong absorbance in the infrared region to be useful in PDT.

Various substituted phenoxy groups were attached to the phthalocyanine skeleton. This provided a series of electron-donating and withdrawing groups that allowed the study of their effects on the photophysical, photochemical and electrochemical properties. By attaching biological active compounds to the phthalocyanines it was hoped to synthesize complexes that would increase cellular uptake and tumour selectivity.

A brief discussion on the general synthesis of Pc complexes follows.

2.1.1 General synthesis of phthalocyanine complexes

2.1.1.1 Metal-free Phthalocyanines

The original syntheses of metal-free phthalocyanines (**10**) (H_2Pc) were performed by heating o-cyanobenzamide (**9**) in ethanol under reflux (Scheme 2.1 (a)) to yield the blue product in low yield.[2] Higher yields (40%) were obtained when catalysts like magnesium, antimony metal and magnesium salts were added and the reaction mixture was heated to over 230°C, Scheme 2.1 (b).

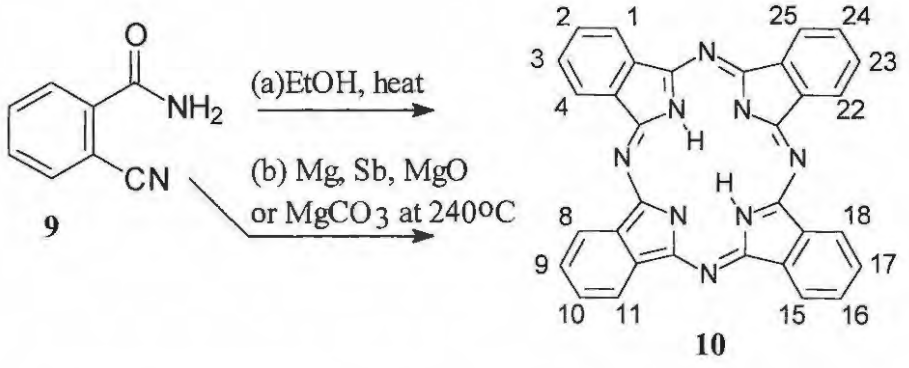

Scheme 2.1 Synthesis of metal-free phthalocyanine (**10**) using o-cyanobenzamide (**9**) as starting material.

When phthalonitrile (**11**) is used as starting material, a very easy synthesis is afforded upon treatment with sodium or lithium in n-pentanol (Scheme 2.2) or other alcohols, at 135-140°C to give the disodium or dilithium phthalocyanine which could be demetallated with concentrated H_2SO_4 or glacial acetic acid.[3,4] Good yields were obtained and reaction times were often shorter than 30 minutes. In 1980 and 1983 Tomada *et al.*[5,6] reported the reaction of phthalonitrile in alcohols with 1,5-diazabicyclo[4.3.0]non-5-en (DBN) or 1,8-diazabicyclo[5.4.0]undec-7-ene (DBU) as strong bases. They obtained metal-free and

metallated phthalocyanines in 70 and 80% yields, respectively. A detailed comparative study by Wöhrle *et al.*,[7] where different organic bases, for example 2-*N,N*-dimethylaminoethanol (DMAE), 1,2,3,6-tetrahydropyridine (THP), triethylamine (TEA), pyridine (Py), triphenylphosphine (TPP), 1,5,7-triazabicyclo[4.4.0]dec-5-en (TBD) and 2-*tert*-butylimino-2-diethylamino-1,3-dimethyl-perhydrodiazophophorin (BEMP) were used, showed that the weaker bases like Py, TEA and THP do not form phthalocyanines. No significant difference was observed in terms of improved yields between the slightly stronger bases TBD and BEMP compared to DBU and DBN.

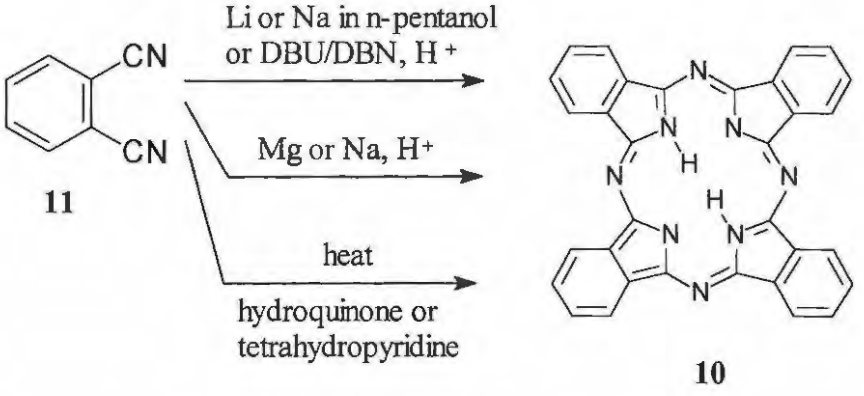

Scheme 2.2 Synthesis of metal-free phthalocyanine (**10**) using phthalonitrile (**11**) as reagent.

Phthalonitrile (**11**) can also be fused with magnesium or sodium metal (Scheme 2.2) above 200°C to give the magnesium and sodium phthalocyanines which can be demetallated with concentrated H_2SO_4. Using reducing agents like hydroquinone, tetrahydropyridine or 4,4'-dihydroxobiphenyl as co-reactants and fusing at 180°C in a sealed tube yielded the phthalocyanine (**10**) in 43% yield (Scheme 2.2).[8,9]

Phthalonitrile (**11**) can easily be converted into 1,3-diiminosoindoline (**12**) by bubbling gaseous ammonia into a methanol solution of the phthalonitrile at room temperature

(Scheme 2.3).[10] For insoluble phthalonitriles methanol[11] or methanol-dioxane[12] under reflux will give the same results. When the 1,3-diiminosoindoline was heated in the presence of a hydrogen donor such as succinonitrile or boiling tetralin, the metal-free phthalocyanine was produced in 34 and 45% yields respectively. It was later shown that by heating a substituted 1,3-diiminosoindoline (**12**) in 2-*N,N*-dimethylaminoethanol the substituted metal-free phthalocyanine (**10**) can be obtained in 85% yield (Scheme 2.3).

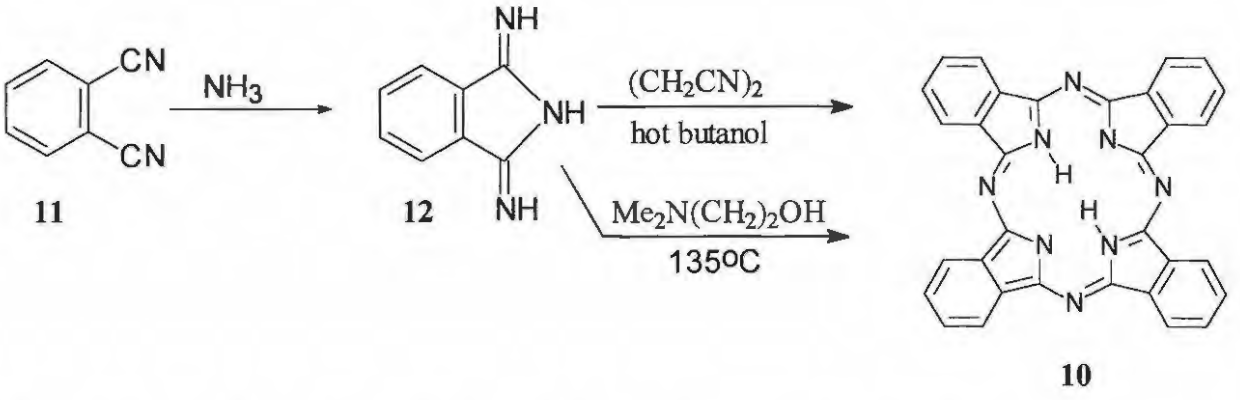

Scheme 2.3 Synthesis of metal-free phthalocyanines (**10**) using 1,3-diiminosoindoline (**12**) as reagent.

2.1.1.2 Metallated phthalocyanines (MPc)

Substituted or unsubstituted phthalic acid (**13**), phthalic anhydride (**14**), phthalimide (**15**) or phthalamide (**16**) (Scheme 2.4) together with urea are often used instead of phthalonitrile, and catalysts such as ammonium molybdate or zirconium tetrachloride may be employed[13,14,15] to yield metallated substituted phthalocyanines.

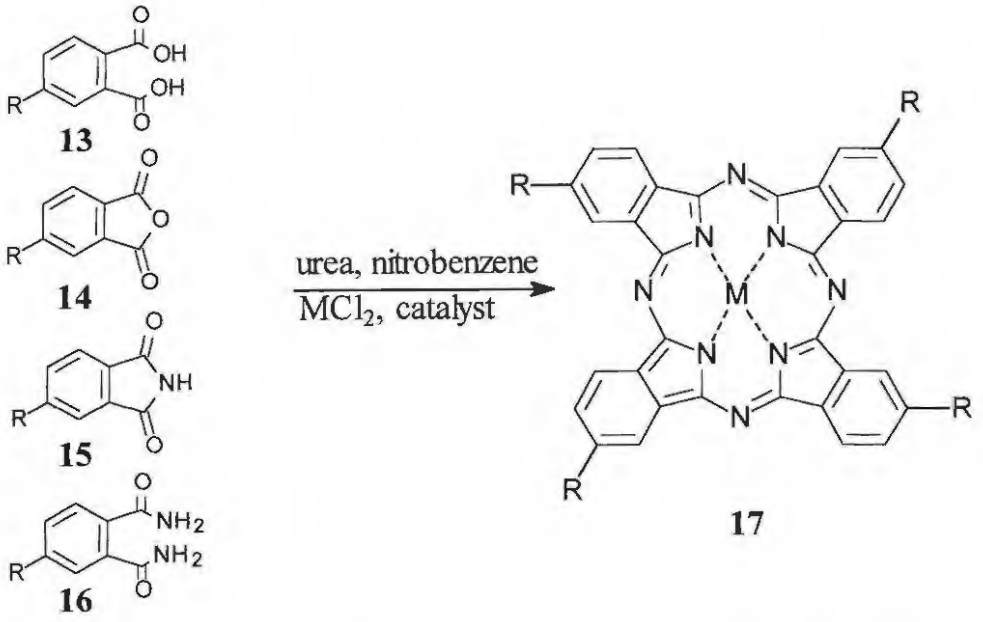

Scheme 2.4 Synthesis of metallated phthalocyanines using substituted phthalic acid (**13**), phthalic anhydride (**14**), phthalimide (**15**) or phthalamide as starting materials.

Reactions between phthalonitrile, 1,3-diiminosoindoline or o-cyanobenzamide and a finely devided metal, metal hydride or metal chloride may also be employed to yield the particular metallated phthalocyanine. Metal-free phthalocyanines are also metallated by refluxing with the appropriate metal or metal salt in solvents like quinoline or DMF, Equation 2.1. Linstead showed that 1,3-diiminosoindoline (**12**) in hot formamide in the presence of $NiCl_2$ gave the nickel phthalocyanine in 96% yield.[16]

$$PcH_2 + MX_2 \xrightarrow[\text{reflux}]{\text{solvent (e.g. quinoline or DMF)}} PcM + 2HX \qquad \text{.....(2.1)}$$

2.1.1.3 Unsymmetrically substituted phthalocyanines

In order to synthesize unsymmetrically substituted phthalocyanines the mixed condensation method where two differently substituted 1,3-diiminoisoindolines are employed will yield a statistical mixture of compounds that are likely to be inseparable by chromatographic methods. However, if one of the substituted-1,3-diiminoisoindolines were attached to an insoluble polymer and reacted with a large excess of a second diiminoisoindoline in solution, an unsymmetrically substituted phthalocyanine can be formed exclusively on the polymer and subsequently liberated from the polymer. A good example would be a polymer-bound trityloxyalkoxy-1,3-diiminoisoindoline (**18**) condensed with 5-isopropoxy-1,3-diiminoisoindoline (**19**)[17,18] in a mixed diiminoisoindoline condensation in 2-*N,N*-dimethylaminoethanol to give, after Soxhlet extraction to remove 2,9,16,23-tetraisopropoxyphthalocyanine and mild acid treatment, unsymmetrical tetrasubstituted 2-(6'-hydroxyhexoxy)-9,16,23-triisopropoxy-phthalocyanine (**20**) in 24% yield (Scheme 2.5).

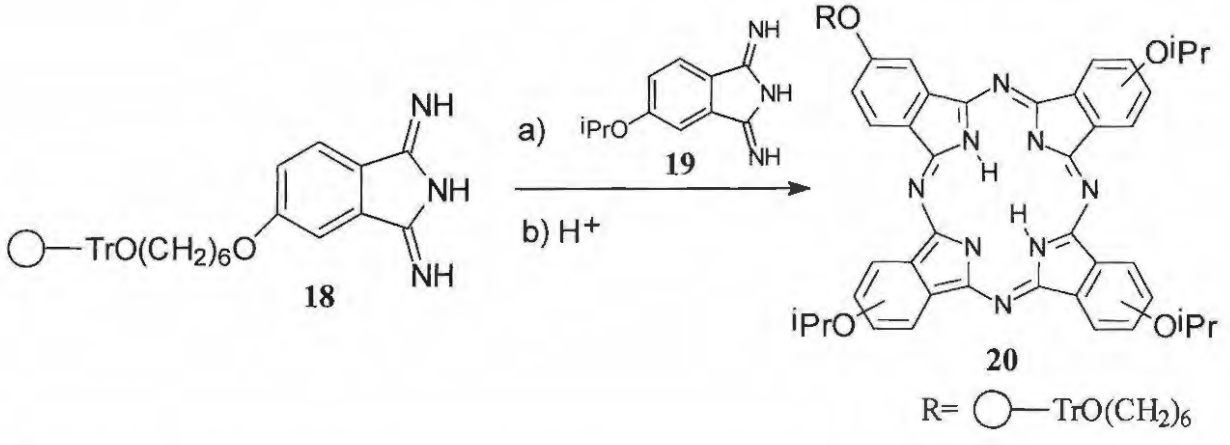

Scheme 2.5 Synthesis of an unsymmetrical phthalocyanine (**20**) using polymers.

Another method used to prepare unsymmetrically substituted phthalocyanines makes use of subphthalocyanines (Scheme 2.6). This typically yields a monosubstituted phthalocyanine. The subphthalocyanine (**21**) and is prepared by heating a 1 M solution of boron trichloride in n-hexane and 1-chloronaphthalene with the substituted or unsubstituted phthalonitrile of interest.[19,20,21] Reaction of **21** with a differently substituted phthalonitrile or diiminoisiindoline (**15**) yields the unsymmetrically substituted phthalocyanine (**22**).

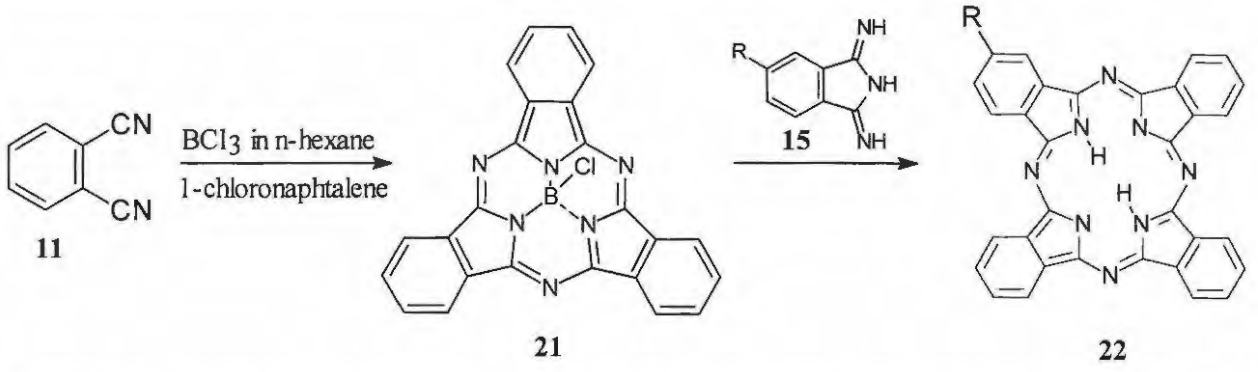

Scheme 2.6 Synthesis of an unsymmetric phthalocyanine (**22**) using subphthalocyanine (**21**) as an intermediate.

2.1.1.4 Synthesis of zinc, germanium(IV) and tin (IV) phthalocyanines

In this study metal free, zinc(II), germanium(IV) and tin (IV) phthalocyanines have been synthesized and therefore a short review on the general synthesis of these complexes follows.

Zinc phthalocyanines

In addition to the general synthesis of MPc already discussed, the zinc phthalocyanine may be prepared from phthalonitrile and zinc dust[22] or from dilithium phthalocyanine and zinc chloride in absolute ethanol.[23] Zinc phthalocyanines are in general very easy to synthesize

and yield, availability and cost of starting materials will determine the synthesis of choice. A variety of ring substituted ZnPc complexes have been reported, but this work reports for the first time the synthesis of ZnPc complexes substituted with biologically active compounds, namely cholesterol and estrone. ZnPc complexes containing eight phenoxy groups are also not commonly found in literature and this work reports on the synthesis of ZnPc containing a series of substituted phenoxy groups.

Germanium(IV) and tin(IV)phthalocyanines

The Cl_2GePc (**23**) complex is formed in a reaction of $GeCl_4$ and phthalonitrile (**11**) in quinoline under reflux, Scheme 2.7.[24,25] The Cl_2GePc (**23**) complex may also be formed by the reaction of $GeCl_4$ with the metal-free phthalocyanine and is very resistant to hydrolysis. Hydrolysis will only occur through reprecipitation from concentrated H_2SO_4 (Scheme 2.7). The $(OH)_2Ge(IV)Pc$ (**24**) will react easily with either phenols or alcohols to form metal ethers in condensation reactions on the axial position.[26]

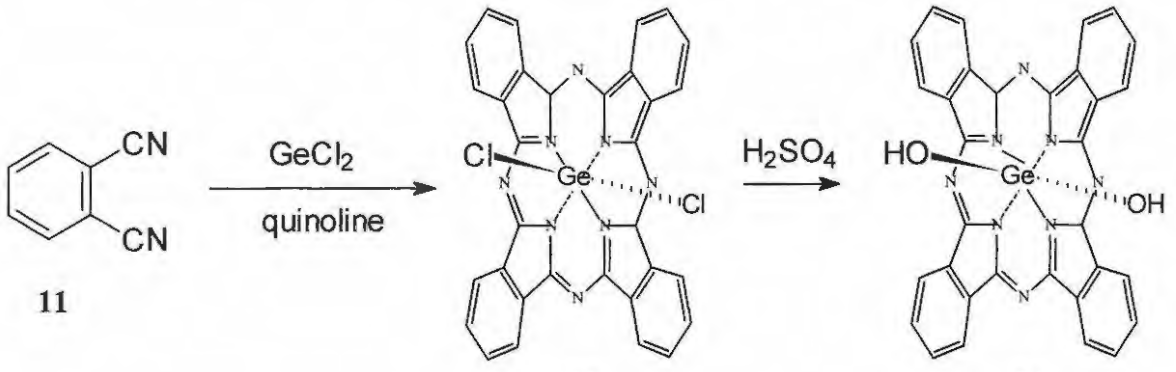

11 **23** **24**

Scheme 2.7 Synthesis of germanium(IV)phthalocyanines.

The reaction between phthalonitrile (**11**) and stannous chloride is violently exothermic and results in the formation of $Cl_2Sn(IV)Pc$ (**25**) (Scheme 2.8). No hydrogen chloride is

evolved and the process involves an unique direct addition.[27] A reaction of the metal-free phthalocyanine with stannic or stannous chloride also gives $Cl_2Sn(IV)Pc$ (**25**).[28] Hydrolysis is attained by first synthesizing Sn(II)Pc (**26**) through reduction of $Cl_2Sn(IV)Pc$ (**25**) with $SnCl_2$. Compound **26** is then heated in 1-chloronaphthalene in the presence of iodine, yielding $I_2Sn(IV)Pc$ (**27**), which is more readily hydrolized, Scheme 2.8.[29] $(OH)_2SnPc$ (**28**) also allows axial condensation reactions with phenols, but the alkoxy derivatives are unstable.[30]

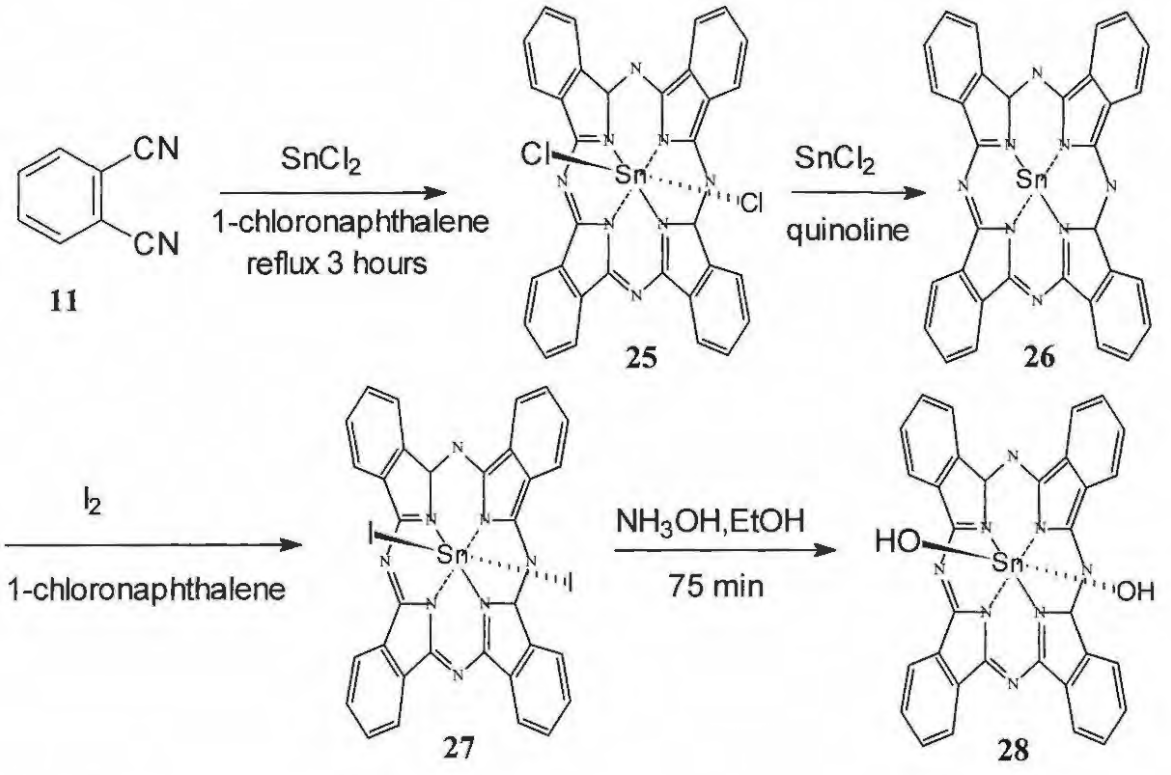

Scheme 2.8 Synthesis of tin(IV)phthalocyanines.

The preferred solvent for the reactions depicted in Scheme 2.8 is the high boiling 1-chloronaphthalene. A recent publication showed how 5,6-dialkoxy-1,3-diiminoisoindolines as well as their phthalonitrile derivatives have been heated in a microwave with $GeCl_4$ and $SnCl_4$ in quinoline and 1-chloronaphthalene respectively to yield these phthalocyanines in high yield within 15 minutes.[31]

There are only a few reports on the synthesis of ring substituted Ge(IV)Pc and Sn(IV)Pc complexes.[32,33] Ge(IV)Pc complexes containing a variety of axial substituents including cholesterol, have been reported.[34] This work reports on the peripheral substitution of Ge(IV)Pc and Sn(IV)Pc with the steroid estrone as well as the axial substitution of Sn(IV)Pc with estrone. A few Ge and Sn phthalocyanine complexes substituted with eight phenoxy derivatives are included.

2.1.2 Mechanism of phthalocyanine formation

Phthalocyanines can be prepared by many different routes and therefore many different mechanisms are involved. In the synthesis of substituted phthalocyanines via sodium or lithium) n-pentoxide in pentanol, Borodkin[35] isolated a sodium derivative of methoxy-iminoisoindoline (**29**) (Figure 2.1) as an intermediate. Later Hurley *et al.*[36] isolated the nickel complexes (**30**) and (**31**) shown in Figure 2.1 as intermediates leading to nickel phthalocyanines. A dimeric lithium salt (**32**) was later also isolated and shown to condense to a tetranitrophthalocyanine.[37] Although some ideas exists as to how phthalocyanines are formed, a lot of studies still need to be done.

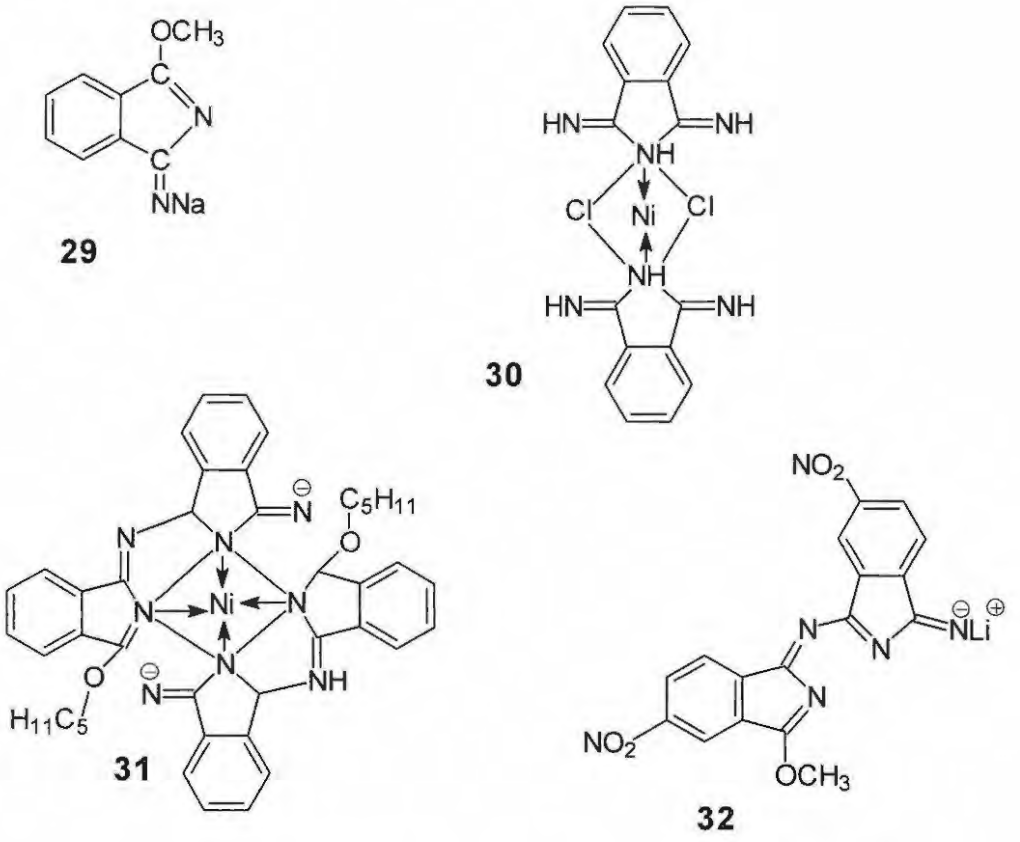

Figure 2.1 Intermediates isolated during phthalocyanine synthesis.[29,30,31]

2.1.3 Characterization of phthalocyanine complexes

2.1.3.1 UV/Visible spectroscopy

Metallated phthalocyanines have very distinct UV/Visible spectra with a strong characteristic band in the visible region called the Q-band and a weaker absorption in the UV region called the B or the Soret band. The Q-band arises from the absorption of light of a certain frequency and the consequent excitation of electrons from the highest occupied molecular orbital (HOMO) namely the a_{1u} (π) to the lowest unoccupied molecular orbital (LUMO), namely the e_g (π^*). The transition from a_{2u} to e_g results in the B-band that forms part of the electronic spectra (Figure 2.2).[38]

As can be seen in Figure 2.2b the metal-free phthalocyanine has a split Q band. This is the result of a difference in symmetry, that is, the metallated phthalocyanine has a D_{4h} symmetry and the metal-free phthalocyanine a D_{2h} symmetry.

The UV/Visible spectra are influenced by co-ordinating solvents, different central metals, peripheral and axial ligands.[39,40]

By making use of spectroelectrochemistry it can be observed whether reduction or oxidation occurs on the metal or on the Pc ring. Reduction from MPc^{2-} to MPc^{3-} (where Pc^{2-} represents the phthalocyanine dianion) leads to the formation of bands between 500 and 600nm.[41] This anion radical can be reduced further by succesive addition of electrons to the LUMO up to MPc^{6-}. The absorption bands of the ring reduced Pc are significantly weaker than that of the original MPc^{2-} due to the ring perturbations.[42] Reduction of the central metal normally only shows a shift in the position of the Q-band but not a significant change in intensity.[43]

Oxidation occurs through removal of electrons from the HOMO, allowing transitions from the lower lying e_g orbitals to the singly occupied HOMO. Intensity is lost and a new broad band is formed between 700 and 800 nm and another at 500 nm.

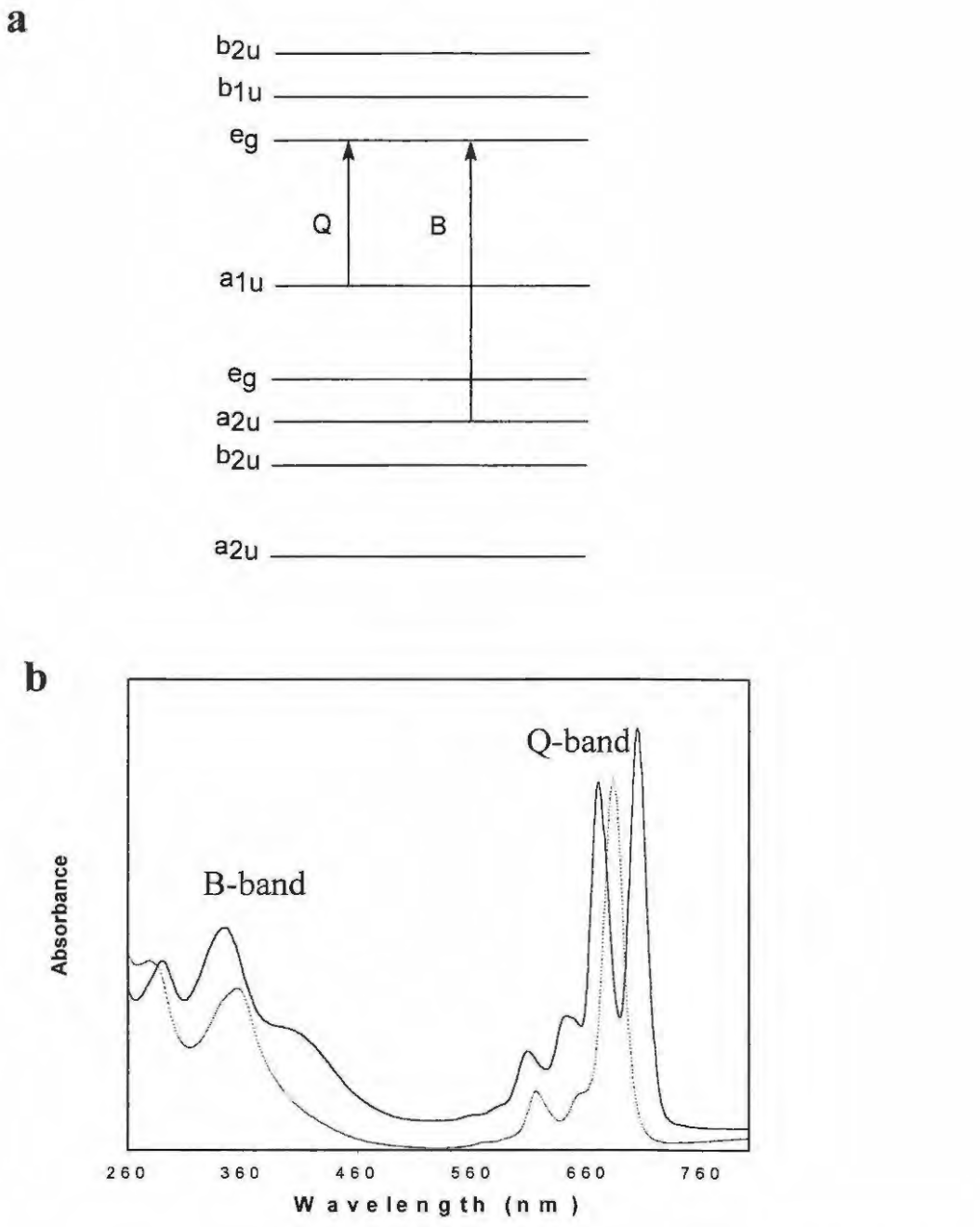

Figure 2.2 a) Electronic transitions between the HOMO and the LUMO giving rise to the characteristic Q-band and Soret-band in a typical UV/visible spectrum. b) Absorption spectra of metallated (---) and metal-free (solid line) phthalocyanine with the Q – and B band as indicated.

2.1.3.2 Infrared spectroscopy

Most metallated phthalocyanines have very similar infrared spectra. The lower symmetry of the metal-free phthalocyanine probably accounts for a more complex spectrum. The band at 3030 cm^{-1} is assigned to the aromatic C-H stretching vibration, the 1610 and 1475 cm^{-1} bands to C-C ring skeletal stretching vibrations and the 720 cm^{-1} bands to C-H out of plane bending vibrations.[44] The metal-free phthalocyanine has a band near 3298 cm^{-1} assigned to the N-H stretching vibration.[45] Metal sensitive bands are observed at about 1490 and 1410 and differ with about 10 cm^{-1} between, for example, SnPc (1493 and 1416 cm^{-1}) and PbPc (1484 and 1404 cm^{-1}).[46]

2.1.3.3 ^1H Nuclear magnetic resonance spectroscopy

The basic unsubstituted phthalocyanine molecule is highly symmetric and shows distinct resonances at lower field due to the deshielding effect of the induced secondary field in the 18-membered phthalocyanine ring. Two resonances of equal intensity are observed due to protons a and b in Figure 2.3.

^1H NMR spectra of Pc complexes become increasingly complicated upon addition of axial and peripheral substituents and as a decrease in symmetry is observed.

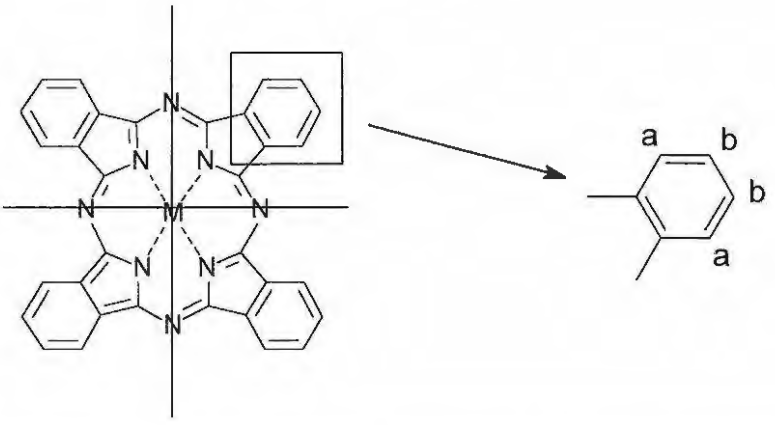

Figure 2.3 A figure indicating the highly symmetric phthalocyanine molecule and the protons (a and b) responsible for the two resonances observed.

2.2 Results and discussion

2.2.1 Synthesis of 4,5-dichlorophthalonitrile (37) (Scheme 2.9)

4,5-Dichlorophthalonitrile (**37**) is used as one of the precursors in the synthesis of octa(phenoxy)phthalocyanines and its synthesis will therefore be discussed (Scheme 2.9). Inexpensive 4,5-dichlorophthalic acid (**33**) was available in the laboratory and was therefore used as starting material from which 4,5-dichlorophthalonitrile (**37**) was synthesized according to the method used by Wöhrle *et al.*[47] The 4,5-dichlorophthalic anhydride (**34**) was synthesized by gently heating 4,5-dichlorophthalic acid in acetic anhydride for 5 hours upon which the product is obtained in 93% yield. Care was taken during this step against overheating. The next step where 4,5-dichlorophthalic anhydride (**34**) was heated under reflux in formamide for 3 hours to afford 4,5-dichlorophthalimide (**35**) proceeded without effort with a yield of 95%. Conversion of 4,5-dichlorophthalimide (**35**) into the 4,5-dichlorophthalamide (**36**) (71%) proceeded over a period of 2 days in the presence of 25% ammonium hydroxide. The last step involved a reaction of 4,5-dichlorophthalamide (**36**) with thionyl chloride in dry distilled DMF at low temperature between 0 and 5°C during a 5 hour time period and at room temperature for 24 hours to yield the 4,5-dichlorophthalonitrile (**37**) in 72% yield. The overall yield in this four step synthesis adds up to a satisfying 45%.

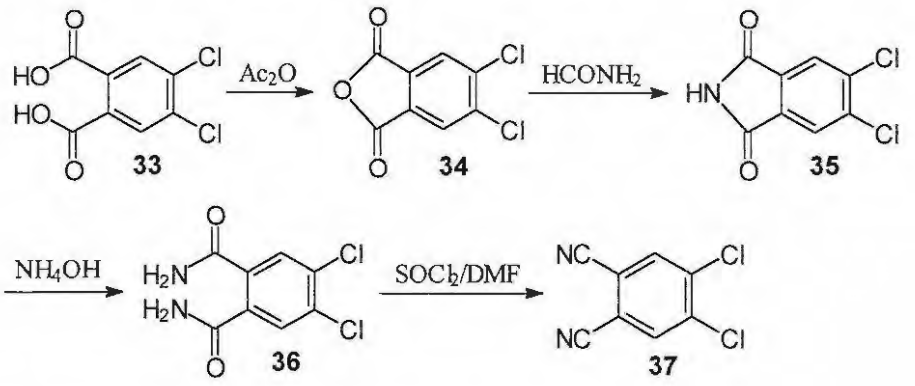

Scheme 2.9 Synthesis of 4,5-dichlorophthalonitrile (**37**).

2.2.2 Synthesis of 2,3,9,10,16,17,23,24-octa(phenoxy)phthalocyanines (Scheme 2.10)[†]

A known method according to Wöhrle *et al.*[40] was used to synthesize the 4,5-di(substituted phenoxy)phthalonitrile (**38**) and the octa(substituted phenoxy)phthalocyanine complex (**39**).

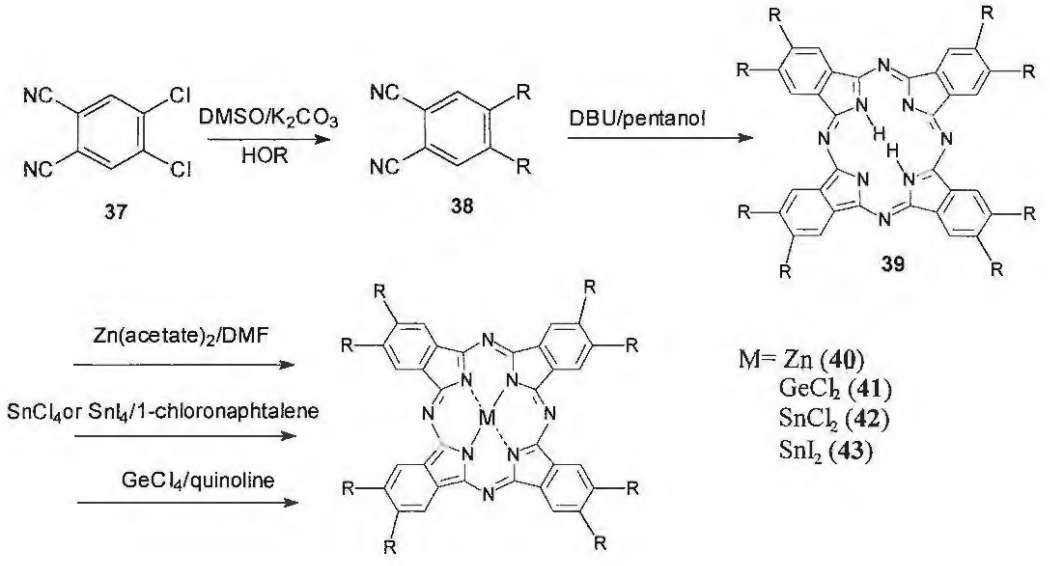

Scheme 2.10 Synthesis of 2,3,9,10,16,17,23,24-octa(substituted phenoxy)phthalocyanines.

[†] This work is published as "Suzanne E. Maree and Tebello Nyokong, **Syntheses and photochemical properties of octasubstituted phthalocyaninato zinc complexes**, *J. Porphyrins and Phthalocyanines*, **5**, 782 (2001)." and submitted as "Suzanne E. Maree, D. Phillips and Tebello Nyokong, **Syntheses, photophysical and photochemical studies of germanium and tin phthalocyanine complexes**, *In Press*".

Table 2.1 Structures, abbreviations and numbering of the substituents from Scheme 2.10.

2,3,9,10,16,17,23,24-octa(R)phthalocyanine where R =	**Abbreviation**	**Number**
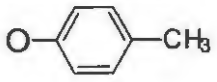 *p*-methylphenoxy	H_2OpMPPc ZnOpMPPc	**39a** **40a**
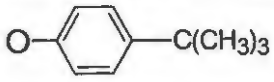 *p-tert*-butylphenoxy	H_2OTBPPc ZnOTBPPc	**39b** **40b**
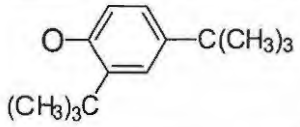 di-*tert*-butylphenoxy	H_2ODTBPPc ZnODTBPPc	**39c** **40c**
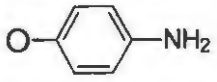 *p*-aminophenoxy	H_2OAPPc ZnOAPPc	**39d** **40d**
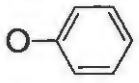 phenoxy	H_2OPPc ZnOPPc Cl_2GeOPPc Cl_2SnOPPc I_2SnOPPc	**39e** **40e** **41e** **42e** **43e**
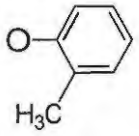 *o*-methylphenoxy	H_2OMPPc ZnOMPPc Cl_2GeOMPPc Cl_2SnOMPPc	**39f** **40f** **41f** **42f**
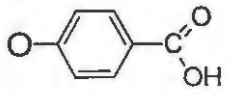 *p*-carboxyphenoxy	H_2OCPPc ZnOCPPc	**39g** **40g**
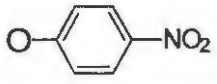 *p*-nitrophenoxy	H_2ONPPc ZnONPPc	**39h** **40h**
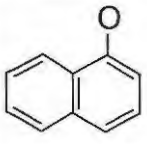 1-naphtoxy	H_2ONaphPc ZnONaphPc	**39i** **40i**
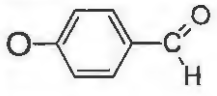 *p*-formylphenoxy	H_2OAldPPc ZnOAldPPc	**39j** **40j**
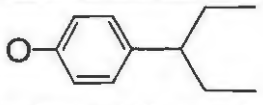 *p*-amylphenoxy	H_2OAmPPc ZnOAmPPc	**39k** **40k**

Scheme 2.10 represents the synthesis of the octa(substituted phenoxy)phthalocyanines (**39**) and Table 2.1 gives a summary of the complexes synthesized, the abbreviations as well as the numbering system that will be used.

The synthesis of the 4,5-di(substituted phenoxy)phthalonitrile (**38**), requires that an appropriate phenoxy derivative of choice is stirred with 4,5-dichlorophthalonitrile (**37**) at 90°C in DMSO with K_2CO_3 addition at 5 minute intervals for 40 minutes, Scheme 2.10. According to this published method the reaction should only be stirred for another 30 minutes, but it was found that higher yields and purity of compound **38** were obtained with less of the monosubstituted phthalonitrile if the reaction was allowed to continue for another 3 hours. The reaction is a simple nucleophilic substitution reaction with general yields between 58 - 80%. After recrystallization no further purification is needed and ^1H NMR spectrums confirmed good purity. Singlet peaks (7.00-7.20 ppm) defined the benzene rings while the hydrogen atoms on the phenoxy aromatic rings resonated as two doublets that may be found between 6.90 and 8.40 ppm. The unsymmetrically substituted phenoxy groups, e.g. **38c** and **38f**, showed the appropriate multiplicity according to the n+1 rule. FTIR spectra showed characteristic C-O stretches at ~1280 and 1210 and C≡N stretches at 2229.

Formation of the metal-free phthalocyanine (**39**) proceeded by heating with DBU, a strong organic base, in pentanol for 16 hours, Scheme 2.10. It is quite interesting to note that the phenoxy groups with more electron-donating groups, for example **39a**, **39b**, **39c** and **39k** shows cyclotetramerization within the first 20 minutes whereas the more electron-withdrawing groups, for example the **39d**, **39g**, **39h** and **39j** only turns blue-green after 40 minutes to an hour. Good yields (40-60%) were already found after 8 hours for the more

electron-donating groups. These yields are only obtained after 16 hours for the more electron-withdrawing groups.

It should also be noted that in general amino substituted phthalocyanines (**39d**) could not be successfully synthesized from amino substituted phthalonitriles, because a dark brown polymer was formed upon heating. This was overcome by synthesizing the H_2ONPPc (**39h**) first and then reduction with Na_2S in water to yield **39d** in up to 95% yield.

Figure 2.4 shows typical ^{1}H NMR spectrum observed for the metal-free complexes. Aggregation was strongly present for complexes **39d, 39g, 39h, 39j** and was manifested as broad, undefined ^{1}H NMR peaks (Figure 2.4 i), while the more soluble complexes for example **39a**, **39b**, **39c** and **39k** showed well defined peaks (Figure 2.4 ii). The Pc skeleton resonance is observed as a singlet at about 9 ppm for H_2ODTBPPc (**39c**) and the protons on the phenoxy group as a singlet and two doublets, each integrating for 8 protons.

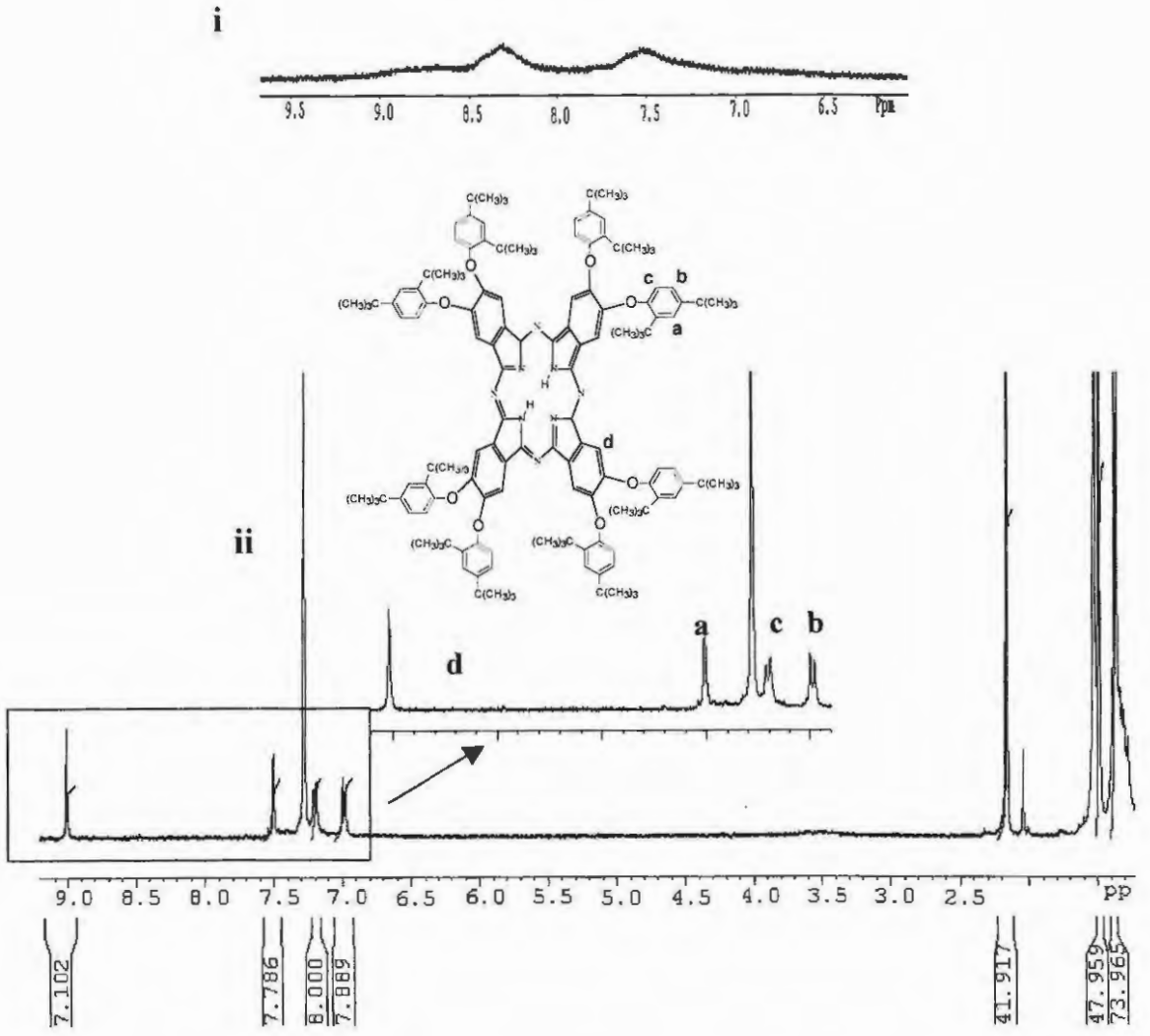

Figure 2.4 ^{1}H NMR of i) H_2ONPPc (**39h**) and ii) H_2ODTBPPc (**39c**) showing the extend of aggregation and hydrogen bonding present with H_2ONPPc (**39h**) and the absence thereof with H_2ODTBPPc (**39c**).

It was decided in this study to insert the metal after the phthalocyanine had been formed and purified. Although this was an easy procedure, each metal required different experimental procedures according to different mechanisms involved.

Insertion of zinc was accomplished by dissolving the metal-free phthalocyanine (**39**) in DMF and addition of excess zinc acetate (Scheme 2.10). This step was usually complete within 10 to 20 minutes and the collapse of the split to a single Q-band is followed by

UV/Visible spectroscopy. UV/Vis spectra show Q-bands with wavelength values as given in Table 2.2.

Table 2.2 UV/Visible data of metallated octa(substituted phenoxy) phthalocyanine complexes. Solvent chloroform unless indicated otherwise.

Compound	UV/Vis, λ_{max}(log ε):
40a[a]	679 (5.12), 652 (4.30), 613 (4.63), 368 (4.56)
40b	683 (5.16), 655 (4.31), 615 (4.34), 357 (4.61)
40c	686 (4.85), 657 (3.93), 619 (3.97), 345 (4.33)
40d[a]	683 (5.23), 651 (4.73), 618 (4.69), 345 (5.03)
40e[a]	680 (5.32), 652 (4.50), 613 (4.50), 364 (4.91)
40f	682 (5.14), 655 (4.34), 615 (4.35), 348 (4.64)
40g[a]	678 (4.47), 644 (4.04), 623 (4.04), 337 (4.36)
40h[a]	678 (5.31), 639 (4.73), 616 (4.63), 345 (5.04)
40i	694 (-), 668 (-), 624 (-), 430 (-)[b]
40j[a]	679 (4.35), 651 (3.74), 618 (3.66), 352 (4.32)
40k	684 (4.94), 654 (4.18), 616 (4.17), 348 (4.48)
41e	692 (5.16), 663 (4.40), 623 (4.40), 362 (4.75), 349 (4.62), 294 (4.52)
41f	690 (5.20), 669 (4.66), 621 (4.46), 365 (4.81), 346 (4.74), 274 (4.91)
42e	707 (4.86), 677 (4.08), 637 (4.06), 373 (4.31), 302 (4.06)
43e	708 (4.82), 680 (4.09), 638 (4.05), 371 (4.23), 297 (4.09)
42f	708 (5.45), 681 (4.64), 637 (4.62), 372 (4.90), 301 (4.73)

[a] Solvent DMSO.
[b] Not soluble enough for extinction coefficient determinations.

The ^{1}H NMR spectra very distinctly showed a downfield shift of the singlet that defines the benzene rings of the phthalocyanine skeleton from between 7.00-7.20 ppm of the 4,5-di(substituted phenoxy)phthalonitrile (**38**) to between 8.00-9.00 ppm of the ZnPc complexes due to the deshielding effect of the highly conjugated aromatic ring system (Table 2.3). Once again, aggregation limited the ^{1}H NMR spectra to broadened peaks that were unresolved especially with **40d**, **40g**, **40h** and **40j** which may form additional hydrogen bonding. Quite interestingly it was found that the ZnOpMPPc (**40a**) shows low

solubility. This was overcome by synthesizing the ZnOMPPc (**40f**) where the absolute symmetry was broken and amazingly a significant increase in solubility was observed.

Table 2.3 Yields and spectral data of metallated octa(substituted phenoxy)phthalocyanines (**40a-k, 41e, 41f, 42e, 42f, 43e**).

Compound	Yield	^{1}H NMR (in $CDCl_3$ unless indicated otherwise)	FTIR (KBr)
40a[a]	40	8.52 (s, 8H, CH-pc) 7.45 (d, 16H, CH-phenoxy) 7.34 (d, 16H, CH-phenoxy) 2.28 (s, 24H, CH_3)	2916, 2855, 1580, 1486, 1398, 1269, 1223, 739
40b	62	8.52 (s, 8H, CH-pc) 7.45 (d, 16H, CH-phenoxy) 7.34 (d, 16H, CH-phenoxy) 2.28 (s, 24H, CH_3)	2916, 2855, 1580, 1486, 1398, 1269, 1223, 739
40c	65	9.01 (s, 8H, CH-pc), 7.51 (d, 8H, CH), 7.20 (dd, 8H, CH), 6.99 (d, 8H, CH), 1.54 (s, 144H, CH_3), 11 (s, 144H, CH_3)	2955, 2870, 1600, 1486, 1394, 1278, 1208, 823
40d[a]	44	8.31 (s, 8H, CH-pc), 7.40 (d, 16H, CH-phenoxy), 6.75 (d, 16H, CH-phenoxy)	3458, 3366, 3221 (NH); 1584, 1500; 1253, 1207; 742
40e[a]	60	8.70 (s, 8H, CH-pc) 7.51 (t, 8H, CH-phenoxy) 7.32 (m, 24H, CH-phenoxy)	1584, 1486, 1398, 1268, 1204, 743
40f	51	8.32 (s, 8H, CH-pc) 7.22 (d, 8H, CH-phenoxy) 7.03 (m, 24H, CH-phenoxy) 2.21 (s, 24 H, CH_3)	2947, 2924 (C-H); 1581, 1490; 1398; 1269, 1223; 739
40g[a]	58	8.12 (s, 8H, CH-pc), 8.01 (d, 16H, CH-phenoxy), 7.18 (d, 16H, CH-phenoxy)	1686 (C=O), 1589, 1498, 1398, 1291, 1212, 771
40h[a]	46	8.89 (s, 8H, CH), 8.32 (broad s, 32 H, CH)	1596; 1520 (NO_2 asym.); 1485; 1342 (NO_2 sym.), 1248; 739
40i	56	8.63 (s, 8H, CH-pc), 7.80 (m, 24H, CH-naph), 7.40 (m, 24H, CH-naph), 7.21 (d, 8H, CH-naph)	3053, 1595, 1505, 1447, 1398, 1276, 1211, 743
40j[a]	52	9.94 (s, 8H, aldehyde), 8.07 (broad s, 8H, CH-pc), 7.47 (broad d, 16H, CH-phenoxy) 7.14 (broad d, 16H, CH-phenoxy)	1694 (C=O), 1595, 1497, 1269, 1211, 743
40k	77	8.55 (s, 8H, CH-pc) 7.26 (d, 16H, CH-phenoxy) 7.05 (d, 16H, CH-phenoxy) 1.63 (m, 32H, CH_2) 1.34 (d, 8H, CH) 0.69 (t, 48H, CH_3)	2962, 2908, 2870 (C-H); 1583, 1501; 1400; 1295, 1219; 827
41e	65	9.08 (s, 8H, CH-pc) 7.52 (t, 16H, CH-phenoxy) 7.31 (m, 24H, CH-phenoxy)	1585, 1487; 1410; 1276, 1205; 743, 686
41f	54	8.89 (s, 8H, CH-pc) 7.43 (d, 8H, CH-phenoxy) 7.34 (t, 8H, CH-phenoxy) 7.23 (m, 8H, CH-phenoxy) 7.21 (d, 8H, CH-phenoxy) 2.43 (s, 24H, CH_3)	2962, 2924; 1583, 1493; 1406; 1272, 1224; 743
42e	44	9.08 (s, 8H, CH-pc) 7.52 (t, 16H, CH-phenoxy) 7.32 (m, 24H, CH-phenoxy)	1585, 1486; 1394; 1272, 1207; 737, 687
43e	59	9.09 (2s, 8H, CH-pc) 7.54 (t, 16H, CH-phenoxy) 7.34 (m, 24H, CH-phenoxy)	1581, 1485; 1394; 1269, 1223; 740
42f	45	8.86 (s, 8H, CH-pc) 7.34 (d, 8H, CH-phenoxy) 7.38 (t, 8H, CH-phenoxy) 7.32 (m, 8H, CH-phenoxy) 7.24 (d, 8H, CH-phenoxy) 2.43 (s, 24H, CH_3)	2962, 2924;1585, 1485; 1392; 1270, 1227; 735

[a] Deuterated DMSO used as solvent.

Inserting tin into the phthalocyanine ring required completely different conditions. Higher energy was required for this much larger atom and therefore a higher boiling point solvent like 1-chloronaphthalene was employed (Scheme 2.10). Anhydrous tin(IV)chloride was used and the mixture refluxed for about 1 hour. Removing a high boiling solvent like 1-chloronaphtalene is always challenging but it was found that the phthalocyanine may be precipitated out by addition of hexane. Soxhlet extraction with methanol and acetone yielded a very pure product which is soluble in chloroform. Only the H_2Pc complexes showing good solubility as well as stability were metallated with tin and germanium to extend the study.

Germanium was inserted with the same ease as for tin (Scheme 2.10), but after about 20 minutes more $GeCl_4$ needs to be added since $GeCl_4$ is a liquid and at these elevated temperatures evaporation becomes a problem. Quinoline was the solvent used for this procedure since it acts as a HCl trap. The reaction mixture turns to a dark brown mixture as soon as the metallation starts taking place. It has been noted in literature that formation of the Sn(IV)Pc occurs through a different mechanism than for Ge(IV)Pc where hydrogen chloride is not one of the products.

Table 2.4 gives the solubility and aggregation properties of metallated octa(substituted phenoxy)phthalocyanines (**40**). The percentage aggregation was calculated as the percentage deviation from Beer's law at absorbance equal to one. It is quite an achievement to synthesize phthalocyanines of good solubility, especially in solvents like chloroform. Good solubility in chloroform was especially observed for the tin and germanium phthalocyanines, most likely due to the presence of the axial ligand.

Table 2.4 Aggregation and solubility data for the metallated octa(substituted phenoxy)phthalocyanines. Good solubility denoted by +, sparingly soluble by ± and not soluble by -. Solvent used for % aggregation is chloroform unless indicated otherwise.

Compound	% aggregation	Solubility	
		Chloroform	DMSO
40a[a]	0	±	±
40b	0	+	-
40c	0	+	-
40d[a]	0	-	+
40e[a]	0	±	+
40f	0	+	+
40g[a]	26	-	+
40h[a]	0	-	+
40i	90	±	-
40j[a]	8	-	±
40k	10	+	-
41e	0	+	±
41f	10	+	±
42e	0	+	±
43e	0	+	±
42f	9	+	±

[a] Solvent DMSO

^{1}H NMR spectra were much more resolved for both the tin and germanium Pc complexes than for those of the zinc phthalocyanines. This is due to the presence of the axial chloro - and iodo groups de-aggregating the Pc molecules (Figure 2.5). The singlet proton resonance of the phthalocyanine benzene ring was more deshielded for the Ge(IV)Pc complexes and Sn(IV)Pc complexes than for that of the ZnPc complexes (Table 2.3). This is explained by the higher electronegativities of the tin and germanium (as well as their charge) consequently causing electron density to be mostly located on the metal centre.

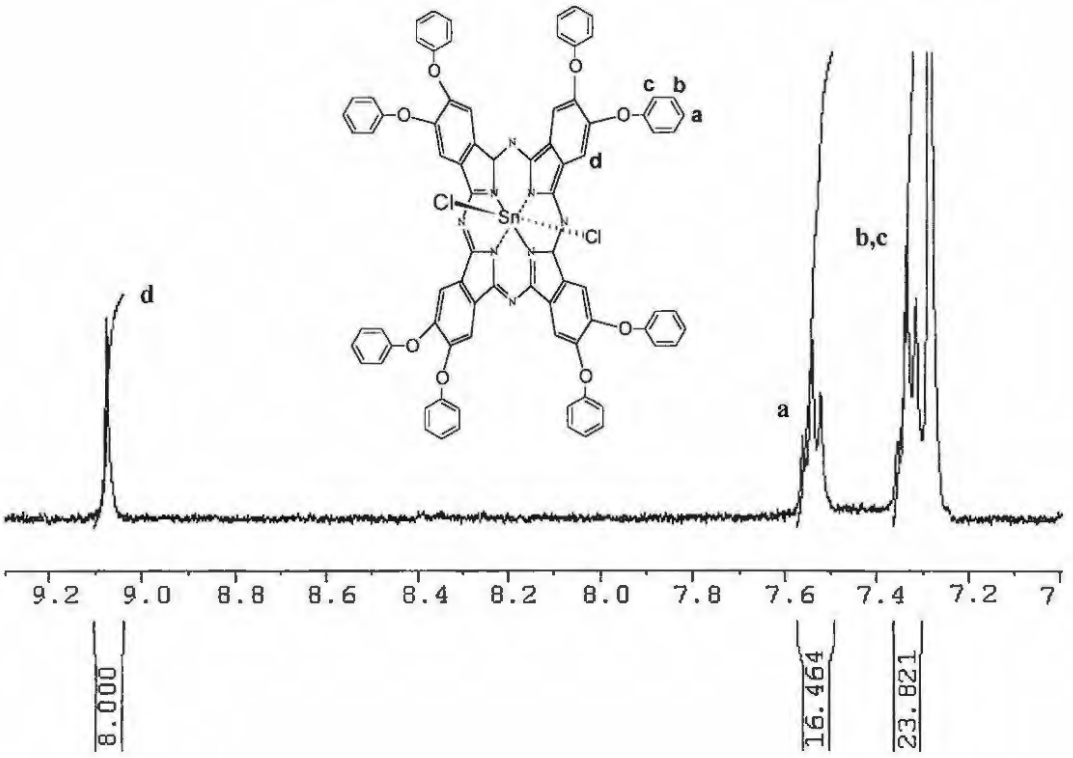

Figure 2.5 ^{1}H NMR of $Cl_2SnOPPc$ (**42f**).

From the UV/Visible data in Table 2.2 it can be seen that the Q-bands of the Ge(IV)Pc complexes (**41e** and **41f**) are on average 10 nm more red shifted than those of the corresponding ZnPc complexes (**40e** and **40f**) and the Sn(IV)Pc complexes (**42e** and **42f**) are up to 30 nm more red shifted as compared to the ZnPc complexes (Figure 2.6). This is due to the raised energy level of the $a_{2u}(\pi)$ HOMO with increased size of the central metal.[48] Strong absorbance in the infrared region is one of the desired properties of a good photosensitizer and this prerequisite has therefore been met successfully. Metal sensitive stretching frequencies[49] were observed for $Cl_2GeOMPPc$ (**41f**) at 1493 and 1406 cm^{-1}, ZnOMPPc (**40f**) at 1490 and 1398 cm^{-1} as well as $Cl_2SnOMPPc$ (**42f**) at 1485 and 1392 cm^{-1}. This increase in stretching frequencies Sn>Zn>Ge was a general trend observed for all complexes with similar peripheral groups.

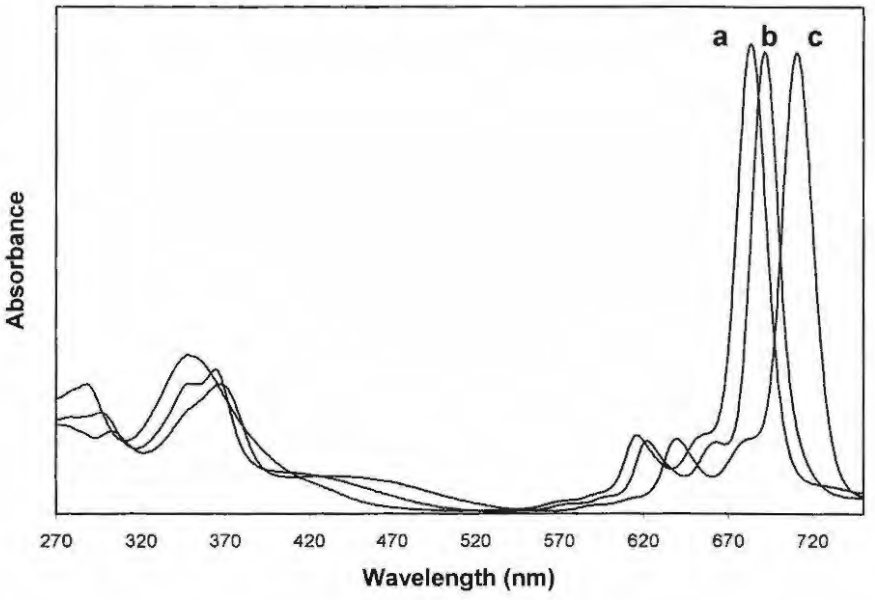

Figure 2.6 Absorbance spectra of a) ZnOMPPc (**40f**), b) Cl_2GeOMPPc (**41f**) and c) Cl_2SnOMPPc (**42f**) in chloroform.

2.2.3 Synthesis of steroid-containing phthalocyanines

2.2.3.1 Synthesis of 2,3,9,10,16,17,23,24-octa(steroid)phthalocyanines (Scheme 2.11)

In order to increase oncotropicity, that is the affinity of the sensitizer to cancer cells, it was decided to derivatize the phthalocyanine entity with steroids. Breast cancer cells are known to over express estrogen receptor,[50] thus providing a potential site for directing photosensitizers. It was therefore decided to make use of the phenolic group contained in estrone to react it with 4,5-dichlorophthalonitrile (**37**) in the same way as discussed before (Section 2.2.1) to yield the pure 4,5-diestrone phthalonitrile (**38l**) in 83% yield (Scheme 2.11).

The H_2OEPc (**39l**) was synthesized and metallated with zinc, germanium and tin (as described in Section 2.2.2) in good yields to give complexes **40l**, **41l** and **42l** that are soluble in chloroform, DMF and DMSO.

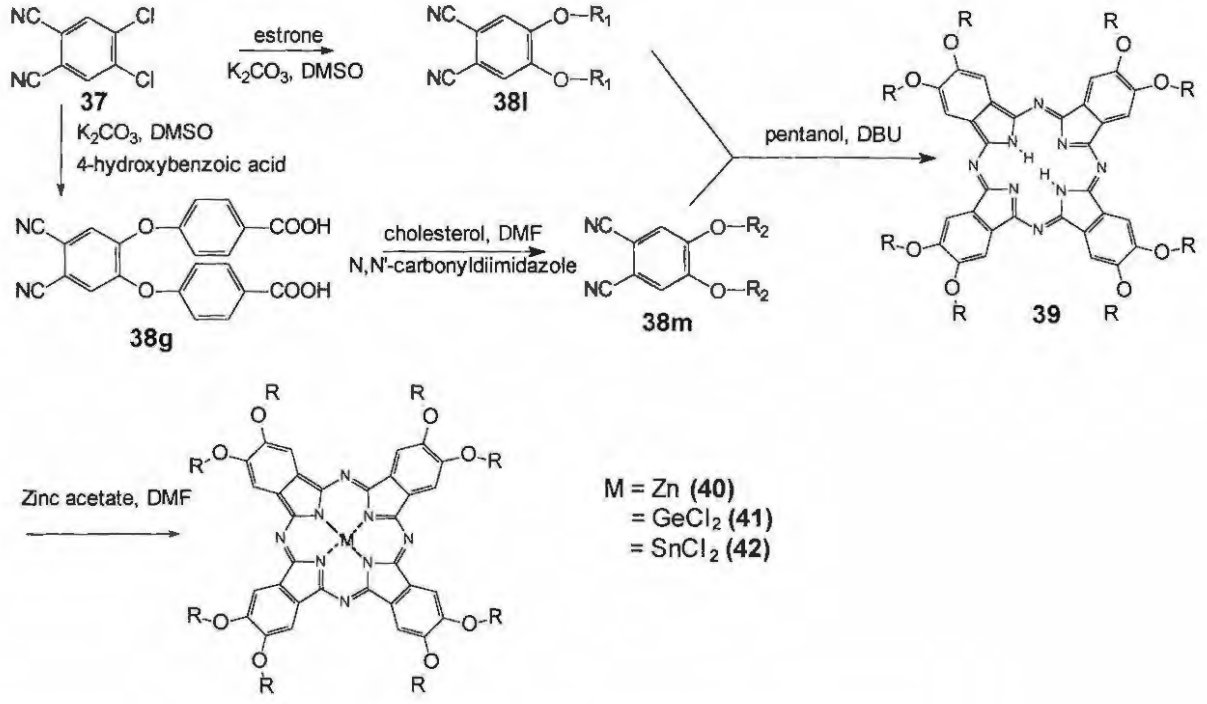

R	Abbreviation	Number
R_1 = 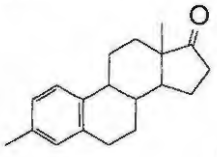 estrone	H_2OEPc ZnOEPc $Cl_2GeOEPc$ $Cl_2SnOEPc$	**39l** **40l** **41l** **42l**
R_2= 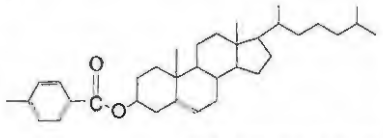 cholesterolester	$H_2OCholPc$ ZnOCholPc	**39m** **40m**

Scheme 2.11 Synthesis of octa(steroid)phthalocyanines.

The characteristic FTIR spectra (Figure 2.7) of 4,5-diestrone phthalonitrile (**38l**) and of H_2OEPc (**39l**) are shown and the strong C-H stretches are observed at about 2930 and 2850 cm^{-1} and the ketone carbonyl stretch at 1739 cm^{-1}. The disappearance of the C≡N stretch upon formation of the phthalocyanine is also indicated.

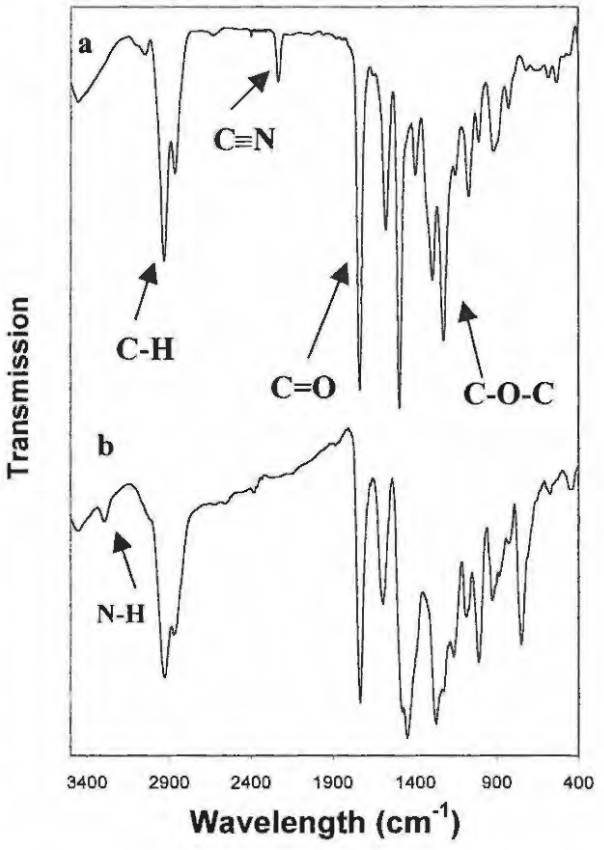

Figure 2.7 Mid IR spectrum of a) 4,5-diestrone phthalonitrile (**38l**) and b) metal-free octa(estrone) phthalocyanine (**39l**).

The ^{1}H NMR spectra of Cl_2GeOEPc and Cl_2SnOEPc are slightly better defined than the ZnOEPc due to the presence of the axially coordinated chloro ligands (Figure 2.8, p. 47). The UV/Vis spectra (Figure 2.9) shows monomeric behaviour and again the GePc and SnPc complexes show shifts to longer wavelengths compared to ZnPc complexes, Table 2.5.

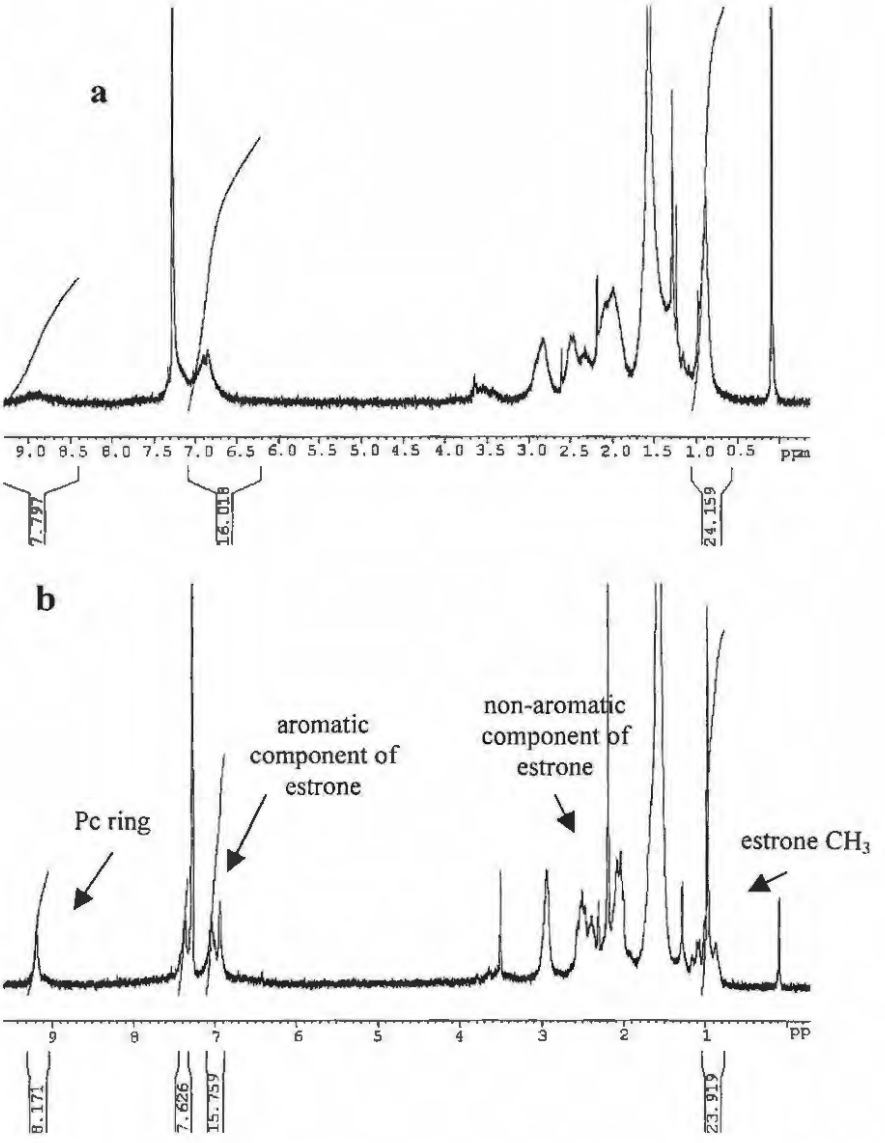

Figure 2.8 ^{1}H NMR of a) ZnOEPc (**40l**) and b) $Cl_2GeOEPc$ (**41l**). The $Cl_2GeOEPc$ shows more defined peaks indicating a lesser degree of aggregation due to the presence of the chloro axial ligand.

Low-density lipoproteins are one of the important factors involved in the selective accumulation of phthalocyanines in tumour tissues, because cancer cells generally express much more low-density lipoprotein receptors than normal cells.[51,52,53] The transport of the photosensitizer by low-density lipoproteins should enhance the selectivity of tumour loading. Thus substitution with cholesterol moieties at the phthalocyanine skeleton may encourage affinity to cancer cells. It has been found that Ge(IV)Pc bearing two axially

ligated cholesterol moieties incorporated into small unilamellar liposomes and injected into mice bearing an intramuscularly implanted fibrosarcoma, is quantitatively transferred to serum lipoproteins and localizes in the tumour tissue with good efficiency. Massive tumour necrosis involving both malignant cells and blood vessels occurred after irradiation.

Since cholesterol contains a non-aromatic alcohol group an intermediate 4,5-di(carboxyphenoxy) phthalonitrile (**38g**) was used to attach the cholesterol to the phthalocyanine ring . By stirring **38g** and the coupling reagent *N,N*-carbonyldiimidazole in DMF for 1 hour, **38g** was converted into a more reactive species and after adding the cholesterol, the formation of **38m** (Scheme 2.11) takes place with stirring at room temperature over 24 hours in 46% yield. The octa(cholesterolester)phthalocyanine (**39m**) may also be synthesized by coupling the cholesterol to the octa(carboxy-phenoxy)phthalocyanine (**39g**). Another synthetic route attempted was to prepare the acid chloride derivative from **39g** by reaction with thionyl chloride. The species formed in this way is highly reactive, but also poses a problem at the same time. The acid chloride is highly sensitive towards moisture and is easily partly, or completely, hydrolysed back to the carboxylic acid.

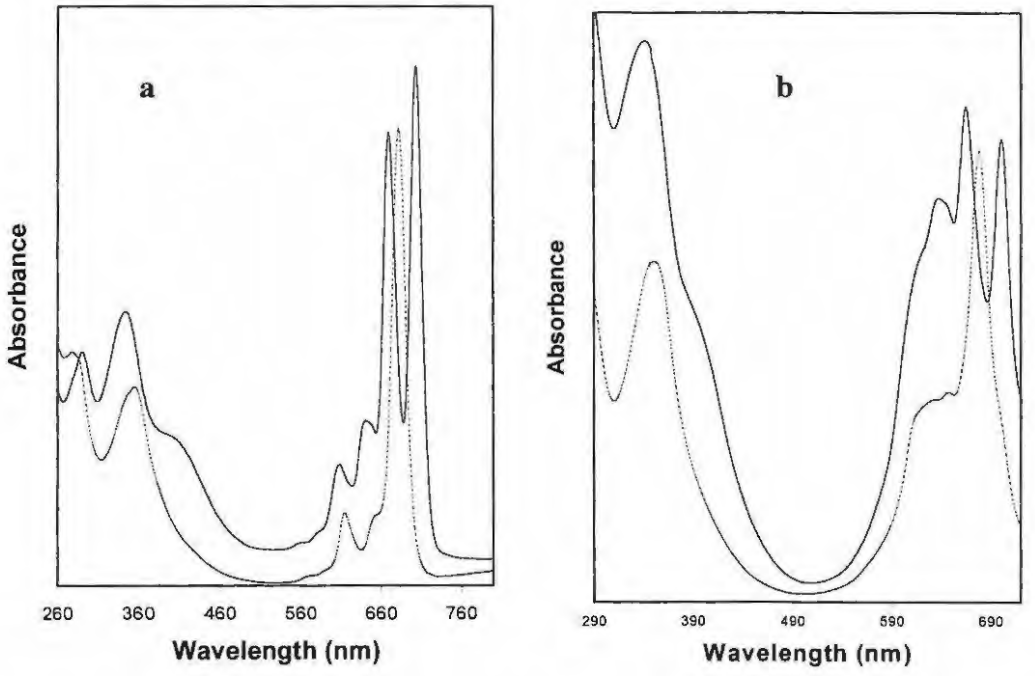

Figure 2.9 UV/Vis spectra of a) ZnOEPc (**40l**) (---) and H_2OEPc (**39l**) (solid), b) ZnOCholPc (**40m**) (---) and H_2OCholPc (**39m**) (solid) in chloroform.

H_2OCholPc (**39m**) was synthesized and metallated with zinc using the same method as described in Section 2.2.2. Compounds containing unreacted carboxylic groups were removed by thin layer chromatograpy using chloroform as eluent leaving the hydrogen bonded carboxy groups on the silica gel. ZnOCholPc (**40m**) shows excellent solubility in chloroform, but was not soluble in DMSO or DMF. This problem was overcome by dissolving ZnOCholPc (**40m**) in one or two drops of chloroform and then diluting with DMSO. The FTIR spectrum showed the distinct ester stretch at 1715 cm^{-1} and the ether stretches at 1272 and 1219 cm^{-1}. The UV/Visible spectrum (Figure 2.9) of H_2OCholPc (**39m**) showed a split Q-band at 700 and 664 and ZnOCholPc (**40m**) a single Q-band at 678 nm. UV/Visible data for all the octa(steroid)phthalocyanines are given in Table 2.4. The estrone containing complexes (**39l** and **40l**) are slightly more redshifted than the cholesterol containing complexes (**39m** and **40m**).

Table 2.5 UV/Visible data of octa(steroid)phthalocyanines.

Compound	UV/Vis, λ_{max}(log ε):
39l	704 (5.16), 669 (5.10), 641 (4.66), 607 (4.52), 401 (4.62), 344 (4.87), 290 (4.81)
40l	684 (4.71), 654 (3.94), 616 (3.94), 348 (4.25)
41l	692 (4.90), 662 (4.09), 622 (4.10), 364 (4.76), 347 (4.35), 296 (4.60)
42l	711 (5.13), 682 (4.13), 640 (4.34), 367 (3.75), 3.02 (2.38)
39m	700 (4.72), 664 (4.71), 636 (4.53), 612 (4.41), 399 (4.32), 345 (4.69).
40m	678 (4.89), 647 (4.53), 632 (4.54), 351 (4.77)

Although very good ^{1}H NMR data (Table 2.6) were obtained for the dicholesterolesterphthalonitrile (**38m**), only broad peaks were observed for H_2OCholPc (**39m**) and ZnOCholPc (**40t**) due to aggregation and the almost polymer-like nature of the complex (Figure 2.10). For **38m**, two doublets at 8.08 and 7.00 ppm integrating for two, were assigned to the protons of the linking phenoxy group and the singlet at 7.32 ppm integrating for two, to the benzene ring (Figure 2.10i). The proton on the cholesterol closest to the ester resonates at 5.42 ppm with an integral equavalent to two protons (two cholesterol groups) and the alkene protons resonate at 4.85 ppm as a multiplet integrating for two protons. The rest of the hydrogen atoms associated with the cholesterol moiety show resonances situated between 0.5 and 2.5 ppm and no further assignments were made due to the complexity of these resonances. The singlet ^{1}H NMR resonance normally observed at 9 ppm for the Pc ring is very weak due to aggregation, but the appropriate resonances from the phenoxy ester group were seen as two broad singlet resonances (typical of polymer-like molecules) integrating for 16 protons each at 8.0 and 6.92 ppm, respectively (Figure 2.10ii). The resonances due to the cholesterol is also situated between 0.5 and 2.5 ppm.

Table 2.6 Yields and spectral data of metallated octa(steroid)phthalocyanines (**40-42l, 40m**).

Compound	Yield	^{1}H NMR (400 MHz, $CDCl_3$)	FTIR (KBr)
40l	84	9.00 (s, 8H, CH-pc) 6.85 (broad s, 24H, CH-estrone) 1.75-3.10 (m, 120H, CH and CH_2 –estrone) 0.90 (s, 24H, CH_3)	2927, 2862 (C-H); 1736 (C=O); 1610; 1490; 1398; 1269,1222; 728
41l	63	9.17 (s, 8H, CH-pc) 7.38 (broad s, 8H, CH-estrone) 7.05 (broad s, 8H, CH-estrone) 6.94 (s, 8H, CH-estrone) 1.75-3.10 (m, 120H, CH and CH_2 –estrone) 0.90 (s, 24H, CH_3)	2923, 2855; 1738 (C=O); 1603, 1493; 1406; 1276, 1222; 733
42l	51	9.22 (s, 8H, CH-pc) 7.41 (broad s, 8H, CH-estrone) 7.07 (broad s, 8H, CH-estrone) 6.97 (s, 8H, CH-estrone) 3.00-1.60 (m, 120H, CH and CH_2 –estrone) 0.98 (s, 24H, CH_3)	2923, 2855; 1738 (C=O); 1603, 1493; 1390; 1276, 1222, 743
40m	84	8.00 (broad s, 16 H, 2',4'-H) 7.52 (broad-s, 8H, 3,6-Pc) 6.92 (broad-s, 16 H, 1',5'-H) 5.43 (s, 8H, CH-cholesterol) 4.84 (m, 8H, C=C-cholesterol), 0.80-2.60 (m, 290H, CH,CH_2, CH_3-cholesterol) 0.74 (s, 24H, CH_3-cholesterol).	2940, 2863 (C-H), 1716 (C=O), 1597, 1499 (CH,CH_2), 1453, 1270 (C-O-C), 1218, 759, 690, 621.

UNIVERSITY LIBRARY

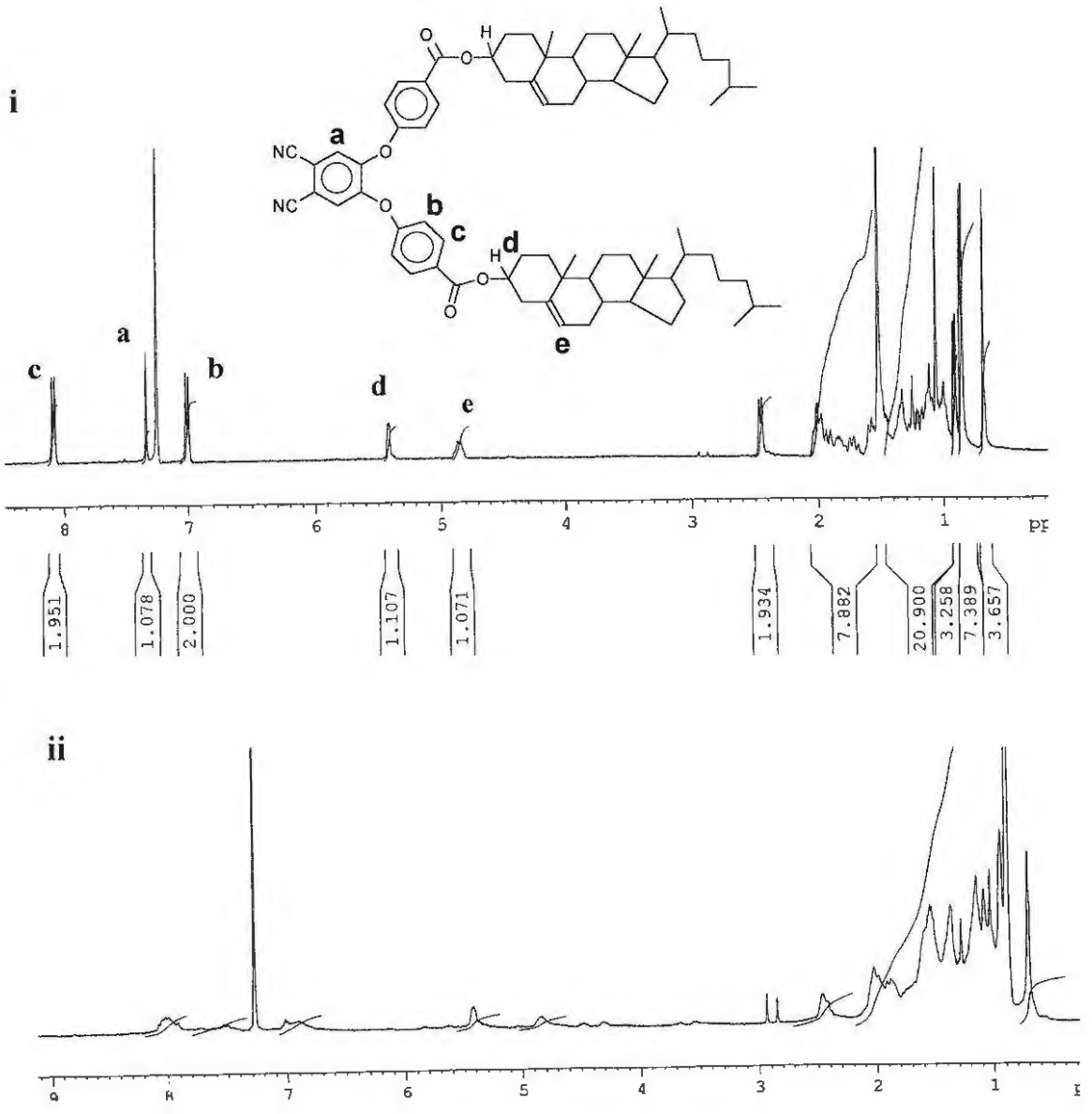

Figure 2.10 ^{1}H NMR of i) dicholesterolesterphthalonitrile (**38m**) and ii) ZnOCholPc (**40m**).

2.2.3.2 Synthesis of zinc tetra(steroid)phthalocyanines (Scheme 2.12)

It has been found that when 3-nitrophthalonitrile reacts with an alcohol or phenolic group of reasonable size, only a single isomer would be obtained when the phthalocyanine is formed. This is due to steric hindrance as was shown by Leznoff *et al.*[54] when 1,8,15,22-tetra-*p*-*n*-butylbenzyloxyphthalocyanine was synthesized as a single isomer in this manner.

Since estrone and cholesterol are relatively large molecules an attempt was made to synthesize the tetra substituted steroid derivatives in the same manner, hoping to obtain a single isomer (Scheme 2.12).

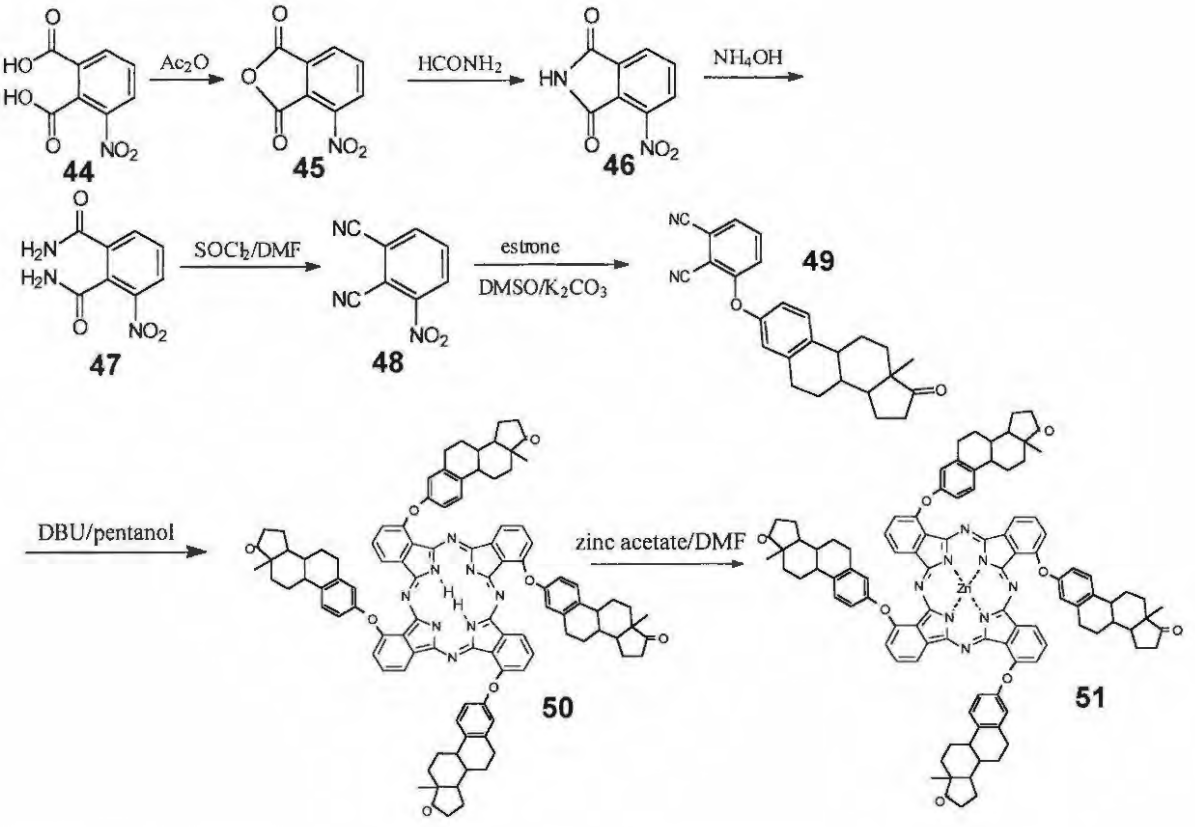

Scheme 2.12 Synthesis of zinc tetra (3-estrone) phthalocyanine (**51**).

The 3-nitrophthalonitrile (**48**) was synthesized by using the same method as described for the synthesis of 4,5-dichlorophthalonitrile (**37**). It was found that the 3-nitro derivatives are more unstable in comparison with the 4,5-dichloro derivatives. An overall lower yield (26%) for the synthesis of 3-nitrophthalonitrile (**48**) was obtained in comparison to that of 4,5-dichlorophthalonitrile (**37**) wich was synthesized in an overall yield of 45%. Special care should be taken in the first step, where the 3-nitrophthalic anhydride (**45**) is formed, to

remove all traces of acetic anhydride before proceding with the next step. If not, all product may be lost by polymerization of some kind.

By stirring estrone and 3-nitrophthalonitrile (**48**) in DMSO in the presence of K_2CO_3 at room temperature for 48 hours, 3-estrone phthalonitrile (**49**) was obtained in 71% yield. Phthalocyanine formation was attempted by using the Li-pentoxide method whereby the 3-estrone phthalonitrile was heated under reflux in a Li/pentanol mixture for 30 minutes. Unfortunately the carbonyl group on the estrone moiety was somehow reduced as its stretching frequency was no longer visible on the infrared spectrum. The DBU/pentanol method was therefore followed as was described for the octa (substituted phenoxy)phthalocyanines and shown in Scheme 2.12 and the tetra (3-estrone) phthalocyanine (**50**) was obtained in 25% yield after 24 hours of refluxing.

Unfortunately, ^{1}H NMR revealed more than one isomer (Figure 2.11). The rotation around the ether bond did not allow enough restriction for the formation of one isomer. A doublet and two triplets. each integrating for four protons, was expected for the Pc ring, but multiplets at 9.10, 8.55 and 7.90 ppm were observed instead. Since the isomers are only regio isomers, it was decided to continue studying the properties of this compound. Metallation was done with zinc as described in Section 2.2.2 to give **51**. Upon metallation the resonance at -0.4 ppm disappeared and is assigned to the N-H proton. An attempt was also made to synthesize the tetra (3-cholesterolester)phthalocyanine, but it appears that this group was too bulky to allow the Pc to form.

The infrared spectra of zinc tetra(estrone)phthalocyanine (**51**) appears similar to that of the zinc octa(estrone)phthalocyanine (**40l**) with the characteristic carbonyl, ether and C-H

stretches. The Q-band (698 nm) of **51** is red shifted by almost 15 nm in comparison with the other steroid containing phthalocyanines.

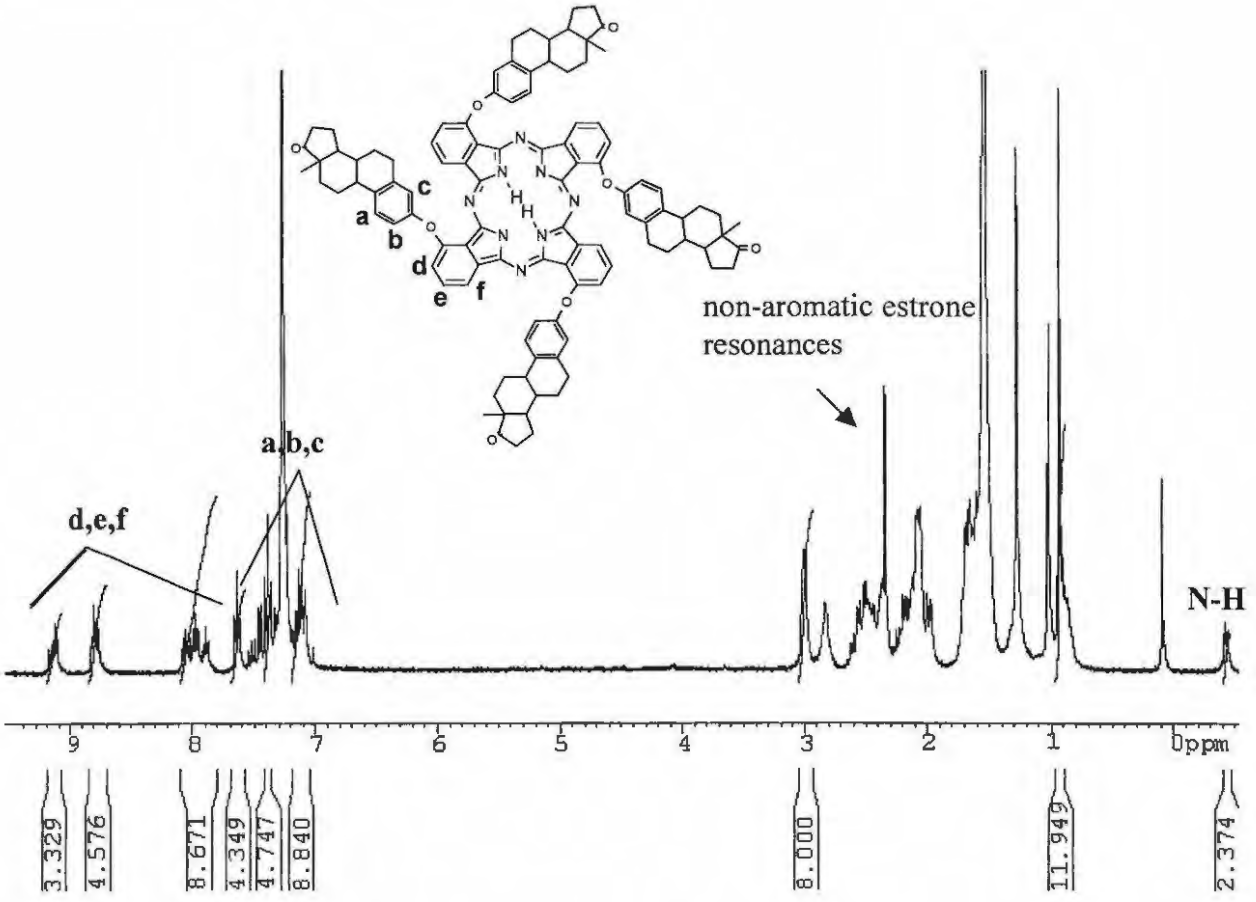

Figure 2.11 ^{1}H NMR of the tetra (3-estrone) phthalocyanine (**50**) showing the presence of several isomers through the presence of multiplets (d,e,f).

2.2.3.3 Synthesis of diestrone tin(IV)phthalocyanine (53) (Scheme 2.13)

The synthesis of the diestrone tin(IV) phthalocyanine ((estrone)$_2$SnPc, **53**) was more or less done according to the procedure that was described by Kenney *et al.*[55] where alcohols were reacted with Si(IV)Pc, Ge(IV)Pc and Sn(IV)Pc. Although it was claimed that axially substituted SnPc complexes are unstable, it was not found to be the case in the present

situation where the phenolic estrone moiety was attached to the central metal to form a stable ether bond.

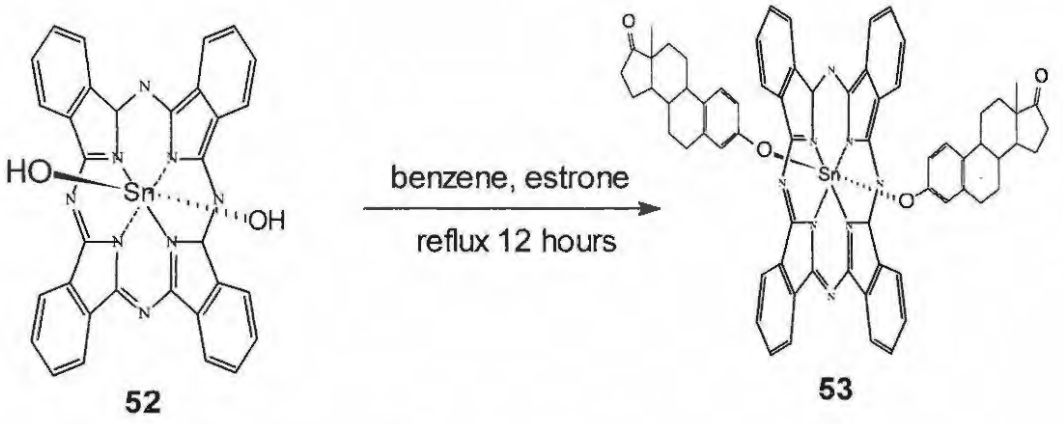

52 **53**

Scheme 2.13 Synthesis of $(estrone)_2SnPc$ (**53**).

The synthesis involves a condensation reaction between $(OH)_2Sn(IV)Pc$ (**52**) and estrone in benzene as solvent (Scheme 2.13). The solvent seems to be of importance since the same reaction was unsuccessful in solvents like DMSO or DMF and yielded an unknown purple product. The reaction time of 12 hours is also significantly longer than for the reaction with alcohols. The solubility of the product is significantly better than that of the dihydroxy tin(IV) phthalocyanine (**52**) due to the presence of estrone as an axial ligand, thereby preventing aggregation.

The ^1H NMR spectrum (Figure 2.12) also shows a curious, though not unexpected, phenomenon. It is noted that the aromatic protons of the estrone moiety are shielded quite substantially (2 ppm or more). This is due to the strong ring current effect of the phthalocyanine shielding the aromatic protons of estrone, indicating strongly that the estrone is co-ordinated on the axial position.

The UV/Visible data showed a strong absorbing Q-band at 692 nm.

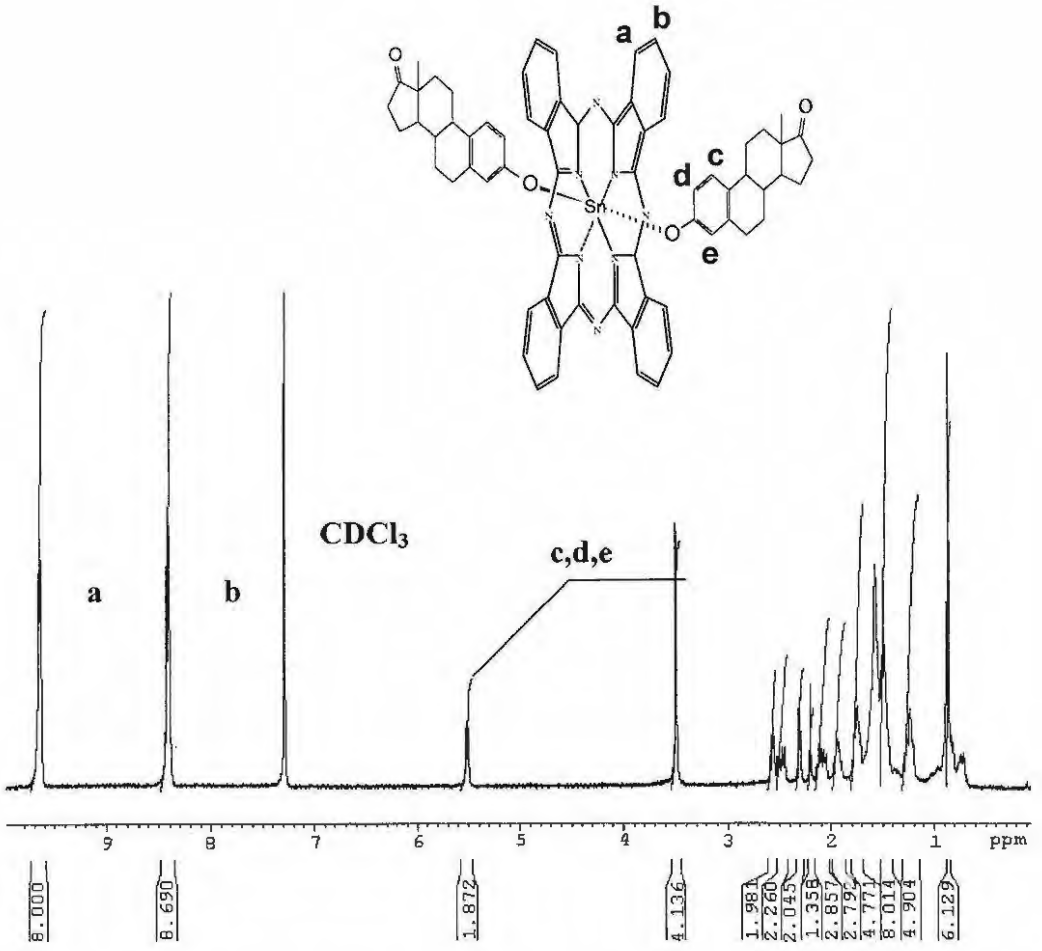

Figure 2.12 ^{1}H NMR of (estrone)$_2$SnPc (**53**).

2.3 Experimental

2.3.1 Materials

Dimethylsulphoxide (DMSO) and 1,8-diazabicyclo[5.4.0]undec-7-ene (DBU) were purchased from Sigma-Aldrich. Cholesterol, estrone, *N,N'*-carbonyldiimidazole as well as the phenol derivatives: phenol, 1-naphtol, *p*-cresol, *p-tert*-butylphenol, 2,4-*tert*-butylphenol, *p*-nitrophenol, *p*-aminophenol, 4-hydroxybenzaldehyde and 4-benzoic acid were purchased from Aldrich. DMSO was dried over alumina and chloroform freshly distilled before use.

2.3.2 Instrumental methods

The complexes were characterized by ^{1}H Nuclear Magnetic Resonance spectroscopy, UV/Visible spectroscopy, Fourier Transform Infrared (FTIR) and elemental analyses. ^{1}H NMR (400 MHz) were recorded using the Bruker EMX 400 NMR spectrometer in $CDCl_3$ or deuterated DMSO as indicated. UV/Visible spectra were recorded using a Varian 500 UV/Vis/NIR spectrophotometer and FTIR spectra (KBr pellets) recorded on a Perkin-Elmer spectrum 2000 FTIR spectrometer.

2.3.3 Synthesis

*2.3.3.1 Synthesis of 4,5-dichlorophthalonitrile (**37**) (Scheme 2.9, p. 34)*

*4,5-Dichlorophthalic anhydride[47] (**34**)*

A mixture of 4,5-dichlorophthalic acid (**33**) (13.5 g, 57.4 mmol) and acetic anhydride (23 ml) was heated under reflux for 5 hours. After cooling, the product (**34**) was filtered, washed with petroleum ether until all acetic anhydide was removed, and air-dried to yield 11.6 g of a white crystalline product (93%).

IR (KBr): ν = 3085 (C-H), 3022 (C-H), 1828 and 1781(anhydride)

*4,5-Dichlorophthalimide[47] (**35**)*

A suspension of 4,5-dichlorophthalic anhydride (**34**) (11.6 g, 51.5 mmol) in formamide (15 ml) was heated under reflux for 3 hours. After cooling the product (**35**) was filtered, washed with water and dried at 60°C to yield 11.0 g of a light yellow crystalline product (95%).

IR (KBr): ν = 3465 (N-H), 1775 and 1722 (imide)

*4,5-Dichlorophthalamide[47] (**36**)*

A suspension of 4,5-dichlorophthalimide (**35**) (11.0, 50.9 mmol) in 25% NH_4OH (150 ml) was stirred for 24 hours and then 33% NH_4OH (50 ml) was added and the stirring was continued for an additional 24 hours. The product (**36**) was filtered off, washed with water and dried at 60°C to yield 8.3 g of a white powder (71%).

IR (KBr): ν = 3420, 3305 and 3152 (N-H), 2794 (C-H), 1657 (C=O)

4,5-Dichlorophthalonitrile[47] *(37)*

Distilled $SOCl_2$ (29 ml) was added under stirring and nitrogen to dry dimethylformamide (42 ml) at 0°C. After two hours dry 4,5-dichlorophthalamide (**36**) (8.3 g, 35.6 mmol) was added and the mixture stirred at 0-5°C for 5 hours and then at room temperature for 24 hours. The product (**37**) was carefully added to ice water, filtered, washed with water and recrystallized from methanol to yield 4.9 g of a yellow crystalline product (72%).
IR (KBr): ν = 2229 (C≡N). ^{1}H NMR(360 MHz, $CDCl_3$): δ_H = 7.93 (s, 2H, CH)

2.3.3.2 *Synthesis of metal-free octa(substituted phenoxy)phthalocyanines*[47] *(39)* *(Scheme 2.10, p.34)*

4,5-Di(substituted phenoxy) phthalonitriles (38a-k)

A solution of the 4,5-dichlorophthalonitrile (**37**) (493 mg, 2.5 mmol) and phenol derivative (7.5 mmol) in dry DMSO (5 ml) was heated with stirring to 90°C under nitrogen. Dry finely, powdered K_2CO_3 (8 x 5 mmol every 5 minutes and 8 x 10 mmol every 5 minutes in the case of 4-hydroxybenzoic acid) was added. The mixture was stirred for an additional 3 hours and added to ice water (50 ml) thereafter. The precipitate was filtered off, washed thoroughly with water and recrystallized from methanol. Products that were not soluble in methanol were washed thoroughly with methanol and air-dried. In the case of 4,5-di(*p*-formyl phenoxy)phthalonitrile (**38j**) the product was extracted with acetone and separated

by TLC using chloroform as solvent and the first band was collected as the product. Spectral analysis data are shown in Table 2.7.

Table 2.7 Yields and spectral data of 4,5-di(substituted phenoxy)phthalonitriles (**38**).

Compound	Yield	^{1}H NMR ($CDCl_3$)	FTIR(KBr)
38a	62	7.36 (d, 4H, CH), 7.26 (d, 4H, CH), 7.01 (s, 2H, CH), 2.22 (s, 6H, CH_3)	2923, 2855 (C-H); 2229 (C≡N); 1575, 1494; 1394; 1292, 1220
38b	78	7.48 (d, 4H, CH-phenoxy) 7.16 (s, 4H, CH) 7.04 (d, 4 H, CH-phenoxy) 1.38 (s, 18 H, CH_3)	2955, 2870 (C-H); 2223 (C≡N); 1581, 1502; 1398; 1295, 1221
38c	56	7.51 (d, 2H, CH), 7.30 (dd, 2H, CH), 7.18 (s, 2H, CH), 6.82 (d, 2H, CH), 1.41 (s, 9H, CH_3), 1.39 (s, 9H, CH_3)	2954, 2870 (C-H); 2229 (C≡N), 1585, 1497; 1394; 1291, 1217
38e	62	7.48 (t, 2H, CH) 7.32 (d, 4H, CH) 7.20 (s, 2H, CH) 7.10 (d, 4H, CH)	2229 (C≡N); 1588, 1490; 1390; 1303 and 1209
38f	72	7.38-7.22 (m, 8H, CH), 7.3 (s, 2H, CH), 2.22 (s, 6H, CH_3)	2924, 2863, 2221 (C≡N), 1577, 1490, 1398, 1294, 1224
38g	74	8.09 (s, 2H, CH), 7.95 (d, 4H, CH), 7.15 (d, 4H, CH)	2229 (C≡N); 1685 (C=O), 1590, 1498; 1397; 1288, 1212
38h	63	8.37 (d, 4H, CH), 7.37 (s, 2H, CH), 7.17 (d, 4H, CH)	2229 (C≡N); 1516 (NO_2 asym.); 1482; 1346; 1341 (NO_2); 1272, 1214
38i	80	7.97 (d, 2H, CH), 7.92 (d, 2H, CH), 7.83 (d, 2H, CH), 7.55 (m, 4H, CH), 7.29 (s, 2H, CH), 7.26 (m, 4H, CH)	2230 (C≡N); 1583, 1503; 1397; 1294, 1213
38j	68	10.06(s, 2H, aldehyde), 8.04 (d, 4H, CH), 7.48 (s, 2H, CH), 7.21 (d, 4H, CH)	2229 (C≡N); 1697 (C=O); 1588, 1497; 1379; 1300, 1214
38k	70	7.42 (d, 4H, CH) 7.18 (s, 2H, CH) 7.03 (d, 4H, CH) 1.69 (m, 8H, CH_2) 1.34 (d, 2H, CH) 0.73 (t, 12H, CH_3)	2962, 2908, 2870 (C-H); 2222 (C≡N); 1580, 1501; 1398; 1295, 1219

*Metal-free octa(substituted phenoxy)phthalocyanines (**39a-c, e-k**)*

Di(substituted phenoxy)phthalonitrile (**38a-c, e-k**) (1 mmol) was heated under reflux in 1-pentanol (50 ml) in the presence of DBU (1 mmol and 3 mmol for the **38g**) for 16 hours. Methanol (50 ml) was added and the precipitate filtered off, washed with methanol and dried at 60°C. Elemental analysis data are shown in Table 2.8.

Table 2.8 Elemental analyses for metal-free octa(substituted phenoxy)phthalocyanines (**39a-k**)

Compound	Elemental analyses
39a	Anal. Calcd. for $C_{88}H_{66}N_8O_8$: C, 77.52; H, 4.88; N, 8.22. Found: C, 76.10; H, 4.68; N, 8.01.
39b	Anal. Calcd. for $C_{112}H_{114}N_8O_8$: C, 79.12; H, 6.76; N, 6.59. Found: C, 78.45; H, 6.73; N, 6.49
39c	Anal. Calcd. for $C_{144}H_{178}N_8O_8$: C, 80.48; H, 8.35; N, 5.21. Found: C, 78.60; H, 9.38; N, 4.28
39d	Anal. Calcd. for $C_{80}H_{58}N_{16}O_8$: C, 47.81; H, 34.67; N, 11.15. Found: C, 47.52; H, 34.85; N, 10.88
39f	Anal. Calcd. for $C_{88}H_{66}N_8O_8$: C, 77.52; H, 4.88; N, 8.22. Found: C, 76.90; H, 5.05; N, 8.16
39h	Anal. Calcd. for $C_{80}H_{42}N_{16}O_{24}.8H_2O$: C, 54.73; H, 3.33; N, 12.78. Found: C, 56.25; H, 1.96; N, 13.06
39i	Anal. Calcd. for $C_{88}H_{66}N_8O_8$: C, 81.44; H, 4.03; N, 6.78. Found: C, 80.13; H, 3.78; N, 6.51
39j	Anal. Calcd. for $C_{88}H_{50}N_8O_{16}.8H_2O$: C, 65.26; H, 4.10; N, 6.92. Found: C, 65.31; H, 3.63; N, 8.10
39k	Anal. Calcd. for $C_{120}H_{130}N_8O_8$: C, 79.53; H, 7.23; N, 6.18. Found: C, 79.66; H, 7.51; N, 6.09

Complexes **39e** and **39g** is not included in Table 2.8, since these complexes have already been characterized in the literature.[47]

*Octa(aminophenoxy)phthalocyanine **(39d)***[56]

Octa(p-nitrophenoxy)phthalocyanine (**39h**) (100 mg, 0.06 mmol) was finely ground and suspended in water (2 ml) containing sodium sulfide nonahydrate (264mg, 1.05 mmol) and the mixture was stirred at 50°C for 24 hours. The dark green product was separated by centrifugation and treated with 1 M hydrochloric acid (10 ml), then stirred in sodium hydroxide (10 ml) for 1 hour and centrifuged again. The product (**39d**) was washed with water (20 ml) and dried at 60°C overnight to yield 81 mg (95%).

*2.3.3.3 Synthesis of metallated octa(substituted phenoxy)phthalocyanines[47] **(40a-k, 41e-f, 42e-f, 43e)**(Scheme 2.10, p.34)*

*Zinc octa(substituted phenoxy)phthalocyanines **(40a-k)***

Metallation proceeded by adding zinc acetate (3 mmol) to a solution of the metal free phthalocyanine (**39a-k**) (1 mmol) in DMF (50 ml) and by refluxing until the split Q-band in the UV/Vis spectrum collapses to a single Q-band (~10 minutes for phenoxy groups with electron-donating substituents and ~20 minutes for those with electron-withdrawing groups). The products (**40a-k**) were centrifuged off after addition of water and washed with methanol/water (1:1) mixture. Spectral analysis data shown in Table 2.3, p. 40.

*Germanium(IV)octa(substituted phenoxy)phthalocyanines **(41e-f)***

A solution of $GeCl_4$ (5 mmol) and octa substituted phthalocyanine (**39e** or **39f**) (1 mmol) in freshly distilled quinoline (10 ml) was refluxed for 1hr or until the split Q-band collapses to one. Additional $GeCl_4$ (5 mmol) was added after 20 minutes. The mixture was cooled, chloroform added, the mixture filtered and the chloroform layer washed with 10 % HCl 5 x 30 ml and the solvent evaporated off. The solid was further washed with diethyl ether to remove remaining impurities and Soxhlet extracted with methanol (8 hours) and then acetone (8 hours). Spectral analysis data shown in Table 2.3, p. 40.

Tin(IV)octa(substituted phenoxy)phthalocyanines ***(42e-f)***

A solution of $SnCl_4$ or SnI_4* (5 mmol) and octa substituted phthalocyanine (**39e** or **39f**) (1 mmol) in 1-chloronaphtalene (10 ml) was heated at 190°C for 45 minutes or until the split Q-band collapses to a single Q-band. The mixture was cooled, hexane added, and the phthalocyanine filtered off. The 1-chloronaphthalene was removed by repetitively washing with diethyl ether until the 1-chloronaphthalene could no longer be detected. The phthalocyanine was dissolved in chloroform, filtered and the solvent removed under vacuum. The product was further Soxhlet extracted with methanol for 16 hours and then acetone 8 hours. Spectral analysis data shown in Table 2.3, p. 40.

*SnI_4 was synthesized[57] by gently heating tin metal (1.2 g) and I_2 (4.0 g) in CCl_4 (7.5 ml) until the reaction was initiated. The reaction was stopped as soon as all I_2 disappeared (colour change of violet to orange red and absence of iodine vapour). The reaction mixture was filtered quickly and the bright orange product allowed to crystallize out.

*2.3.3.4 Synthesis of metallated octa(estrone)phthalocyanines (**40l** and **41l**) (Scheme 2.11 p.45)*

*4,5-Di(estrone)phthalonitrile (**38l**)*

A solution of 4,5-dichlorophthalonitrile (**37**) (74 mg, 0.38 mmol) and estrone (400 mg, 1.48 mmol) in dry dimethylmethoxide (3 ml) was heated to 90°C under nitrogen. Eight portions of K_2CO_3 (53 mg, 0.38 mmol) were added at 5 minute intervals. The solution was stirred for another 3 hours, cooled, the product (**38l**) precipitated out with water, washed with water (3x50ml) and methanol (3x50 ml) and left to air dry, yielding 253 mg of a white powder (83%).

IR(KBr): ν = 2932 and 2854 (C-H), 2229 (C≡N), 1739 (C=O), 1579, 1497, 1394, 1291 and 1227 (C-O-C), 1150, 1070, 1006, 914, 891, 823.

^{1}H NMR (400 MHz, $CDCl_3$): δ_H = 7.41 (d, 2H, CH), 7.17 (s, 2H, CH), 6.91 (d, 2H, CH), 6.86 (d, 2H, CH), 1.45 – 3.05 (m, 30H, CH and CH_2), 0.98 (s, 6H, CH_3). Anal. Calcd for $C_{44}H_{44}N_2O_2$: C, 79.49, H, 6.67, N, 4.21. Found: C, 78.88, H, 6.84, N, 3.94.

*Metal-free octa(estrone)phthalocyanine (**39l**)*

A suspension of 4,5-di(estrone)phthalonitrile (**38l**) (100 mg, 0.151 mmol) and DBU (46 mg, 0.3 mmol) in pentanol (3 ml) was heated under reflux for 8 hours. The reaction mixture was allowed to cool and the product was isolated by additon of methanol (5 ml) and stirring for 15 min. and consequent centrifugation. Purification through column separation (neutral alumina, $CHCl_3$) yielded metal-free octa(estrone)phthalocyanine (**39l**) 80 mg (84%).

IR(KBr): ν = 3290 (N-H), 2927(C-H), 2862(C-H), 1736(C=O), 1596, 1478, 1449, 1274(C-O-C), 1227, 1166, 1086, 1010, 926, 880, 823, 749.

UV/Vis ($CHCl_3$): λ_{max} (log ε)= 704 (5.16), 669 (5.10), 641 (4.66), 607 (4.52), 401 (4.62), 344 (4.87), 290 (4.81).

^1H NMR (400 MHz, $CDCl_3$): δ = 0.90 (s, 26H, NH_2 and CH_3), 1.75 – 3.10 (m, 120H, CH and CH_2), 6.91 (s, 24H, CH (estrone)), 8.94 (s, 8H, CH).

Anal. Calcd for $C_{44}H_{44}N_2O_2$: C, 79.43, H 6.74, N, 4.21. Found C, 73.68, H, 6.33, N, 3.81.

Metallated octa(estrone)phthalocyanine ***(40-42l)***

Metallation proceeded as described in Section 2.3.3.3. Spectral analysis data are shown in Table 2.9.

Table 2.9 Yields and spectral data of metallated octa(estrone)phthalocyanines (**40-42l**).

Compound	Yield	^1H NMR (400 MHz, $CDCl_3$)	FTIR (KBr)
40l	84	9.00 (s, 8H, CH-pc) 6.85 (broad s, 24H, CH-estrone) 1.75-3.10 (m, 120H, CH and CH_2 –estrone) 0.90 (s, 24H, CH_3)	2927, 2862 (C-H); 1736 (C=O); 1610; 1490; 1398; 1269,1222; 728
41l	63	9.17 (s, 8H, CH-pc) 7.38 (broad s, 8H, CH-estrone) 7.05 (broad s, 8H, CH-estrone) 6.94 (s, 8H, CH-estrone) 1.75-3.10 (m, 120H, CH and CH_2 –estrone) 0.90 (s, 24H, CH_3)	2923, 2855; 1738 (C=O); 1603, 1493; 1406; 1276, 1222; 733
42l	51	9.22 (s, 8H, CH-pc) 7.41 (broad s, 8H, CH-estrone) 7.07 (broad s, 8H, CH-estrone) 6.97 (s, 8H, CH-estrone) 3.00-1.60 (m, 120H, CH and CH_2 –estrone) 0.98 (s, 24H, CH_3)	2923, 2855; 1738 (C=O); 1603, 1493; 1390; 1276, 1222, 743

*2.2.3.5 Synthesis of Zinc octa(cholesterolester)phthalocyanine (**40m**) (Scheme 2.11, p.45)*

*4,5-Di(cholesterolesterphenoxy) phthalonitrile (**38m**)*[58]

N,N'-carbonyldiimidazole (76 mg, 0.46 mmol) was added to a solution of the 4,5-di(carboxyphenoxy)phthalonitrile (**38g**) (100 mg, 0.46 mmol) in dry dimethylformamide (2 ml) and stirred under N_2 for 1 hour at 40°C. Cholesterol (387 mg, 1.0 mmol) and DBU (304 mg,2 mmol) was added and the reaction mixture was stirred at 40°C for 24 hours. The product (**38m**) was precipitated out by addition of water, centrifuged and purified by thin layer chromatography (eluent: chloroform, base: silica gel) to yield **38m** as a white powder (46%).

IR (KBr): 2940, 2865 (C-H), 1717 (C=O), 1588, 1502 (CH,CH_2), 1465, 1280 (C-O-C), 1219, 1162, 1114, 1014, 910.

^{1}H NMR (360 MHz, $CDCl_3$): 8.08 (d, 4 H, 2',4'-H) 7.32 (s, 2H, 3,6-H) 7.00 (d, 4 H, 1',5'-H) 5.42 (s, 2H, CH-cholesterol) 4.85 (m, 2H, C=C-cholesterol), 0.80-2.50 (m, 82 H, CH,CH_2, CH_3-cholesterol) 0.66 (s, 6H, CH_3-cholesterol).

Anal. Calcd for $C_{76}H_{96}N_2O_6$: C, 80.53, H, 8.54, N, 2.47. Found: C, 77.89, H, 8.66, N, 2.16.

*Metal-free octa(p-cholesterolesterphenoxy)phthalocyanine (**39m**)*

A suspension of 4,5-di(cholesterolester)phthalonitrile (**38m**) (50 mg, 0.044 mmol) and DBU (12 mg, 0.08 mmol) in pentan-1-ol was heated under reflux for 8 hours, cooled down, methanol added and the product (**39m**) centrifuged off and dried at 60°C to yield 24 mg (49%).

IR (KBr): 2938, 2865 (C-H), 1715 (C=O), 1600, 1501 (CH, CH_2), 1461, 1374, 1272 (C-O-C), 1219, 1162, 1110, 1008, 880, 849, 762.

UV/Vis ($CHCl_3$), λ_{max}(log ε): 700 (4.72), 664 (4.71), 636 (4.53), 612 (4.41), 399 (4.32), 345 (4.69).

^{1}H-NMR (400 MHz, $CDCl_3$): 8.01 (broad-s, 16 H, 2',4'-Pc) 7.52 (broad-s, 8H, 3,6-Pc) 6.95 (broad-s, 16 H, 1',5'-Pc) 5.41 (s, 8H, CH-cholesterol) 4.86 (m, 8H, C=C-cholesterol), 0.80-2.60 (m, 322 H, CH, CH_2, CH_3-cholesterol) 0.72 (s, 26H, NH-Pc and CH_3-cholesterol).

Anal. Calcd. $C_{304}H_{378}N_8O_{24}$: C, 80.67, H, 8.37, N, 2.47. Found: C, 78.82, H, 9.52, N, 2.22.

*Metallated octa(p-cholesterolesterphenoxy)phthalocyanine (**40m**)*

Metallation proceeded through heating under reflux octa(cholesterolester)phthalocyanine (**39m**) (20 mg, 0.0044mmol) with zinc acetate (5 mg, 0.04 mmol) in a DMF:chloroform (1 ml:3.5 ml) mixture for 1 hour* to yield 17 mg (84%) crude product (**40m**). Further purification was done by TLC seperation using chloroform as solvent.

IR (KBr): 2940, 2863 (C-H), 1716 (C=O), 1597, 1499 (CH,CH_2), 1453, 1270 (C-O-C), 1218, 1162, 1107, 1015, 883, 852, 759, 690, 621.

UV/Vis ($CHCl_3$), λ_{max}(log ε): 678 (4.89), 647 (4.53), 632 (4.54), 351 (4.77).

^{1}H-NMR (360 MHz, $CDCl_3$): 8.00 (broad s, 16 H, 2',4'-H) 7.52 (broad-s, 8H, 3,6-Pc) 6.92 (broad-s, 16 H, 1',5'-H) 5.43 (s, 8H, CH-cholesterol) 4.84 (m, 8H, C=C-cholesterol), 0.80-2.60 (m, 290H, CH,CH_2, CH_3-cholesterol) 0.74 (s, 24H, CH_3-cholesterol).

Anal. Calcd. $C_{304}H_{394}N_8O_{24}Zn$: C, 79.52, H, 8.25, N, 2.44. Found: C, 70.65, H, 8.78, N, 2.38.

*The reaction must be followed by UV/Vis spectra. The ratio of the two solvents must be such that the phthalocyanine is dissolved (chloroform) as well as the zinc acetate (DMF) and solvent may be added if metallation does not proceed. With the correct ratio metallation may proceed within 15 minutes. Alternatively 1-chloronaphtalene may be used as solvent but then soxhlet extraction with methanol for at least 8 hours in methanol and acetone will be necessary.

*2.3.3.6 Synthesis of zinc tetra(estrone)phthalocyanine (**51**)[59] (Scheme 2.12, p. 53)*

The same procedure was followed for the synthesis of 3-nitrophthalonitrile (**45**) as for the synthesis of 4,5-dichlorophthalonitrile (**37**) (Section 2.3.3.1 p. 59).

*3-Nitrophthalic anhydride (**45**)*

A mixture of 3-nitrophthalic acid (**44**) (13.5 g, 57.4 mmol) and acetic anhydride (23 ml) was heated under reflux for 5 hours. After cooling the product was filtered, washed with petroleum ether until all acetic anhydide was removed and air-dried to yield 11.6 g of a light yellow crystalline product (90%).

IR(KBR): ν = 1734 and 1699(anhydride) 1534 (NO_2 asym), 1349 (NO_2 sym).

*3-Nitrophthalimide (**46**)*

A suspension of 3-nitrophthalic anhydride (**45**) (11.6 g, 51.5 mmol) in formamide (15 ml) was heated under reflux for 3 hours. After cooling, 3-nitrophthalimide (**46**) was filtered off, washed with water and dried at 60°C to yield 11.0 g (90%).

IR(KBR): ν = 3465 (N-H), 1772 and 1730 (imide), 1538 (NO_2 asym), 1356 (NO_2 sym).

*3-Nitrophthalamide (**47**)*

A suspension of 3-nitrophthalimide (**46**) (11.0, 50.9 mmol) in 25% NH_4OH (150 ml) was stirred for 24 hours and then 33% NH_4OH (50 ml) was added and the stirring was continued for an additional 24 hours. The product was filtered off, washed with water and dried at 60°C to yield 8.3 g (42%).

IR(KBR): ν = 3420, 3335 and 3297 (N-H), 2794 (C-H), 1672 (C=O), 1541 (NO_2 asym), 1353 (NO_2 sym).

*3-Nitrophthalonitrile (**48**)*

Distilled $SOCl_2$ (29 ml) was aded under stirring and nitrogen to dry dimethylformamide (42 ml) at 0°C. After two hours dry 3-nitrophthalamide (**47**) (8.3 g, 35.6 mmol) was added and the mixture stirred at 0-5°C for 5 hours and then at room temperature for 24 hours. The product (**48**) was carefully added to ice water, filtered, washed with water and recrystallized from methanol to yield 4.9 g (76%).

IR(KBR): ν = 3081 (C-H), 2239 (C≡N), 1534 (NO_2 asym), 1349 (NO_2 sym)

*3-Estronephthalonitrile (**49**)*[54]

A mixture of 3-nitrophthalonitrile (**48**) (80 mg, 0.46 mmol), estrone (125 mg, 0.46 mmol) and dry K_2CO_3 (64 mg, 0.46 mmol) in dry DMSO (2 ml) was stirred under N_2 for 4 days. The product was precipitated out with water, filtered, washed with water and methanol and air dried to yield 146 mg of **49** (71 %).

IR(KBR): ν = 2924, 2863 (C-H), 2229 (C≡N), 1737 (C=O), 1490, 1459, 1272, 1215. ^{1}H-NMR (360 MHz, $CDCl_3$): 7.56 (t, 1H, CH-benzene) 7.45 (d, 1H, CH), 7.36 (d, 1H, CH) 6.9 (d, 1H, CH) 6.88 (s, 1H, CH) 3.00-1.40 (m, 16 H, estrone) 0.95 (s, 3H, CH_3-estrone)

*Metal-free tetra(estrone)phthalocyanine (**50**)*

The 3-estrone phthalonitrile (**49**) (395 mg, 1 mmol) was heated under reflux in 1-pentanol (50 ml) in the presence of DBU (150 mg, 1 mmol) for 24 hours. The reaction was cooled, methanol (50 ml) added and the precipitate filtered off, washed with methanol and dried at 60°C for 3 hours to give 99 mg of **50** (25%).

IR(KBR): ν = 2921, 2846, 1733, 1603, 1476, 1249, 747

*Zinc tetra(estrone)phthalocyanine (**51**)*

Metallation proceeded by stirring a mixture of tetra(estrone)phthalocyanine (**50**) (11 mg, 0.007 mmol) and zinc acetate (9 mg, 0.07 mmol) in DMF (1 ml) at 100°C for 10 minutes (until split Q-band formed one band), poured into water (3 ml) and the precipitate centrifuged off. The product (**51**) was washed with MeOH/water (1:1) solution (3x20 ml) and the product dried at 60°C for 3 hours to yield 10 mg (85%).

IR(KBR): ν = 2921, 2846, 1733 (C=O), 1603, 1476, 1249, 747

UV/Vis ($CHCl_3$), λ_{max}(log ε): 698 (5.13), 628 (4.67), 380 (4.70), 330 (4.85)

^{1}H-NMR (360 MHz, $CDCl_3$): 9.10 (m, 4H, CH-pc) 8.55 (m, 4H, CH-pc) 7.90 (m, 4H, CH-pc), 7.45 (m, 4H, CH-estrone) 7.18 (m, 4H, CH-estrone) 6.89 (d, 4H, CH-estrone) 0.8-3.1 (m, 84H, CH, CH_2, CH_3-estrone).

2.2.3.7 Synthesis of diestrone tin(IV)phthalocyanine (53)[60] (Scheme 2.13, p. 56)

A mixture of dihydroxy tin(IV)phthalocyanine (**52**) (100 mg, 0.19 mmol), estrone (200 mg, 0.76 mmol) and benzene (20 ml) was heated under reflux for 16 hours and the benzene evaporated off. The solid was Soxhlet extracted with methanol for 3 hours and dried at 60°C for 3 hours to yield 132 mg of **53** (89%).

IR(KBR): ν = 2923, 2854 (C-H), 1737 (C=O), 1462, 1339, 1283, 773, 746, 722.

UV/Vis ($CHCl_3$), λ_{max}(log ε): 692 (5.36), 660 (4.59), 624 (4.59), 356 (4.90), 338 (4.81), 292 (4.93)

^{1}H-NMR (360 MHz, $CDCl_3$): 9.64 (s, 8H, CH-pc) 8.42 (s, 8H, CH-pc) 5.53 (d, 2H, CH-estrone) 3.50 (s, 4H, CH-estrone) 2.50-1.10 (m, 34H, CH, CH_2-estrone), 0.92 (s, 6H, CH_3)

Anal. Calcd.: C, 74.97; H, 7.05; N, 13.99. Found: C, 74.83; H, 6.99; N, 13.87.

2.4 Conclusion

A series of octa substituted phthalocyanines has been synthesized in order to study the effect of different substituents on the photophysical, photochemical and electrochemical properties. The syntheses are easy and yield single isomers. A few steroid containing phthalocyanines have also been succesfully synthesized and may prove useful in tumour localization. Significant increase in solubility as well as a shift of the Q-band towards the infrared region have been observed.

2.5 References

1. A.B.P. Lever and C.C. Leznoff, *Phthalocyanines, Properties and Applications,* Eds., Vol.1, Chapter 1, VCH: New York, 1989
2. A. Braun and J. Tcherniac, *Ber. Deut. Chem. Ges.*, **40**, 2709 (1907)
3. P.A. Barret, C.E. Dent and R.P. Linstead, *J. Chem. Soc.,* 1719 (1936)
4. R.P. Linstead and A.R. Lowe, J. Chem. Soc., 1022 (1934)
5. H. Tomada, S. Saito and S. Shiraishi, *Chem. Lett.,* 1277 (1980)
6. H. Tomada, S. Saito and S. Shiraishi, *Chem. Lett.,* 313 (1983)
7. D. Wöhrle, G. Schnurpfeil and G. Knothe, *Dyes and Pigments,* **18**, 91 (1992)
8. A.W. Snow, J.R. Griffith and N.P. Marulla, *Macromolecules,* **17**, 1614 (1984)
9. U.S. Patent Appl. 768004 (1986); *Chem. Abstr.*, **105**, 145325f (1986)
10. P.J. Brach, S.J. Grammatica, O.A. Ossanna and L. Weinberger, *J. Heterocyclic Chem.*, **7**, 1403 (1970)
11. C.C. Leznoff, S.M Marcuccio, S. Greenberg, A.B.P. Lever and K.B. Tomer, *Can. J. Chem.*, **63**, 623 (1985)
12. W.A. Nevin, W. Liu, S. Greenberg, M.R. Hempstead, S.M. Marcuccio, M. Melnik, C.C. Leznoff and A.B.P. Lever, *Inorg. Chem.*, **26**, 891 (1987)
13. F.H. Moser, U.S. Patent 2,469,663 (1949)
14. F.H. Moser and A.L. Thomas, *Phthalocyanine Compounds*, Monograph No. 157, American Chemical Society, Washington, D.C., 44, 1963
15. F.S. Palmer and P.F. Gross, U.S. Patent 2,413,191 (1946)
16. J.A. Elvidge and R. P.Linstead, *J. Chem. Soc.*, 3536 (1955)
17. C.C. Leznoff and T.W. Hall, *Tet. Lett.*, **23**, 3023 (1982)
18. T.W. Hall, S. Greenberg, C.R. McArthur, B.Khouw and C.C. Leznoff, *Nouv. J. Chim.*, **6**, 653 (1982)
19. A. Meller and A.Ossko, *Monatsh. Chem.*, **103**, 150 (1972)
20. A. Weitemeyer, H. Kliesch and D. Wöhrle, *J. Org. Chem.*, **60**, 4900 (1995)
21. N. Kobayashi, R. Kondo, S. Nakajima and T. Osa, *J. Am. Chem. Soc.*, **112** 9640 (1990)
22. P.A. Barret, C.E. Dent and R.P. Linstead, *J. Chem. Soc.*,1719 (1936)
23. P.A. Barrett, D.A. Frye and R.P. Linstead, *J. Chem. Soc.*, 1157 (1938)
24. R.D. Joyner and M.E. Kenney, *J. Am. Chem. Soc.*, **82**, 5790 (1960)
25. R.G. Linck, J.N. Esposito and M.E. Kenney, *J. Inorg. Nucl. Chem.*, **24**, 299 (1962)

26. M.E. Kenney, *J. Inorg. Nucl. Chem.*, **28**, 899 (1966)
27. P.A. Barret, C.E. Dent and R.P. Linstead, *J. Chem. Soc.*, 1723 (1936)
28. P.A. Barret, C.E. Dent and R.P. Linstead, *J. Chem. Soc.*,1719 (1936)
29. W.J. Kroenke and M.E. Kenney, *Inorg. Chemistry*, **3**, 251 (1964)
30. M.E. Kenney, *J. Inorg. Nucl. Chem.*, **28**, 899 (1966)
31. C. Ungurenasu, *Synthesis*, **10**, 1729 (1999)
32. B.D. Rihter, M.E. Kenney, W.E. Ford and M.A.J. Ford, *J. Am. Chem. Soc.*,**112**, 8064 (1990)
33. M. Hanack, K. Mitulla, G. Pawlowski and L.R. Subramanian, *J. Organomet. Chem.*, **204**, 315 (1981)
34. H.-G. Capraro, K. Schieweck, R. Hilfiker, M. Ochsner, U. Isele, P. van Hoogevest, R. Naef and M. Baumann, *Proc. SPIE*, **2078**, 158 (1994)
35. V.F. Borodkin, *Zh. Prikl. Khim.*, **31**, 813 (1958); *J. Appl. Chem. USSR*, **31**, 803 (1958)
36. T.J. Hurley, M.A. Robinson and S.I. Trotz, *Inorg. Chem.*, **6**, 389 (1967)
37. S.W. Oliver and T.D. Smith, *J. Chem. Soc. Perkin Trans II*, 1579 (1987)
38. S. Basu, *Indian J. Phys.*, **28**, 511 (1954)
39. M. J. Stillman, and T. Nyokong in C. C. Leznoff and A. B. P. Lever (ed.) Phthalocyanines: Properties and applications, VCH, Volume 1, Chapter 3 (1998)
40. B. W. Dale, *Trans. Faraday Soc.*, **65**, 311 (1969)
41. M. J. Stillman, *Phthalocyanines: Properties and Applications*, Eds., C. C. Leznoff and A. B. P. Lever (eds), Vol.3, VCH, 1993: New York, Chapter 5.
42. A. B. P. Lever, M. R. Hempstead, C. C. Leznoff, W. Liu, M. Melnik, W. A. Nevin and P. Seymour, *Pure and Appl. Chem.*, **58**, 1467 (1986)
43. T. Nyokong, Z. Gasyna and M. J. Stillman, *J. Am. Chem. Soc.*, 309 (1986)
44. W.J. Kroenke and M. E. Kenney, *Inorg. Chem.*, **3**, 696 (1964)
45. A. N. Sidorov and I.P. Kotlyar, *Opt. I Spektr.*, **11**, 175 (1961)
46. W.J. Kroenke and M.E. Kenney, *Inorg. Chem.*, **3**, 697 (1964)
47. D. Wöhrle, M. Eskes, K. Shigehara and A. Yamada, *Synthesis*, 194 (1993)
48. M. Gouterman, *J. Chem. Phys.*, **30**, 1139 (1959)
49. W.J. Kroenke and M.E. Kenney, *Inorg. Chem.*, **3**, 696 (1964)
50. D.A. James, N. Swamy, N. Paz, R.N. Hanson and R. Ray, *Bioinorg. Med. Chem. Lett.*, **9**, 2379 (1999)

51. F. Gineva, S. Biffanti, A. Pagnan, R. Biolo, E. Reddo and G. Jori, *Cancer Let.*, **49**, 59 (1990)

52. C. Milanesi, F. Sorgoto and G. Jori, *British J. Cancer*, **61**, 846 (1990)

53. H. L. L. M. van Leengoed, V. Cuomo, A. A. C. Versteeg, N. Vanderveen, G. Jori and W. M. Star, *British J. Cancer*, **64**, 840 (1994)

54. C.C. Leznoff, M. Hu, C.R. McArthur and Y. Qin, *Can. J. Chem.*, **72**, 1990 (1994)

55. R. Rafaeloff, F.J. Kohl, P.C. Krueger and M.E. Kenney, *J. Inorg. Nucl. Chem.*,**28**, 899 (1966)

56. B.N. Achar, G.M. Fohlen, J.A. Parker and J. Keshavayya, *Polyhedron*, **6**, 1463 (1987)

57. T. Moeller and D.C. Edwards, *Inorg. Synth.*, Vol. IV, p. 120.

58. B.S. Furniss, A.J. Hannaford, P.W.G. Smith and A.R. Tatchell, *Vogel's Textbook of Practical Organic Chemistry,* 5th ed, Addison Westley Longman Limited, England, p. 1079-1080 (1989)

59. C.C. Leznoff, M. Hu, C.R. McArthur, Y. Qin and J.E. van Lier, *Can. J. Chem.*, **72**, 1990 (1994)

60. M.E. Kenney, *J. Inorg. Nucl. Chem.*, **28**, 901 (1966)

Chapter 3
Photophysical and Photochemical Properties

-Chapter 3-

3.1 Introduction

The potency of a drug in photodynamic therapy is determined by its ability to produce a photocytotoxic species, namely singlet oxygen on interaction with light. The ability to produce singlet oxygen is measured as the singlet oxygen quantum yield (Φ_Δ). This is, however, not the single important property that needs to be investigated. Photochemical studies also usually reveal the stability of compounds when exposed to light. Photostability is important when it comes to storage lifetime of these potential medical drugs, in other words whether these drugs will show the same consistency after a certain period of time or whether certain precautions should be taken in order to preserve the drug against light. When it comes to *in vivo* considerations, photostability may be just as important. Drugs used in photodynamic therapy (PDT) do not localise 100% in tumour cells and lower concentrations are present in normal cells. Thus, if light is shone through tissue, destruction of normal cells may occur. However, at low concentrations photodegradation of the drug may occur even before significant damage of the normal cells occurs.

In this study the aim was to investigate the effect of peripheral substituents with different electronegativities, as well as axial ligands on the photochemical and photophysical properties of phthalocyanines. The effect of bio-active substituents on the properties of phthalocyanines was also investigated. Photophysical properties include triplet and fluorescence lifetimes and quantum yields, and photochemical properties including the study of the photodegradation of these complexes as well as singlet oxygen quantum yields.

A brief discussion on photodynamic therapy and the theory behind the photophysics and photochemistry follow.

3.1.1 Photodynamic therapy

Figure 3.1 shows the Jablonski diagram[1] which shows that after a photon is absorbed by the sensitiser in its ground state, a short-lived electronically excited singlet species is formed (Equation 3.1).

$$P + h\nu \rightarrow {}^1P^* + h\nu \rightarrow {}^3P^* \qquad \text{.....(3.1)}$$

where P is the sensitizer.

The excited species will relax back to the ground state or convert to the triplet state through any of the following processes:

1. Radiative transitions including fluorescence, delayed fluorescence or phosphorescence
2. Radiationless transitions through internal conversion or intersystem crossing which involves the conversion of the singlet spin state to the triplet state. The triplet state has a relatively long lifetime (microseconds to milliseconds) and favours bimolecular processes
3. Vibrational relaxation, energy transfer or quenching

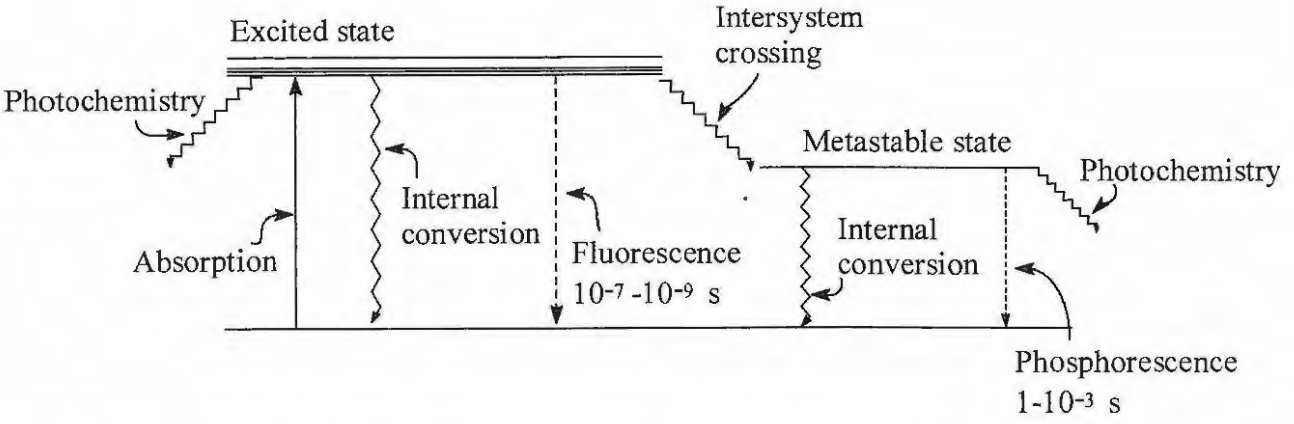

Figure 3.1 Jablonski diagram.

These processes are in competition with one another and depending on the magnitudes of the rate constants, e.g. if the rate constant of fluorescence is smaller than the radiotionless deactivation, the excited species will be depleted predominantly by the radiationless route and fluorescence will be weak or not detectable.

The sensitiser readily transfers its energy to ground-state molecular oxygen to produce singlet oxygen that may react with the substrate. Oxygen is unique in that its ground state is the triplet state. The energy required for the singlet to triplet transition being 22 kcal mol^{-1}, that is 1274 nm in terms of wavelength.[2]

Ground state oxygen has two unpaired electrons in the antibonding orbitals (Figure 3.2). In the presence of a magnetic field three separate electronic configurations for the two unpaired electrons can be distinguished, that is, both spins up, both spins down or one up and one down.[3] This is why the ground state of oxygen is called the triplet state

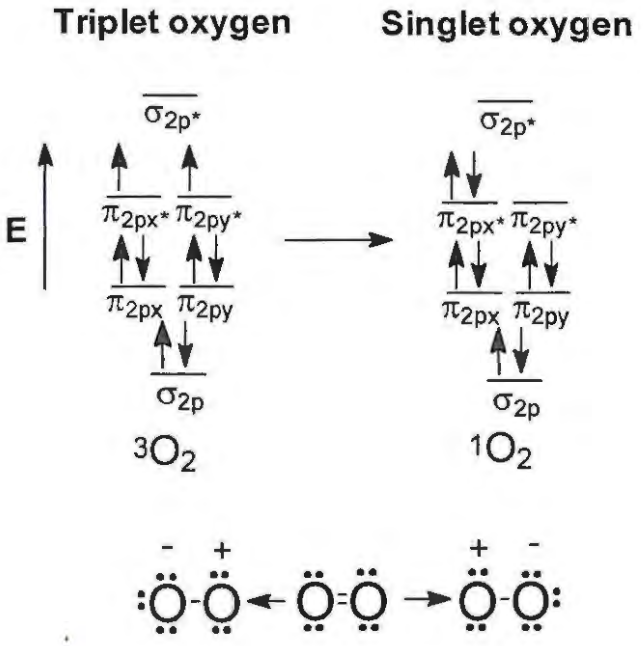

Figure 3.2 Molecular orbital diagrams with the electron distribution in triplet (left) and singlet (right) oxygen. At the bottom the zwitterionic character of oxygen is depicted.[5]

Pairing of two electrons into the π^*_{2p} antibonding orbital, due to interaction with the sensitiser, renders the singlet oxygen extremely reactive due to the destabilization of the molecule. Singlet oxygen has a lifetime of $4x10^{-6}$ s in water, $50\text{-}100x10^{-6}$ s in lipids and $0.6x10^{-6}$ s in cellular environment. The short lifetime in water is explained by the fact that the stretching energy of oxygen-hydrogen is approximately the same as the excited state energies of the singlet oxygen. The reaction sphere of this species has a limited radius of less than 0.02 μm.[5]

Two proposed mechanisms exists for cell destruction. Type II reactions are dependent on oxygen concentrations and are intermediated by the already discussed singlet oxygen (Equations 3.2 to 3.4). [4,5]

Type II:

$$P \xrightarrow{h\nu} {}^1P^* \xrightarrow{ISC} {}^3P^* \quad \text{.....(3.2)}$$

$${}^3P^* + {}^3O_2 \rightarrow P + {}^1O_2 \quad \text{.....(3.3)}$$

$${}^1O_2 + S \rightarrow \text{tumour necroses} \quad \text{.....(3.4)}$$

where P is the photosensitizer, S the substrate and ISC intersystem crossing.

In the Type I (Equations 3.5 to 3.10) mechanism the excited sensitizer may react directly with the targetted biomolecules in close proximity through electron exchange in anoxic (oxygen poor) environments, thereby producing an oxidized substrate and reduced sensitizer. The oxidized substrates or radicals and peroxides then cause tumour necrosis.

Type I:

$${}^3P^* + O_2 \rightarrow P^{+\cdot} + O_2^{-\cdot} \quad \text{.....(3.5)}$$

$${}^3P^* + S \rightarrow Pc^{-\cdot} + S^{+\cdot} \quad \text{.....(3.6)}$$

$$P^{-\cdot} + O_2 \rightarrow P + O_2^{-\cdot} \quad \text{.....(3.7)}$$

$$O_2^{-\cdot} \xrightarrow{H^+} HO_2^{\cdot} \quad \text{.....(3.8)}$$

$$HO_2^{\cdot} + S\text{-}H \rightarrow H_2O_2 + S^{\cdot} \quad \text{.....(3.9)}$$

$$S^{\cdot+}, S^{\cdot}, H_2O_2 \rightarrow \text{tumour necrosis} \quad \text{.....(3.10)}$$

Depending on the oxygen concentration as well as the direct environment of these sensitisers, both Type I and Type II mechanisms may occur simultaneously. Type II is reported to dominate during PDT.[6] Foote[7] suggested that Type II may become predominant under hypoxic (oxygen rich) conditions and high concentrations of the

sensitizer. Cells containing less than 5% oxygen show resistance to PDT and the use of a lower fluence rate during treatment may enhance tissue destruction.[8,9]

Proteins and unsaturated lipids containing double bonds are very susceptible to attack by singlet oxygen due to the presence of double bonds. The imidazole- and indole-containing amino acids, namely histidine and tryptophan, react with $^1O_2$ to produce endoperoxides that subsequently release hydroxyl radicals. These radicals may further react with cellular components. Sulfur-containing amino acids, such as methionine, are oxidised by $^1O_2$ to sulfoxides. The hydroxyl radicals ($OH^{\cdot}$) are considered as the most toxic oxygen species and readily reacts with most molecules.[10] The reactivity of the superoxide radical ion ($O_2^{\cdot-}$) depends on the environment in which it is formed. In aqueous solution, Equation 3.11 occurs:

$$O_2^{\cdot-} + H_2O \leftrightarrow HO_2^{\cdot} + OH^- \qquad .....(3.11)$$

with $pk_a \sim 4.8$ and $pH = pk_a + \log\frac{[O_2^{\cdot-}]}{[HO_2^{\cdot}]}$. In the pH range 6.5 - 8 (physiological range) the ratio of the superoxide radical ion to the hydroxyl radical is approximately 100:1 and therefore the superoxide radical ion is mainly the reactive species. However, at the membrane surface a drop in pH is observed due to the negative charge and more of the reactive hydroxyl species would be present.

The catalytic nature of these sensitizers is appreciated when it is realised that following the transfer of the photosensitizer's energy to molecular oxygen, the former returns to its electronic ground state and provided that sufficient oxygen is available, singlet oxygen is

produced several times from the same concentration of the sensitizer. With time, singlet oxygen may react with and degrade the sensitizer.

3.1.1.1 Equations for the determination of singlet oxygen quantum yields

Photochemistry may be defined as chemical transformations or reactions that take place as a response to the activation of a molecule by light. As was discussed before, a triplet excited state of the sensitizer is the reactive species. The efficiency of the sensitizer is expressed in quantum yield, that is, the number of molecules of interest formed for each photon of light absorbed. A variety of methods for the determination of quantum yields have been developed and described.[11,12,13,14]

The singlet oxygen quantum yield for this study was determined by allowing a quencher to react with singlet oxygen (Φ_Δ) as soon as it was produced. 1,3-Diphenylisobenzofurane (DPBF) was chosen since its disappearance is easily followed by its decrease in absorption maxima at 416 nm. The disappearance of this peak is related to the singlet oxygen quantum yield in the following ways:

$$O_2(^1\Delta_g) \xrightarrow{k_d} O_2\,(^3\Sigma_g) \qquad \text{(Natural decay)} \qquad \text{.....(3.12)}$$

$$O_2(^1\Delta_g) + \text{DPBF} \xrightarrow{k_q} \text{Oxidation products} \qquad \text{(Chemical quenching)} \qquad \text{.....(3.13)}$$

$$O_2(^1\Delta_g) + \text{DPBF} \xrightarrow{k_p} O_2\,(^3\Sigma_g) + \text{DPBF} \qquad \text{(Physical quenching)} \qquad \text{.....(3.14)}$$

$$\text{MPc} + O_2(^1\Delta_g) \rightarrow O_2\,(^3\Sigma_g) + \text{MPc} \qquad \text{(Physical quenching)} \qquad \text{.....(3.15)}$$

$$\text{MPc} + O_2(^1\Delta_g) \rightarrow \text{Chemical reaction} \qquad \text{(Chemical quenching)} \qquad \text{.....(3.16)}$$

Equation 3.14 is not important and can be ignored since DPBF acts exclusively as a chemical quencher in organic solvents.[15,16] Singlet oxygen quantum yield does not depend on the sensitizer concentration and therefore physical quenching through Equation 3.15 may be ignored. Furthermore, the reaction rate of the sensitizer with the singlet oxygen (Equation 3.16) is negligible compared to its rate of the reaction with the DPBF. Therefore it is only Equations 3.12 and 3.13 that are relevant to the decay of $O_2(^1\Delta_g)$. The rate of disappearance of DPBF in the presence of singlet oxygen is given by Equation 3.17:

$$-\frac{[DPBF]}{dt} = k_q[DPBF][O_2(^1\Delta g)] \qquad .....(3.17)$$

Application of the steady state approximation for $O_2(^1\Delta_g)$ and rearranging gives Equation 3.18:

$$O_2(^1\Delta g) = \frac{\Phi_\Delta I_{abs}}{k_q[DPBF] + k_d} \qquad .....(3.18)$$

Substitution of Equation 3.18 in 3.17 gives 3.19:

$$\frac{-[DPBF]}{dt} = \frac{k_q\Phi_\Delta I_{abs}[DPBF]}{k_d + k_q[DPBF]} \qquad .....(3.19)$$

where I_{abs} the amount of light absorbed by the sensitizer and Φ_Δ the singlet oxygen quantum yield. Since

$$\Phi_{DPBF} = \frac{\frac{-d[DPBF]}{dt}}{I_{abs}} \qquad \text{.....(3.20)}$$

subtitution of 3.20 into 3.19 gives Equation 3.21

$$\Phi_{DPBF} = \frac{k_q \Phi_\Delta [DPBF]}{k_d + k_q[DPBF]} \qquad \text{.....(3.21)}$$

At low DPBF concentrations, $k_d >> k_q[DPBF]$ and Equation 3.21 becomes Equation 3.22

$$\Phi_{DPBF} = \frac{k_q \Phi_\Delta [DPBF]}{k_d} \qquad \text{.....(3.22)}$$

The reaction kinetics are first order at these low DPBF concentrations, whereas at high DPBF concentrations a zero-order law is obeyed which means that the reaction rate becomes independent of the concentration of the DPBF. This is not desired in this situation and therefore a low DPBF concentration was employed. Equation 3.22 may be written as Equation 3.23 for the MPc complexes under study

$$\Phi_{DPBF}^{MPc} = \Phi_\Delta^{MPc} \frac{k_q}{k_d} [DPBF]^{MPc} \qquad \text{.....(3.23)}$$

where Φ_{DPBF}^{MPc} represents the quantum yield for DPBF in the presence of the phthalocyanine (MPc), $\Phi_\Delta{}^{MPc}$ is the singlet oxygen quantum yield in the presence of MPc

and $[DPBF]^{MPc}$ is the concentration of DPBF in the presence of MPc. ZnPc was employed as a standard and Equation 3.22 may be written as Equation 3.24

$$\Phi_{DPBF}^{ZnPc} = \Phi_{\Delta}^{ZnPc} \frac{k_q}{k_d} [DPBF]^{ZnPc} \quad \text{.....(3.24)}$$

Where Φ_{DPBF}^{ZnPc} is the quantum yield of DPBF in the presence of ZnPc and Φ_{Δ}^{ZnPc} the singlet oxygen quantum yield of ZnPc and $[DPBF]^{ZnPc}$ is the concentration of DPBF in the presence of ZnPc.

Using the ratio of Equation 3.23 over Equation 3.24, the Φ_{Δ} of the unknown MPc can be determined using Equation 3.25

$$\Phi_{\Delta}^{MPc} = \Phi_{\Delta}^{ZnPc} \times \frac{\Phi_{DPBF}^{MPc}}{\Phi_{DPBF}^{ZnPc}} \times \frac{[DPBF]^{ZnPc}}{[DPBF]^{MPc}} \quad \text{.....(3.25)}$$

Φ_{DPBF} may be defined by the known Equation 3.26:

$$\Phi_{DPBF} = \frac{(C_o - C_t)V}{I_{abs} \times t} \quad \text{.....(3.26)}$$

Where V is the sample volume, t the photolysis time, C_o the initial concentration and C_t the concentration after photolysis time t. I_{abs} is the absorbed light and is determine by Equation 3.27

$$I_{abs} = \frac{\alpha S I}{N_a} \qquad \text{.....(3.27)}$$

where S is the irradiated cell area, I the light intensity, N_a Avogadro's number and α the fraction of light absorbed. The following Equation is then obtained by substituting Equation 3.27 into 3.26 and then 3.26 into 3.25:

$$\Phi_{\Delta}^{MPc} = \Phi_{\Delta}^{ZnPc} \times \frac{(C_o - C_t)^{MPc}}{(C_o - C_t)^{ZnPc}} \times \frac{(\alpha\, t)^{ZnPc}}{(\alpha\, t)^{MPc}} \times \frac{[DPBF]^{ZnPc}}{[DPBF]^{MPc}} \qquad \text{.....(3.28)}$$

Where $(C_o-C_t)^{MPc}$ and $(C_o-C_t)^{ZnPc}$ are the changes in DPBF concentration in the presence of MPc and ZnPc respectively. The photolyses time in the presence of ZnPc and MPc are given by t^{ZnPc} and t^{MPc} respectively. S,V and N_a cancel out since they are the same for both MPc and ZnPc as I also cancels out if the same interference filter is used. α is calculated from experimental data and will be discussed in the Experimental section.

3.1.1.2 Equations for the determination of photodegradation quantum yields

Photodegradation quantum yields (Φ_D) are calculated by Equation 3.29, similar to Equation 3.26:

$$\Phi_D = \frac{(C_o - C_t)V}{I_{abs} \times t} \qquad \text{.....(3.29)}$$

with V the sample volume, t irradiation time, C_o the initial phthalocyanine concentration and C_t the phthalocyanine concentration after irradiation time t. I_{abs} is the absorbed light and is determined by Equation 3.27 above.

First order kinetics apply to only the first 15% of the bleaching process and therefore C_o and C_t should be taken at 0% and about 10% bleaching, respectively for accurate results. Knowing the extinction coefficients and the absorbance, the concentrations may be obtained from Beer's law using $A = \varepsilon\ c\ l$ with ε the extinction coefficient, c the concentration and l the pathlength of the cell.

3.1.1.3 Equations for the determination of triplet quantum yields and triplet lifetimes

Triplet lifetimes

Deactivation of the triplet state, ^3M, to the ground state, S_0, can be described by the following Equation 3.30:[17]

$$\frac{-d[^3M]}{dt} = k_1[^3M] + k_2[^3M][S_0] + 2k_3[^3M]^2 \qquad \text{.....(3.30)}$$

where k_1 is the measured first order rate constant and is the sum of the radiative and non-radiative unimolecular decay processes. In most cases, for molecules in solution, the radiative process from the triplet state, i.e. phosphorescence, is negligible. The second term in the equation is due to quenching of the excited triplet state by ground state molecules, i.e. self-quenching and the final term is due to quenching of the triplet by another triplet

state i.e. triplet-triplet annihilation. At low sensitizer concentrations and low laser powers, only the first term in the equation is important and the rate constant k_1 is obtained from a first-order plot i.e. $\ln\frac{[^3M]_0}{[^3M]_t}$ *vs* t from $\ln\frac{[^3M]_0}{[^3M]_t} = k_1 t$ where $[^3M]_0$ and $[^3M]$ are the triplet concentrations at time zero and t respectively. The change in triplet concentration with time is directly proportional to the transmittance and thus the voltage change measured on the oscilloscope. Thus the change in absorbance, ΔA, can be calculated using the Beer-Lambert law, Equation 3.31:

$$\Delta A = \varepsilon \Delta c l = \ln \frac{I_0}{I} = \ln \frac{V\infty}{V\infty - \Delta V} \qquad \text{.....(3.31)}$$

where l = 1cm pathlength, V_∞ is the 0 – 100% voltage and ΔV is the change in voltage observed. A linear plot of ln(A) versus time thus gives a gradient k_1 and its reciprocal the triplet lifetime, $\tau_t = 1/k_1$.

Triplet quantum yields

Triplet extinction coefficients, ε_t, were determined by the singlet depletion method.[18] The phthalocyanine triplet state (max ~ 490nm) does not absorb in the same region as the ground state (max ~680nm) and thus Equation 3.32 applies:

$$\varepsilon_t = \frac{(\Delta A)_{490}\,\varepsilon_s}{(\Delta A)_{680}} \qquad \text{.....(3.32)}$$

Triplet quantum yields were determined by the relative method, [29] using zinc phthalocyanine as a standard (ZnPc = 0.25 in DMSO[19]) with Equation 3.33:

$$\Phi_x = \frac{\Phi_{st}(\Delta A\}_x \varepsilon_{st}}{(\Delta A)_{st} \varepsilon_x} \qquad \text{.....(3.33)}$$

Where Φ_X and Φ_{st} are the triplet quantum yields for the sample and the standard, respectively. $(A)_x$ and $(A)_{st}$ and ε_x and ε_{st} are the triplet absorbances and the triplet extinction coefficients of the unknown and standard respectively.

3.1.1.4 Equations for the determination of fluorescence quantum yields and fluorescence lifetimes

Fluorescence lifetimes

If a first order radiative process is experimentally observed, it may be assumed that no other decay process exists but that which is being studied. The electronically excited species will thus decay radiatively to the ground state and the process may therefore be formulated as in Equations 3.34 and 3.35:

$$\frac{d[M^*]}{dt} = -A_{u1}[M^*] \qquad \text{.....(3.34)}$$

$$\therefore [M^*] = M_o * e^{-A_{u1}t} \qquad \text{.....(3.35)}$$

where A_{u1} is the Einstein coefficient, which is the number of times per second that an excited state emits a photon. The radiative lifetime is defined by Equation 3.36:

$$\tau_0 = \frac{1}{A_{u1}} \qquad \text{.....(3.36)}$$

which is the time taken to diminish the population to 1/e of its initial concentration. This first order exponential decay may be recorded by a pulsed laser able to pulse at picosecond (ps) intervals.[20] The lifetime is important because it determines the time available for the fluorophore to interact with or diffuse in its environment.

The most important application that has arisen from the fluorescence of phthalocyanines and porphyrins is the imaging of tumour tissue as tumours are slightly more selective to these macrocycles. Fluorescence lifetimes for phthalocyanine compounds typically range from 1 to 7 ns.[21]

Fluorescence quantum yields

Fluorescence quantum yields, that is, the number of emitted photons relative to the number of absorbed photons, may be determined by a relative method using a reference material. Compounds that have known fluorescence quantum yields in specific solvents such as ZnPc in DMSO (Φ_F = 0.18[19]) may be used for comparitive determinations. These measurements involve the absorption spectra as well as the emission spectra of a sample wherein the optical density is less than 0.1. Low concentrations are essential to avoid

quenching. The fluorescence quantum yields may thus be determined using Equation 3.37 (derived in the same manner as for the singlet oxygen quantum yields):

$$\Phi_F = \Phi_{F(std)} \frac{Area_s . A_{std} . \eta_s^2}{Area_{std} . A_s . \eta_{std}^2} \quad \text{.....(3.37)}$$

Where $Area_s$ and $Area_{std}$ is the respective areas of the sample and standard (determined by simply adding up the relative emission of the Q-band and its vibrational bands.) A_s and A_{std} are the absorptions at the respective excitation wavelengths of the sample and standard. Different excitation wavelengths may be used for excitation. η_s and η_{std} are the refractive indexes of the solvents used for the sample and standard, respectively.

3.2 Results and discussion

3.2.1 Photochemistry

3.2.1.1 Singlet oxygen quantum yields (Φ_Δ)

Zinc phthalocyanine complexes

In the determination of singlet oxygen quantum yields (Φ_Δ), the decay of DPBF in the presence of the photosensitizer is monitored upon irradiation with light. The intensity of the light is low enough so the phthalocyanine remains unaffected as can be seen in Figure 3.3. Equation 3.28 was used in calculating the singlet oxygen quantum yields.

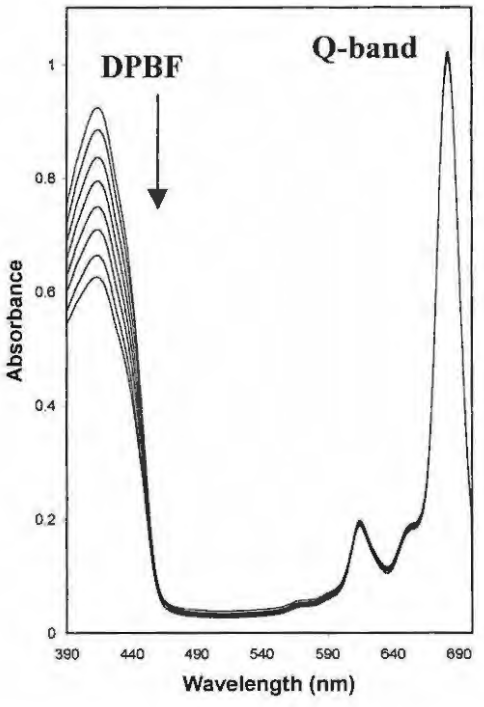

Figure 3.3 Singlet oxygen determinations of zinc octa(phenoxy)phthalocyanine (**40e**) showing the decrease in the DPBF while the Q-band of the phthalocyanine remains constant.

It can be seen in Table 3.1 that the ZnPc complexes containing more electron-donating (e.g. **40a-c**, **40f**, **40k** and **40m**) groups tend to have higher singlet oxygen quantum yields (0.44 - 0.73) whereas the opposite is true for the more electron-withdrawing (**40h**, **40j**, **40g**) groups (<0.44). There are so many factors involved that may influence the Φ_Δ of these compounds, for example aggregation, but it seems that the group electronegativities are significantly predominant in this situation. It appears that group electronegativities are related to the wavelength of the Q-band, since longer wavelengths are observed for complexes with more electron-donating groups and *vice versa*. Figure 3.4 shows the relation of wavelength of the Q-band *vs* Φ_Δ (therefore group electronegativities *vs* Φ_Δ) to be exponential.

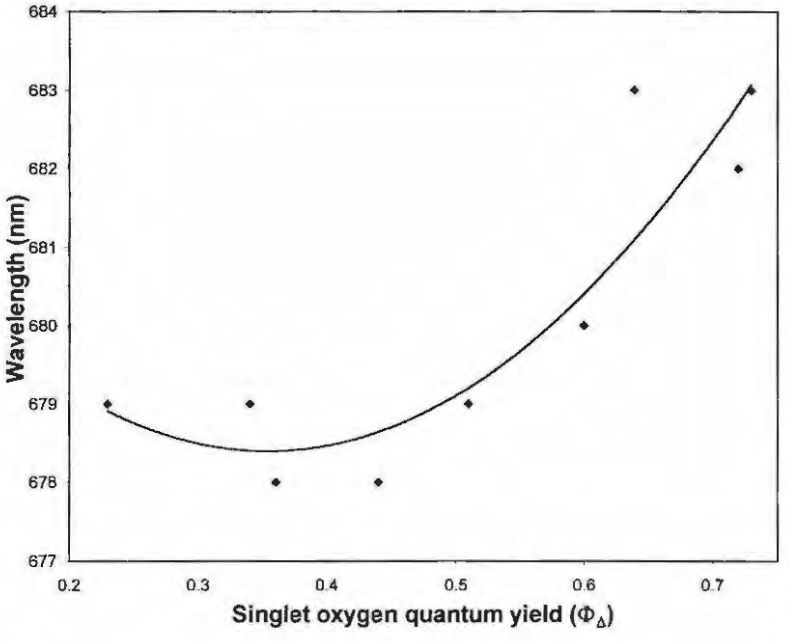

Figure 3.4 Graph of wavelength versus singlet oxygen quantum yield (Φ_Δ).

The exceptions are ZnOAPPc (**40d**) due to its radical scavenging properties and the highly aggregated ZnONaphPc (**40i**). The ZnODTBPPc (**40c**) was very unstable and even at lower light intensities the Q-band decreased as the DPBF decreased. Since part of the light

energy is used for degrading **40c** a lower than expected singlet oxygen quantum yield is obtained.

It is also interesting to note that because the ZnPc complex containing the phenoxy group with the methyl group in the *orto*-position (**40a**) is more soluble than the methyl group in the *para*-position (**40f**), a significant Φ_Δ difference of 0.21 is observed. The difference may also be attributed to the substituent in the *ortho*-position having a stronger influence on the properties of the Pc.

Table 3.1 Singlet oxygen quantum yields (Φ_Δ) using chloroform as solvent unless indicated otherwise.

Compound	**singlet oxygen quantum yields** (Φ_Δ)
ZnOpMPPc (**40a**)	0.51
ZnOTBPPc (**40b**)	0.73
ZnODTBPPc (**40c**)	0.44
ZnOAPPc (**40d**)	0.07[a]
ZnOPPc (**40e**)	0.60[a]
ZnOMPPc (**40f**)	0.72
ZnOCPPc (**40g**)	0.23[a]
ZnONPPc (**40h**)	0.36[a]
ZnONaphPc (**40i**)	0.01
ZnOAldPPc (**40j**)	0.34[a]
ZnOAmPPc (**40k**)	0.46
Cl_2GeOPPc (**41e**)	0.18
Cl_2GeOMPPc (**41f**)	0.24
Cl_2SnOPPc (**42e**)	0.22
I_2SnOPPc (**43e**)	0.29
Cl_2SnOMPPc (**42f**)	0.34
ZnOEPc (**40l**)	0.64
Cl_2GeOEPc (**41l**)	0.18
Cl_2SnOEPc (**42l**)	0.23
ZnOCholPc (**40m**)	0.44
Zn(estrone)$_4$Pc (**51**)	0.64
(estrone)$_2$SnPc (**53**)	0.22
Cl_2SnPc	0.37
Cl_2SiOPPc	0.14

[a] DMSO used as solvent.

The zinc tetra(3-estrone)phthalocyanine (**51**) gave approximately the same Φ_Δ (0.64) value as for the zinc octa(estrone)phthalocyanine (**40l**) but shows the advantage of being redshifted by about 15 nm. ZnOCholPc (**40m**) shows satisfactory Φ_Δ (0.44) in spite of being strongly aggregated.

Germanium and Tin phthalocyanine complexes

The ZnPc complexes in general gave higher singlet oxygen quantum yields than the Ge(IV)Pc and Sn(IV)Pc complexes. The synthesized germanium and tin phthalocyanine complexes discussed in this work all contain axial ligands, which prevent aggregation. Thus, other factors such as the lifetime and quantum yields of the excited states, as well as the photostability of the complexes, will predominate in determining the magnitudes of the Φ_Δ values. Table 3.1 shows the Φ_Δ of the germanium and tin octaphenoxy phthalocyanine complexes. Complexes containing the phenoxy group substituted with the *o*-methyl phenoxy group (**41f** and **42f**), show a slightly higher Φ_Δ values than Cl_2GeOPPc (**41e**) and Cl_2SnOPPc (**42e**) respectively. When Φ_Δ of Cl_2GeOPPc (**41e**) and Cl_2SnOPPc (**42e**) complexes are compared with the corresponding silicon complex (Cl_2SiOPPc) from the literature ($\Phi_\Delta = 0.14$)[22] in Table 3.1, it is seen that the Φ_Δ increases with increase in the size of the central metal as follows: Si(IV)<Ge(IV)<Sn(IV). This is explained by the heavy atom effect as follows:[23] singlet to triplet state transitions are forbidden but still occur due to spin-orbit coupling. Electrons have spin angular moments as well as magnetic moments. A change in the direction of magnetic moment of an electron is therefore observed during a singlet to triplet conversion, since the electron changes its spin. Magnetic interaction which is provided by the magnetic field produced by the orbital motion of the charged electron becomes inevitable and the magnetic moment of the

spinning electron becomes coupled to the orbital magnetic field. Thus the $Cl_2SnOPPc$ (**42e**) has a larger Φ_Δ value than the less heavy $Cl_2GeOPPc$ (**41e**) which in turn has a larger Φ_Δ than the lighter $Cl_2SiOPPc$. Comparison between $Cl_2SnOPPc$ (**42e**) and $I_2SnOPPc$ (**43e**) shows that a higher Φ_Δ value is observed for the latter. The heavier iodide ion will give larger triplet state quantum yield, resulting in larger Φ_Δ values.

Comparing unsubstituted phthalocyanine ring with the octaphenoxy substituted ring, and considering the same axial ligands and central metal ion, e.g comparing $Cl_2SnOPPc$ (**42e**) with Cl_2SnPc, shows that much larger Φ_Δ values (Φ_Δ = 0.37) are obtained for the unsubstituted ring than for the substituted ring (Φ_Δ = 0.22). The former are more soluble than the latter, based on this fact alone higher Φ_Δ values would be expected for the $Cl_2SnOPPc$ (**42e**) compared to the Cl_2SnPc complex. The observation of a lower Φ_Δ value for the $Cl_2SnOPPc$ (**42e**) species suggests that some quenching of the excited state in the presence of the phenoxy groups may occur. The $(estrone)_2SnPc$ (**53**) complex gave a Φ_Δ value (Φ_Δ = 0.22) that is much lower than that obtained in the presence of the chloride axial ligands in Cl_2SnPc (Φ_Δ = 0.37). There does not seem to be much difference in the Φ_Δ values when estrone in located on the axial position compared to when it is located as a substituent for the phenoxy groups located on the phthalocyanine ring (e.g. comples **53** and **42l**).

3.2.1.2 Photodegradation

Zinc phthalocyanine complexes

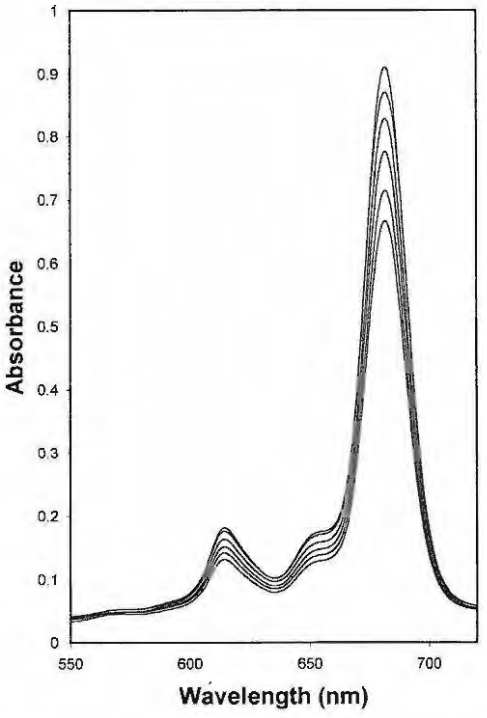

Figure 3.5 Photodegradation spectrum of zinc octa(phenoxy)phthalocyanine (**40e**).

Photobleaching or photodegradation is a process whereby conjugated chromophore structure of the phthalocyanine ring degrates. Typical photodegradation behaviour of ZnPc complexes in the presence of light is shown in Figure 3.5. Phthalocyanines often cause their own degradation in the presence of light having high intensity. These potent complexes produce radicals (for example singlet oxygen) that will destroy the phthalocyanine molecule by a mechanism proposed by Schnurpfeil *et al.* (Figure 3.6).[24] This mechanism suggests singlet oxygen cycloaddition to phthalocyanine pyrrole units resulting in the macrocycle destruction and formation of phthalimide. Photodegradation studies are therefore undertaken to study the behaviour of phthalocyanines in the presence of light and to determine how stable they are. Their stabilities are expressed as

photodegradation quantum yields (quantum cm^{-2} s^{-1}), which is an indication of how many molecules are degraded per quantum light. The photodegradation quantum yields were determined using Equation 3.29.

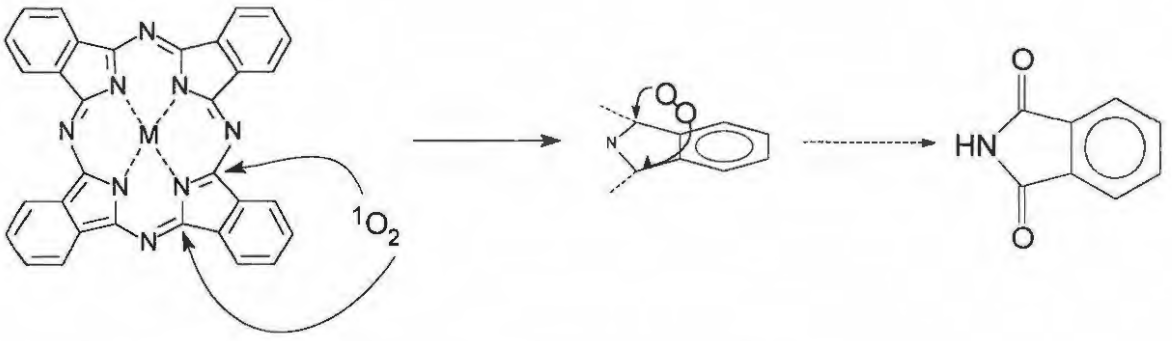

Figure 3.6 Proposed mechanism for photodegradation.[24]

It was observed that the complexes containing substituents that have more of an electron-withdrawing character (e.g. **40d**, **40e**, **40g**, **40h**, **40j**) tend to stabilise the phthalocyanine molecule in the presence of light with photodegradation quantum yields (Φ_D) in the order of 10^{-5}-10^{-6} quantum cm^{-2} s^{-1}. Lower stability was found for the more electron-donating groups (e.g. **40a-c**, **40f**, **40k**) with Φ_D in the order of 10^{-3} quantum cm^{-2} s^{-1}. Complexes with higher stability (**40d**, **40g**, **40h**, **40j**) are those with lower singlet oxygen quantum yields and those with lower stability (e.g. **40a-c**, **40f**, **40k**) have higher singlet oxygen quantum yields. This gives an indication that singlet oxygen may indeed be involved in the photodegradation of the phthalocyanine complexes. The ZnOAPPc (**40d**) shows relatively high stability of 10^{-6} quantum cm^{-2} s^{-1} and is explained by the singlet oxygen quenching abilities of the amino groups.

Table 3.2 Photodegradation quantum yields.

Compound	Photobleaching quantum yield (quantum cm^{-2} s^{-1})
ZnOpMPPc (**40a**)	$2.12x10^{-5}$
ZnOTBPPc (**40b**)	$4.64x10^{-3}$
ZnODTBPPc (**40c**)	$7.66x10^{-3}$
ZnOAPPc (**40d**)	$8.58x10^{-6}$
ZnOPPc (**40e**)	$2.53x10^{-5}$
ZnOMPPc (**40f**)	$4.81x10^{-3}$
ZnOCPPc (**40g**)	$2.36x10^{-6}$
ZnONPPc (**40h**)	$1.41x10^{-5}$
ZnONaphPc (**40i**)	$2.53x10^{-3}$
ZnOAldPPc (**40j**)	$5.04x10^{-5}$
ZnOAmPPc (**40k**)	$1.98x10^{-3}$
ZnOEPc (**40l**)	$2.75x10^{-5}$
ZnOCholPc (**40m**)	$1.11x10^{-3}$
$Zn(estrone)_4Pc$ (**51**)	$2.60x10^{-6}$

The involvement of singlet oxygen in the photodegradation process was further confirmed by performing the photodegradation experiments in deuterated solvents. It is known that singlet oxygen has a longer lifetime in deuterated solvents and will therefore react with the phthalocyanine to a greater extent. An increased rate of degradation in deuterated DMSO indicative of the involvement of singlet oxygen, was observed. When diazabicyclooctane (DABCO) a singlet oxygen scavenger, was added, a decreased rate was observed (Figure 3.7).

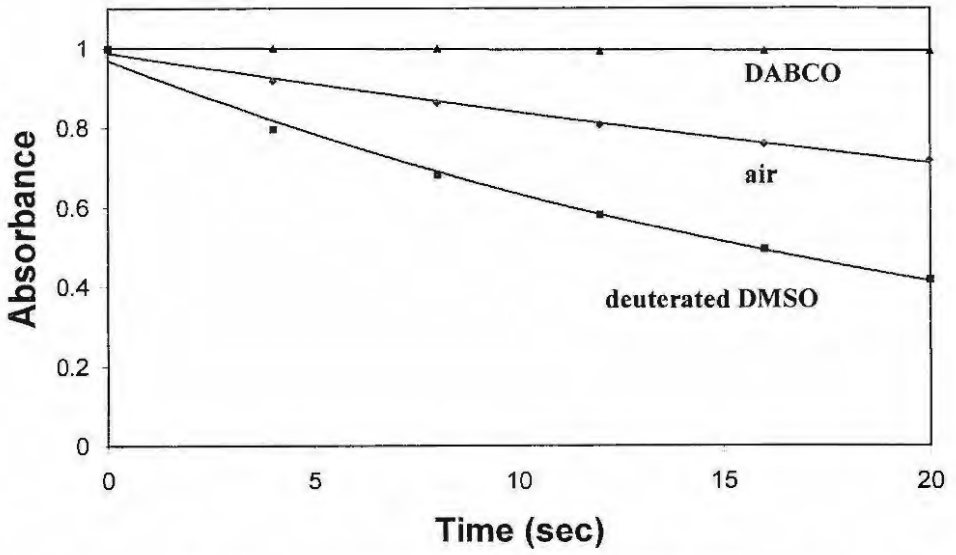

Figure 3.7 Effects of DABCO, air saturated DMSO and deuterated DMSO on the singlet oxygen production of zinc octa(estrone)phthalocyanine (**40l**).

The relatively high stability of the zinc octa(carboxyphenoxy)phthalocyanine (**40g**) may also be partly explained by the fact that the phthalocyanine exists as an aggregate in DMSO that is observed as a broadened peak with a broad shoulder at about 692 nm. Upon irradiation some of the light energy is used in what is thought to be disaggregation following with photodegradation (Figure 3.8).

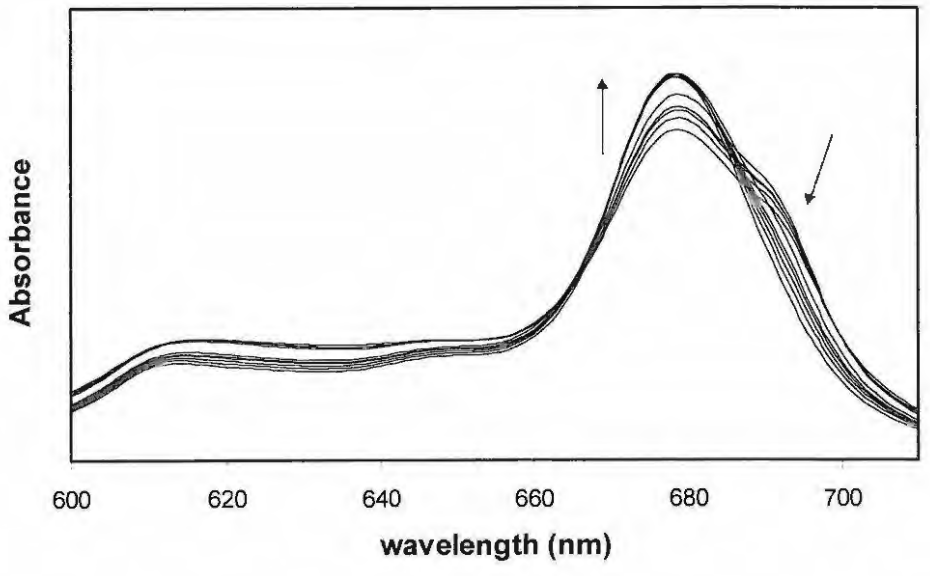

Figure 3.8 Disaggregation of zinc octa(carboxyphenoxy)phthalocyanine (**40g**) upon irradiation.

Zinc tetra(3-estrone)phthalocyanine (**51**) shows the highest stability of all the biologically active ZnPc complexes (Φ_D= 2.6x10^{-6} quantum cm^{-2}s^{-1}) with ZnOEPc (**40l**) and ZnOCholPc (**40m**) having Φ_D in the order of 10^{-3} quantum cm^{-2}s^{-1}.

Germanium and tin phthalocyanine complexes

Upon photobleaching of the GePc complexes a phototransformation is observed (Figure 3.9).

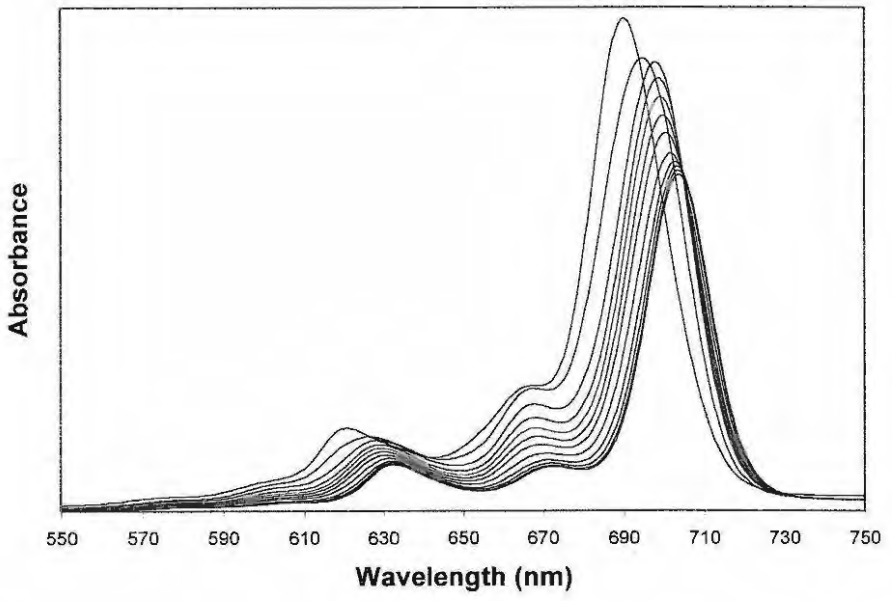

Figure 3.9 Phototransformation of solutions of $(Cl)_2$GeOMPPc (**41f**) in DMSO.

Figure 3.9 shows spectroscopic changes observed on photolysis of solutions of Cl_2GeOMPPc (**41f**) in DMSO. All GePc complexes (**41e**, **41f** and **41l**) showed similar behaviour. The spectral changes involves a shift of about 10 nm of the Q-band to longer wavelengths and is accompanied by a decrease in the absorbance of the whole spectrum. A clear photobleaching process is identified by a decrease in Q and B bands without shift in wavelength.

The nature of the product obtained following photolysis of the GePc complexes needs further investigation. Phototransformation of $Cl_2SiOPPc$ to the hydrolysed $(OH)_2SiOPPc$ has been reported by our group.[25] Cl_2GePc complexes are known to readily hydrolyse to $(OH)_2GePc$ in pyridine solutions containing aqueous ammonia,[26] with spectral changes consisting of a shift to shorter wavelengths. When $Cl_2GeOMPPc$ (**41f**) was hydrolysed in pyridine in the presence of ammonia, a shift to shorter wavelengths typical of hydrolysis of Cl_2GePc and Cl_2SiPc was observed. Thus, spectral changes shown in Figure 3.9 are not a result of the hydrolysis of $(Cl)_2GeOMPPc$ (**41f**) to $(OH)_2GeOMPPc$.

For the GePc derivatives spectroelectrochemistry revealed the exact same process as was observed with photolysis as will be discussed in Chapter 4, and could be used to explain the phototransformation process described above.

As stated above spectral changes shown in Figure 3.9 were observed only for the germanium phthalocyanine complexes. For the tin phthalocyanine complexes, photodegradation occurred by a decrease in the Q band as is expected, no shift in the wavelength of the Q band was observed. It was, however, observed that if the photolysed solution containing tin phthalocyanine derivatives was left to stand for about 2 minutes, the Q band was regenerated. The recovery of the Q band was found to occur much faster if oxygen was bubbled through the solution following photolysis and no recovery was observed if nitrogen was bubbled through the solutions. These observations suggest the involvement of reduction products during the photobleaching process. In the presence of oxygen, recovery occurs faster due to the reoxidation of the phthalocyanine reduction products. The formation of reduction products has been implicated during the photodegradation of germanium porphyrazine complexes,[27] with spectral changes showing the presence of ring reduced products being observed. There was no spectral evidence for

the formation anion radicals for the SnPc complexes, probably because only small amounts are present. A mechanism similar to that proposed before for germanium porphyrazine complexes may be proposed here for the photoinduced photodegradation process of SnPc complexes. In this mechanism, electron or hydrogen atom transfer from the solvent (S-H in the scheme below) to the excited phthalocyanine molecule (Pc*) may be assumed as the first step in the photodegradation process (Equation 3.39).

$$Pc^* + S\text{-}H \rightarrow Pc^{\bullet -}(PcH^{\bullet}) + S\text{-}H^{\bullet +}(S^{\bullet}) \quad \text{.....(3.39)}$$

$$Pc^{\bullet -}(PcH^{\bullet}) + O_2 \rightarrow Pc + O_2^{\bullet -}(HO_2^{\bullet}) \quad \text{.....(3.40)}$$

$$S\text{-}H^{\bullet +}(S^{\bullet}) \xrightarrow{O_2} \text{peroxides} \quad \text{.....(3.41)}$$

$$O_2^{\bullet -}(HO_2^{\bullet}) \xrightarrow{S\text{-}H} H_2O_2 \quad \text{.....(3.42)}$$

$$Pc^{\bullet -}(PcH^{\bullet}) \xrightarrow{O_2} \text{oxidized products} \quad \text{.....(3.43)}$$

$$Pc \xrightarrow{H_2O_2,\ peroxides} \text{oxidized products} \quad \text{.....(3.44)}$$

Interaction of semi-reduced dye radicals with oxygen results in the recovery of the dye according to Equation 3.40. Equations 3.41 to 3.44 represent further possible reactions that may occur. Photolysis in the presence of a free radical scavenger, DABCO, resulted in the increase in the photodegradation rates. DABCO scavenges the radicals hence inhibiting the recovery process occurring due to the reoxidation of the phthalocyanine anion radicals. Inhibition of the recovery process would result in a faster degradation of the phthalocyanine species.

3.2.2 Photophysics

3.2.2.1 Triplet lifetimes and quantum yields

Zinc phthalocyanine complexes

ZnPc complexes do not contain axial ligands and therefore aggregation at higher concentrations will cause quenching and consequent lower than expected triplet quantum yields (Φ_T) and triplet lifetimes (τ_T). Complexes **40a, 40b and 40c** proved to be unstable upon exposure to laser light and **40d, 40h, 40i** and **40j** did not give detectable triplet decay curves, most likely due to aggregation at the higher concentrations ($1x10^{-5}$ mol dm^{-3}) employed. No attempts were made to study them any further since these characteristics are not desirable for photodynamic therapy. Triplet quantum yields are determined with about 20% error. Triplet quantum yields and triplet lifetimes are listed in Table 3.3.

Table 3.3 Triplet quantum yields and triplet lifetimes. Solvent DMSO.

Compound	$\lambda_{triplet}$	Φ_T	τ_T (μs)
ZnOPPc (**40e**)	500	0.08	238
ZnOMPPc (**40f**)	510	0.03	197
ZnOCPPc (**40g**)	505	0.25	366
ZnOAmPPc (**40k**)	510	0.20	340
Cl_2GeOPPc (**41l**)	500	0.30	340
Cl_2GeOMPPc (**41f**)	510	0.50	168
Cl_2SnOPPc (**42e**)	515	0.19	30
I_2SnOPPc (**43e**)	515	0.19	32
Cl_2SnOMPPc (**42f**)	515	0.45	32
ZnOEPc (**40l**)	510	0.10	210
Cl_2GeOEPc (**41l**)	510	0.20	205
Cl_2SnOEPc (**42l**)	515	0.15	10
ZnOCholPc (**40m**)	505	0.02	220
Zn(estrone)$_4$Pc (**51**)	510	0.08	260
(estrone)$_2$SnPc (**53**)	500	0.08	18

The solvent used for all triplet determinations was DMSO, and for the complexes not readily soluble in DMSO one drop of chloroform was added first to aid solubility, then the DMSO was added. Triplet lifetimes, Table 3.3, for the ZnPc complexes ranged between 197 μs (**40f**) to 366 μs (**40g**) and the triple quantum yields between 0.02 (**40m**) and 0.25 (**40g**).

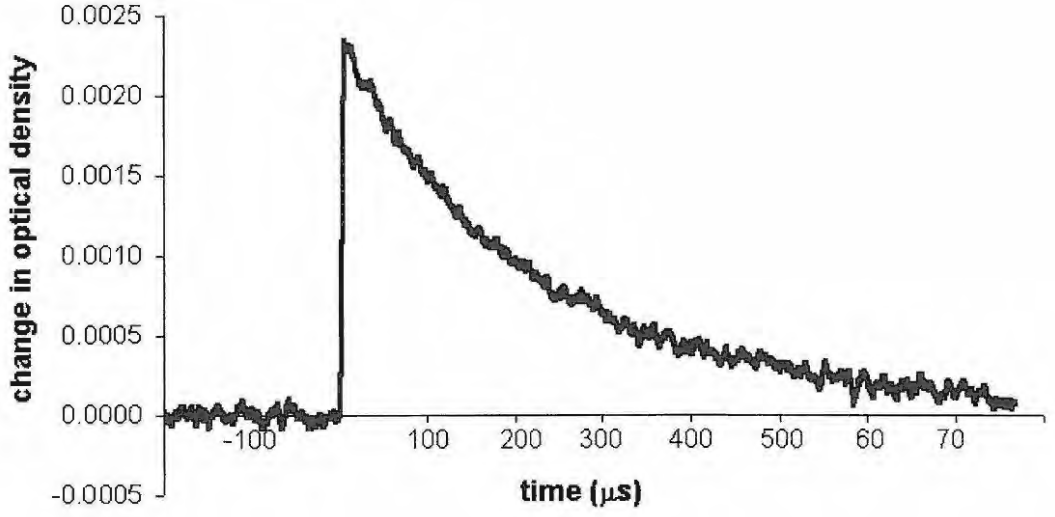

Figure 3.10 Triplet decay of zinc octa(phenoxy)phthalocyanine (**40e**) showing mono exponential decay.

In Figure 3.10 typical triplet state decay is shown. All the ZnPc complexes decayed mono exponentially. The transient spectra observed of complex **40l** on laser excitation is shown in Figure 3.11. The broad band observed near 500 nm has been identified before[28] as the spectra of the triplet ($^3\pi\pi^*$) species of the phthalocyanines. The negative peaks observed correspond to the ground state absorption peaks. The wavelength for the triplet species ranged between 500 and 510 nm, Table 3.3.

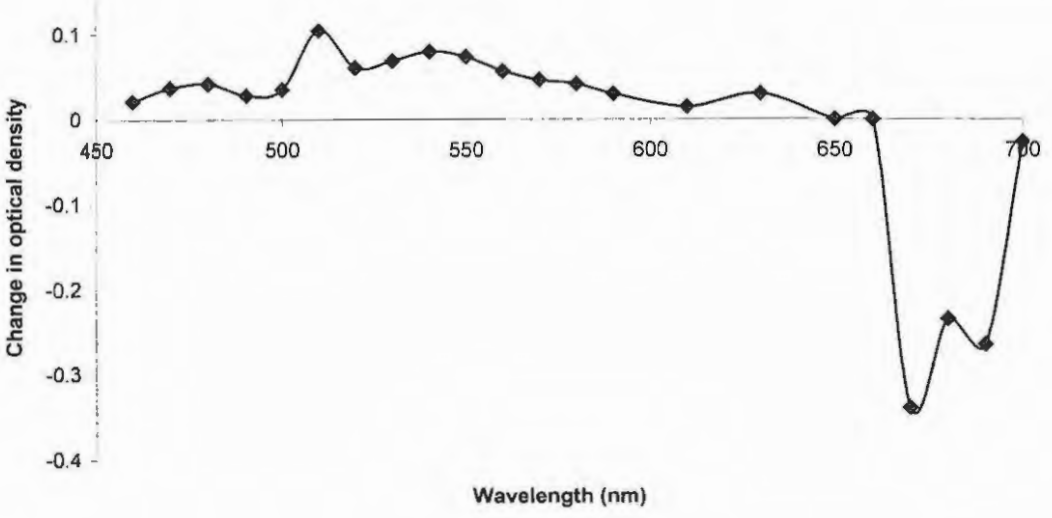

Figure 3.11 Transient spectra of zinc octa(estrone)phthalocyanine (**40l**).

Germanium and tin phthalocyanine complexes

Laser excitation of the GePc and SnPc complexes gave rise to transient absorption spectra in the range of 500 to 515 nm. Table 3.3 lists the triplet state absorption maxima, quantum yields and life times for the GePc and SnPc complexes under discussion. Mono exponential decay for the triplet lifetime was observed for these complexes.

The triplet quantum yields (Φ_T) are generally higher for the GePc (0.20 - 0.50) and SnPc (0.08 - 0.45) complexes than for the ZnPc (0.02 - 0.25) complexes. This is expected and explained by the heavy metal effect with induced spin-orbit coupling for heavier metals. Triplet lifetimes (τ_T) of GePc complexes were very similar to those of the ZnPc complexes, ranging from 168μs to 340μs, whereas the τ_T for the SnPc complexes were almost ten fold shorter than the GePc complexes, ranging from 10μs to 32μs. The heavy atom effect is also not evident when changing the axial ligand from the chloride (**42e**) to the iodide (**43e**).

The SnPc complex containing two estrones on the axial position (**53**) as well as the complex containing the eight peripheral estrone groups (**42l**) showed the shortest τ_T, 18μs and 10μs respectively. This could be attributed to increased quenching through intermolecular collisions due the size of the large estrone molecules.

3.2.2.2 Fluorescence lifetimes and quantum yields

Zinc phthalocyanine complexes

The fluorescence data were recorded in DMSO solutions with absorbances for the ZnPc complexes of less then 0.1 to minimize quenching. The proximity of the wavelengths and shape of the Q-band (~10 nm) and that of fluorescence emission shows that the nuclear configurations of the ground and excited states are the same, therefore no geometrical or structural changes are observed upon excitation of all complexes (Figure 3.12).

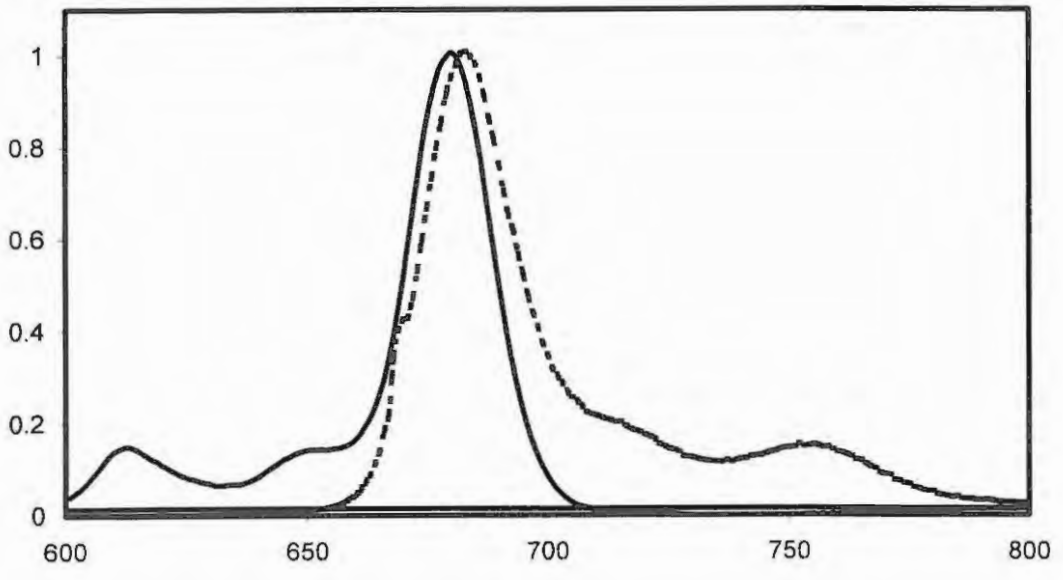

Figure 3.12 Fluorescence spectra (---) and absorbance spectra (solid) of zinc (octa phenoxy) phthalocyanine (**40e**).

Table 3.4 Fluorescence data of zinc phthalocyanine complexes.

Compound	Stokes shift	Φ_F	τ_F (ns)
ZnOAPPc (**40d**)	1	0.05	1.9
ZnOPPc (**40e**)	6	0.20	3.0
ZnOMPPc (**40f**)	7	0.21	2.4
ZnOCPPc (**40g**)	8	0.02	2.7
ZnONPPc (**40h**)	3	0.05	2.2
ZnONaph (**40i**)	6	0.07	2.8
ZnOAmPPc (**40k**)	5	0.20	2.9
Cl_2GeOPPc (**41e**)	6	0.12	0.3
Cl_2GeOMPPc (**41f**)	11	0.31	4.0
Cl_2SnOPPc (**42e**)	15	0.04	0.3
I_2SnOPPc (**43e**)	8	0.04	0.4
Cl_2SnOMPPc (**42f**)	7	0.06	0.4
ZnOEPc (**40l**)	5	0.11	2.9
Cl_2GeOEPc (**41l**)	6	0.21	5.1
Cl_2SnOEPc (**42l**)	7	0.01	0.2
ZnOCholPc (**40m**)	6	0.20	0.3
Zn(estrone)$_4$Pc (**51**)	8	0.06	2.5
(estrone)$_2$SnPc (**53**)	3	0.02	2.2

For ZnPc complexes a mono exponential fluorescence decay profile was observed (Figure 3.13) with Stokes shifts of less than 10 nm (Table 3.4). The quantum yield of fluorescence (Φ_F) of ZnPc complexes varied from 0.02 (**40g**) to 0.21 (**40f**) and the fluorescence life time (ι_F) between 1.9 and 3.0 ns, except for complex **40m** containing cholesterol ring substituents which had a τ_F value of 0.3 ns. This is partially explained by steric effects due to the size of the cholesterol group where collisional energy transfer has quenching of fluorescence as a consequence.[29] The lowest Φ_F values were obtained for ZnOCPPc (**40g**), ZnONaphPc (**40i**), ZnOAPPc (**40d**) and ZnONPPc (**40h**). For complex **40d**, intramolecular quenching of the excited singlet state, by the amino group, will result in low Φ_F values. The highest Φ_F (0.21, complex **40f**) is lower than the values reported for unsubstituted ZnPc complexes.[30] Though differences in solvents employed will account for the differences in Φ_F values, it has been reported that ring substitution in phthalocyanines reduced Φ_F by about 0.1.[31]

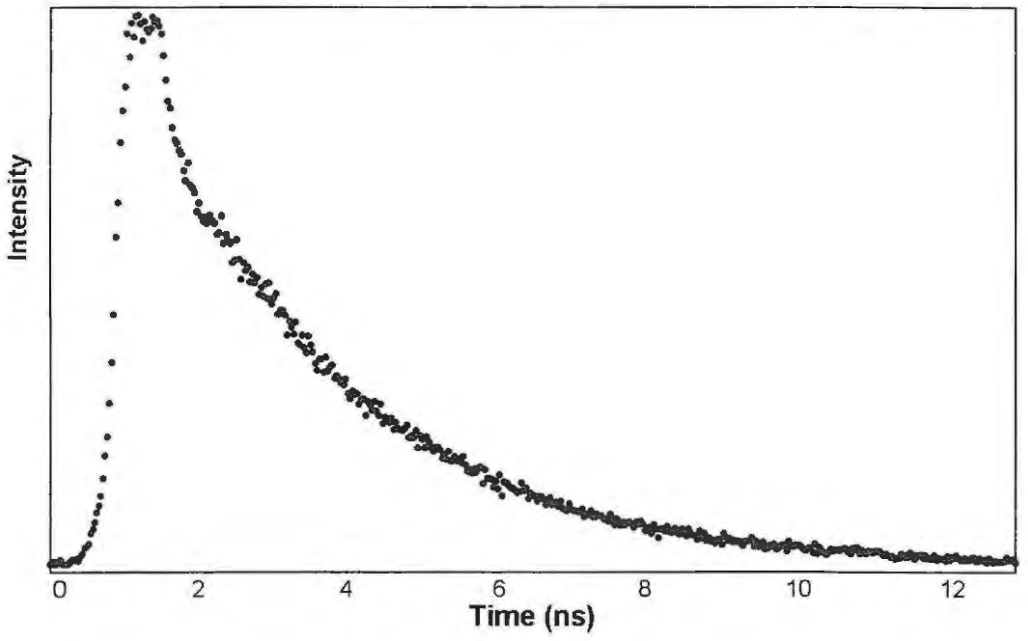

Figure 3.13 Fluorescence decay of zinc octa(estrone)phthalocyanine (**40l**).

It appears that compounds containing phenoxy groups with more electron-donating groups (**40k** and **40l**) have increased Φ_F and τ_F in comparison with the more electron-withdrawing groups (**40d**, **40g** and **40h**).

Germanium and tin phthalocyanine complexes

The τ_F of the GePc complexes (4.0 ns for **41f** and 5.1 ns for **41l**) were significantly higher than the ZnPc (1.9 - 3.0 ns) and SnPc (0.2 - 0.4 ns) complexes with the only exception being Cl_2GeOPPc (**41e**) with a lifetime of 0.3 ns. It was also observed that (estrone)$_2$SnPc (**53**) has a very low fluorescence quantum yield, but a relatively long fluorescence lifetime in comparison with the other SnPc complexes. Change in the axial ligand Cl_2SnOPPc (**42e**) versus I_2SnOPPc (**43e**) had no significant effect on the ϕ_F or τ_F values.

3.3 Experimental

3.3.1 Materials

Dimethylsulphoxide (DMSO), 1,3-diphenylisobenzofuran (DPBF) and diazabicyclo octane (DABCO) were purchased from (Sigma-Aldrich). Zinc phthalocyanine (ZnPc) was kindly donated by Dr. V. Derkacheva from the Organic Intermediates and Dyes Institute, Moscow. DMSO was dried over alumina, and chloroform was freshly distilled before use.

3.3.2 Instrumentation and techniques

3.3.2.1 Singlet oxygen determination and photobleaching

Photochemical experiments were carried out in a spectrophotometric cell of 1 cm pathlength. Typically a 2 ml air saturated solution of the MPc complexes under investigation (concentration range of 0.5 – 1 x 10^{-5} mol dm^{-3}) was introduced to the cell and photolysed in the Q band region of the dye with a General Electric Quartz line lamp (300W). A 600 nm glass cut off filter (Schott) and a water filter were used to filter off ultraviolet and far infrared radiation. An interference filter (Intor, 670nm with a bandwidth of 20 nm) was placed in the light path before the sample (Figure 3.14) under investigation for ZnPc complexes. An Intor 700nm interference filter with bandwidth of 20 nm was used for the tin and germanium phthalocyanine complexes.

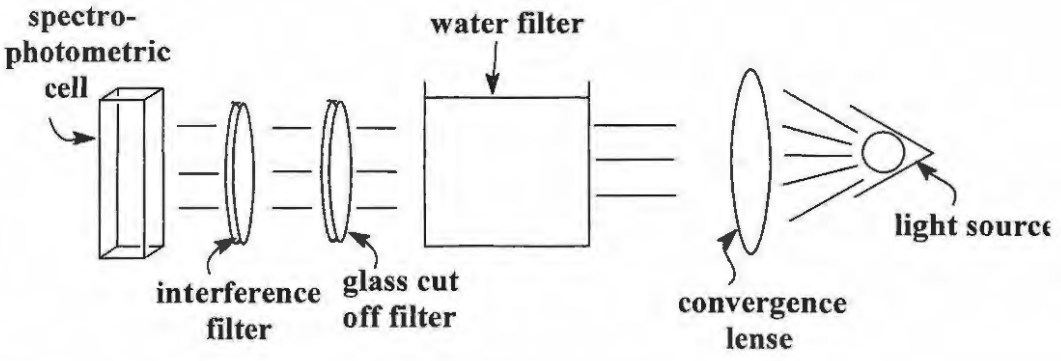

Figure 3.14 Set-up for singlet oxygen determinations.

The light intensity was measured with a power meter (Lasermate) and was found to be 1.5 x 10^{17} photons s^{-1} cm^{-2} for the set-up with the 670 nm interference filter and 7 x 10^{16} photons s^{-1} cm^{-2} for the 700 nm interference filter. The wavelength of the interference filter was chosen such that it was close to the Q band absorption of the phthalocyanine.

To determine the fraction of light that passes through the filter and is actually absorbed by the phthalocyanine, Equation 3.45 was employed. Table 3.5 shows a sample calculation.

Table 3.5 Calculations for fraction of light (α) absorbed by the phthalocyanine.

λ (nm)	T_{filter}	T_{dye}	$1-T_{dye}$	$T_{filter}(1-T_{dye})$
680	0.080	0.70	0.30	0.024
690	0.87	0.65	0.35	0.31
700	0.88	0.28	0.72	0.66
710	0.84	0.11	0.89	0.75
720	0.76	0.24	0.76	0.58
730	0.03	0.67	0.33	0.010
	$\Sigma = 3.46$			$\Sigma = 2.33$

Then

$$\alpha = \Sigma T_{filter}(1-T_{dye}) / \Sigma T_{filter} = 0.67 \quad \text{.....(3.45)}$$

T_{filter} is the light transmitter through the filter (given as a fraction of unity) and T_{dye} is the light transmitted through the dye solution. Thus α is the fraction of the overlap integral of the light received by the sensitizer, the α thus determined was used for Equations 3.27 and 3.28 (Section 3.1.1.1).

The light intensity measured by the power meter (Lasermate) is recorded in J s^{-1} A^{-1} where A is the surface area of the detector and should first be converted to J s^{-1} cm^{-2}. This value is then further converted to photons s^{-1} cm^{-2} by Equation 3.46

$$\Delta E_{\text{at wavelength } \lambda} = hc/\lambda \quad \text{.....(3.46)}$$

where h is Plank's constant and c the speed of light and λ the wavelength of the interference filter. To calculate the number of photons passing per square centimeter per second the total energy read by the power meter should be devided by the particular energy at the wavelength of interest, λ.

The same set-up as described above was used for both the determination of quantum yields of singlet oxygen and photodegradation. The DPBF and phthalocyanine absorbances were both set just below one and the Q-band irradiated by using the appropriate interference filter as explained above. The decrease in the DPBF peak is observed at 416 nm while the Q-band of the phthalocyanine remained unchanged. This is usually done by setting the

light intensity much lower than the light intensity used for photobleaching purposes. Φ_{Δ}^{ZnPc} (for the ZnPc standard) was taken as 0.55[32] in chloroform and 0.67[33] in DMSO. The UV/Visible spectra were recorded using the Cary Varian 500 UV/visible/NIR spectrophotometer.

3.3.3.2 Triplet and fluorescence measurements

The transient absorption spectra and decay kinetics were recorded using a flash-photolysis system. The excitation pulse was provided by an Nd-Yag laser (in frequency-doubled mode, providing 160 mJ, 8 ns pulses of laser light at 0-10 Hz), pumping a Lambda-Physik FL2002 dye laser, Figure 3.15. Single laser pulse energies used ranged from 0.001 to 2 mJ. A 75 W Xenon arc lamp provided the analyzing light. Triplet extinction coefficients were calculated using the singlet depletion method.[34]

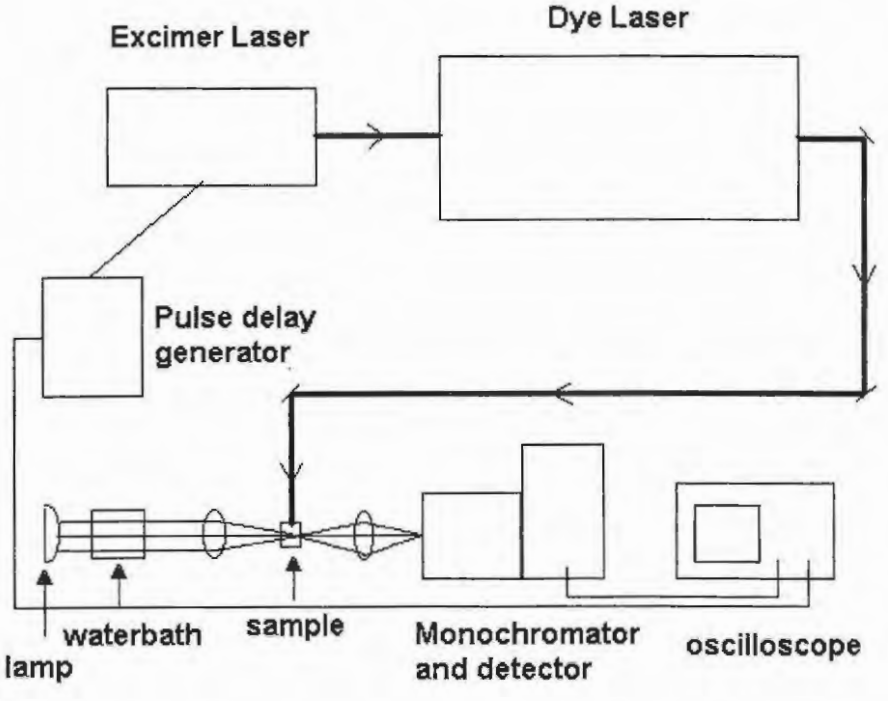

Figure 3.15 Set-up for triplet lifetime and quantum yield determinations.

Absorption and fluorescence spectra were performed on Perkin-Elmer Lambda-15 and SPEX Fluoromax spectrophotometers respectively. Fluorescence decay measurements were made using the time-correlated single-photon method.[35] The excitation source was a frequency-doubled, mode-locked Nd-Yag laser with excitation at 670nm. Detection was via a microchannel plate photomultiplier (Photek) and the instrument response time was up to 300 ps.

The kinetic curves were averaged over 1-8 laser pulses by a Tektronix 2221 A oscilloscope. Fluorescence (Φ_F) and triplet (Φ_T) quantum yields were calculated by a comparitive method using zinc phthalocyanine as a standard ($\Phi_F = 0.18$ and $\Phi_T=0.25$).[19]

3.4 Conclusion

In conclusion, it was shown that most of the complexes discussed in this thesis produced sufficient singlet oxygen to be useful in cell destruction. The more electron-donating substituents show higher singlet oxygen quantum yields and where the central metal is concerned the singlet oxygen quantum yields decrease in the following order Zn>Sn>Ge. Germanium and zinc phthalocyanines show similar triplet lifetimes. Triplet lifetimes of the tin complexes are tenfold shorter than those of germanium and zinc. Germanium as well as zinc phthalocyanines show good fluorescence lifetimes although the zinc complexes have lower fluorescence quantum yields. In terms of photostability it was shown that zinc complexes are more stable if they contain electron-withdrawing complexes. Germanium complexes undergo phototransformation in combination with photobleaching when photolysed. The phototransformation may involve metal reduction. On the other hand tin octaphenoxy phthalocyanine complexes undergo a photobleaching process which is mediated most likely by photoreduction of the phthalocyanine ring. These observations suggest the involvement of Type I (involving electron transfer) mechanism in the photochemical reactions sensitized by these phthalocyanine complexes.

All the estrone containing complexes showed good potential as photo therapy drugs as well as imaging through fluorescence. The cholesterol zinc complex is limited by aggregation but may still be useful as it produces sufficient singlet oxygen. Although the zinc tetra(estrone)phthalocyanine consists of regio isomers it shows excellent stability and photophysical properties.

3.5 References

1. A. Gilbert and J. Baggot, *J. Mol. Photochem.*, 1 (1991)
2. N.J. Turro, *Modern Molecular Photochemistry,* University Science Books: California, 583 (1991)
3. A. Gilbert and J. Baggott, *Essentials of Molecular Photochemistry,* CRC Press: Boca Raton, 501 (1991)
4. C.S. Foote in *Porphyrin Localization and Treatment of Tumors.* D.R.Doiron and C.J. Gomer (eds.)Alan R. Liss: New York, 3 (1984)
5. T.J. Dougherty and I.J. MacDonald, *J. Porphyrins Phthalocyanines,* **5**, 105 (2001)
6. B.W. Henderson and T.J. Dougherty, *Photochem. Photobiol.* **55**, 147 (1992)
7. C.S. Foote in *Porphyrin Localization and Treatment of Tumors.* D.R.Doiron and C.J. Gomer (eds.)Alan R. Liss: New York, 3-18 (1984)
8. H.I. Pass, *J. Natl. Cancer Inst.,* **86**, 443 (1993)
9. K.L. See, I.J. Forbes and W.H. Bettes, *Photochem. Photobiol.*, **39**, 631 (1984)
10. M. Ochsner, *J. Photochem. Photobiol. B: Biol.*, **39**, 1 (1997)
11. W. Spiller, H. Kliesch, D. Wöhrle, S. Hackbarth, B. Röder and G. Schnurpfeil, *J. Porphyrins Phthalocyanines,* **2**, 145 (1998)
12. M.G. Lagorio, L.E. Dicelio and E.A. San Roman, *J. Photochem.Photobiol. B. Biol.,* **3**, 615 (1989)
13. X. Zhang and H. Xu, *J. Chem. Soc. Faraday Trans.*, **89**, 3347 (1993)
14. E.E. Wegner and A.W. Adamson, *J. Am. Chem. Soc.*, **88**, 394 (1966)
15. H.J. Guiraud and C.S. Foote, *J. Am. Chem. Soc.*, **98**, 1984 (1976)
16. M.G. Lagorio, L.E. Dicelio, and E.A. San Roman, *J. Photochem. Photobiol. B. Biol.*, **3**, 615 (1989)
17. S.Dhami, PhD Thesis, Imperial College.
18. R. Bensasson, C.R. Goldschmidt, E. Land and T.G. Truscott, *Photochem. Photobiol,* **28**, 277 (1978)
19. P. Jacques and A. M. Braun, *Helv. Chim. Acta,* **64**, 1800 (1981)
20. N.J.L. Roth, and A. C. Craig, *J. Phys. Chem.*, **78**, 1154 (1974)
21. Lacey, J.A., Phillips, D., Milgrom, L.R., Yahioglu, G. and Rees, R.D., *Photochem. Photobiol.*, **67**, 97 (1998)
22. M.D. Maree, N. Kuznetsova and T. Nyokong, *J. Photochem. Photobiol. A: Chem.* **140**, 117 (2001)

23. J.A. Barltrop and J.D. Coyle, *Principles of Photochemistry*, John Wiley and Sons, p 21-22 (1978)

24. G. Schnurpfeil, A. Sobbi, W. Spiller, H. Kliesch and D. Wöhrle, *J. Porphyrins Phthalocyanines*, **1**, 159 (1997).

25. M.D. Maree, N. Kuznetsova and T. Nyokong, *J. Photochem. Photobiol. A: Chem.*, **140** 117 (2001).

26. C.W. Dirk, T. Inabe, K.F. Schoch and T.J. Marks, *J. Am. Chem. Soc.*, **105**, 1539 (1983)

27. I. Seotsanyana-Mokhosi, N. Kuznetsova and T. Nyokong, *J. Photochem. Photobiol. A: Chem.*, **140**, 215 (2001)

28. G. Ferraudi in *Phthalocyanines: Properties and Applications*, Leznoff CC and Lever ABP (eds), Vol. 1, VCH, 1989: New York, Ch. 4.

29. J.C. Dalton and N.J. Turro, *Mol. Photochem.*, **2**, 133 (1970)

30. S.M. Bishop, A. Beeby, H. Meunier, A. W. Parker, M. S. C. Foley and D. Phillips, *J. Chem Soc. Faraday Trans.*, **92**, 2689 (1996)

31. H.-G. Capraro, K. Schieweck, R. Hilfiker, M. Ochsner, U. Isele, P. van Hoogevest, R. Naef and M. Baumann, *SPIE*, **158**, 2078 (1994)

32. H.-G. Capraro, K. Schieweck, R. Hilfiker, M. Ochsner, U. Isele, P. van Hoogevest, R. Naef and M. Baumann, *Proc. SPIE*, **158**, 2078 (1994)

33. N. Kuznetsova, E. Makarova, S. Dashkevich, N. Gretsova, V. Negrimovsky, O. Kaliya and E. Luk`yanets, *Zh. Obshch. Khim.* **70**, 140 (2000)

34. P.G. Seybold,. and M. Gouterman, Phorphyrins III. Fluorescence Spectra and Quantum yields. *J. Mol. Spectrosc.* 31 (1969)

35. D.V. O'Connor and D. Phillips, *Time correlated Single Photon Counting*, Academic Press, London. (1984)

Chapter 4

Electrochemistry

4.1 Introduction

The importance of studying the electrochemical behaviour of the selected compounds, which may find use in photodynamic therapy, lies in trying to understand how these compounds behave when forced to gain or loose an electron. As this could be part of the overall mechanism taking place *in vitro* it will help us conclude about the stability of these complexes and therefore possible formation of inactive complexes and assist us in resolving unexplained observations or confirm conclusions made by other techniques.

The aims were therefore set to study the electrochemical behaviour of the complexes synthesized and described in Chapter 2, using cyclic voltammetry, a very basic electrochemical technique, as well as spectroelectrochemistry. Spectroelectrochemistry is a useful method to visually observe the electronic changes which occur upon application of a certain potential. It was therefore decided to give a brief background to create a better understanding of these techniques.

4.1.1 Cyclic voltammetry[1]

During a cyclic voltammetry experiment the potential of an electrode is cycled from a starting potential (E_i) to a final potential (E_f) and back to E_i and the resulting current is measured. During this cycle the potential of this working electrode is measured against a reference electrode, for example a saturated calomel electrode (SCE) or silver/silver chloride (Ag|AgCl). The working electrode may be made of solid gold, platinum, glassy carbon matrix or others. During these experiments the solution is kept stationary and is therefore not stirred.

Figure 4.1 displays a typical cyclic voltammogram. A starting potential is applied and scanned e.g. in a negative direction with a cathodic peak appearing as soon as reduction starts taking place. After a maximum current (i_{pc}) is reached, a sudden decline is observed. This is the result of the much slower diffusion of the molecules towards the electrode surface as compared to the reduction of the molecule, that is the immediate solution next to the electrode is depleted of unreduced molecules. Reversing the potential results in an anodic peak and the same behaviour of the current is observed as described for the cathodic peak. Hence the term cyclic voltammetry.

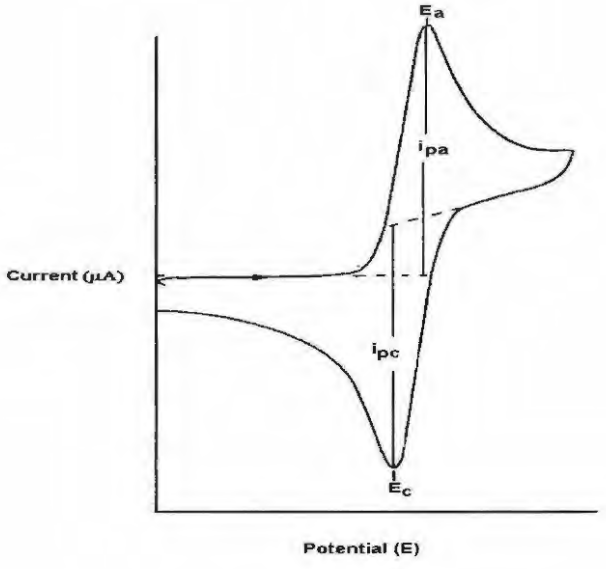

Figure 4.1 A cyclic voltammogram.

4.1.1.1 Interpretation of a cyclic voltammogram[2]

A Nernst reaction is one where the electron transfer is rapid and sufficient enough to assume that the concentration of both the oxidized (O) and the reduced species (R) are in a state of equilibrium. Considering the following half reaction

$O + ne^- \leftrightarrow R$ .....(4.1)

the Nernst equation can be written as

$$E = E^{o'} + \frac{RT}{nF} \ln \frac{[O]_{x=0}}{[R]_{x=0}}$$

.....(4.2)

A reversable system is one in which rapid electron exchange between the species and the working electrode occurs. Situated between E_a and E_c is the formal redox potential, $E^{o'}$ which is approximately equal to the half-wave potential ($E_{1/2}$).

$E^{o'} = ½ (E_{pa} + E_{pc})$ .....(4.3)

Determination of the number of electrons (n) can therefore be done from the peak separation

$\Delta E_p = E_{pa} - E_{pc} = RT/nF$ and at 25 °C $\approx 0.059/n$ .....(4.4)

The peak current (i_p) is described by the Randles-Sevcik equation:

$I_p = (2.69 \times 10^5) n^{3/2} A D^{1/2} C v^{1/2}$ .....(4.5)

Where i_p = peak current in Ampere

n = electron stoichiometry

A = electrode surface (cm^2)

D = diffusion coefficient (cm^2/s)

C = concentration (mol/cm^3)

v = scan rate (V/s)

According to the Randles-Sevcik equation an increase in i_p will occur with an increase in $v^{1/2}$ and is directly related to the concentration. A linear plot of $v^{1/2}$ *versus* i_c or i_a indicates diffusion controlled mass transfer. The relationship between i_p and concentration is of importance to analytical applications as well as to studies concerning electrode mechanisms. The ratio of i_{pa} and i_{pc} is expected to be near unity for simple reversible systems:

$$\frac{i_{pa}}{i_{pc}} = 1 \qquad \text{.....(4.6)}$$

4.1.1.2 Electrochemistry of phthalocyanines

A study of the electrochemistry of phthalocyanines often reveals multiple peaks that may result from metal or phthalocyanine ring centered processes.[3] The phthalocyanine skeleton exists as a dianion (Pc-2) and may be reduced by up to four successive electron transfer processes, which may or may not be reversible (Equation 4.7).

$$Pc(-2) + e^- \rightarrow Pc(-3) + e^- \rightarrow Pc(-4) + e^- \rightarrow Pc(-5) + e^- \rightarrow Pc(-6) \qquad \text{.....(4.7)}$$

Where Pc(-2) is the phthalocyanine dianion.

Oxidation of the ring may also occur (Equation 4.8):

$$Pc(-2) \xrightarrow{-e} Pc(-1) \xrightarrow{-e} Pc\ (0) \qquad \text{.....(4.8)}$$

These ring processes are influenced by the nature of the substituents on the phthalocyanine ring. Figure 4.2 shows a typical cyclic voltammogram of ring based processes.

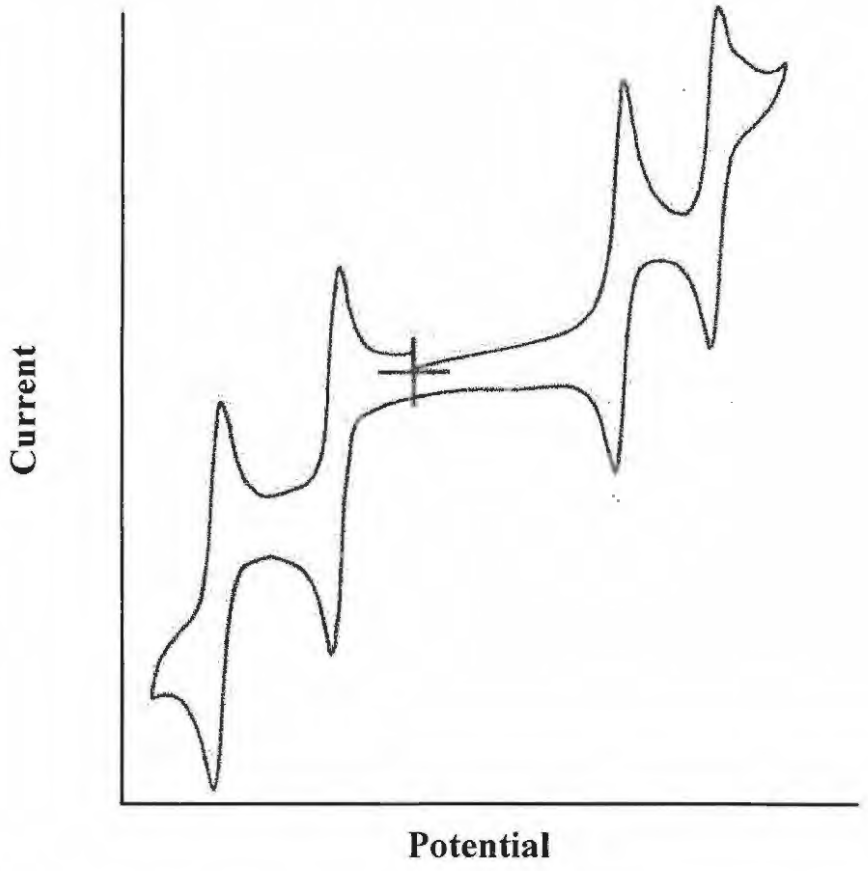

Figure 4.2 Cyclic voltammogram of bis(tri-n-hexylsiloxy)(2,3-naphthalocyanine)silicon.[4]

Any additional electrochemical reactivity results from the redox activity of the metal centre depending on the characteristics of the metal such as the oxidation state, axial ligands and

the solvent used. Metals like cobalt, iron, manganese and chromium have occupied d-orbitals situated between the HOMO and the LUMO gap of the ring and consequently shows electrochemical reactivity. Non-transition metals do not have d-orbitals and only ring processes occur in these phthalocyanines. Metals with higher polarization power tend to be easier to oxidize. Peak separations between the first ring reduction and the first ring oxidation is approximately 1.5 V for phthalocyanines containing main group metals and this correspond to the energy between the HOMO and LUMO in these phthalocyanines.

4.2 Experimental

Cyclic voltammetry data were collected with the BioAnalytical Systems (BAS) model 100 B/W electrochemical workstation. A glassy carbon electrode was used as a working electrode and a platinum wire as an auxiliary electrode. The potentials were internally referenced against ferrocene/ferrocenium (fc^+/fc) couple and these potentials referenced *versus* Saturated Calomel Electrode (SCE). The fc^+/fc has been determined to be 0.46 V in DMF *versus* SCE.[3] Cyclic voltammetry was performed in dry DMSO, or where otherwise stated in dry chloroform, with 0.1 mol dm^{-3} tetrabutylammonium hexafluorophosphate (TEAHP, Aldrich) as the electrolyte. Spectroelectrochemical data were recorded using an optically transparent thin-layer electrochemical (OTTLE) cell connected to a BAS CV 27 voltammograph, containing a Pt grit working and auxiliary and silver wire pseudo reference electrode. UV/Visible spectra were recorded with a Cary 500 UV/vis/NIR spectrophotometer.

4.3 Results and discussion

4.3.1 Cyclic voltammetry

4.3.1.1 Metal-free phthalocyanine complexes

Cyclic voltammetry revealed two ring reduction couples (Couples I and II) and one oxidation couple (Figure 4.3). Sometimes only the anodic component of the oxidation process was observed, hence only the anodic peak potentials are listed. Only a few selected complexes were investigated due to solubility factors. For all complexes, couple I is assigned to the first ring reduction forming the $[H_2Pc(-3)]^-$ species and couple II to the second ring reduction and the formation of $[H_2Pc(-4)]^{2-}$. The oxidation peak is assigned to the $[H_2Pc(-1)]^+$ species. The irreversibility of some of the redox processes suggest disaggregation of the complexes following oxidation or reduction, since at concentrations (10^{-3} M) used for cyclic voltammetry aggregation is expected.

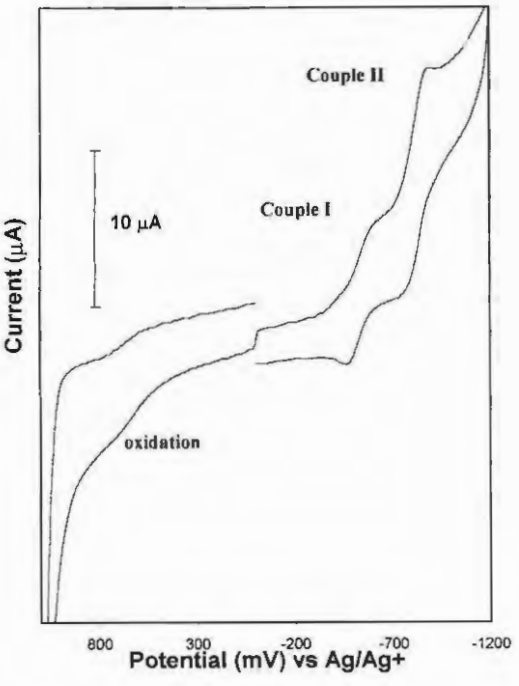

Figure 4.3 Cyclic voltammograph of metal-free octa estrone phthalocyanine. Scan rate 50 mV/s.

The formal redox potentials ($E^{o'}$) for couple II ranges from -908 to -1006 mV and that of couple I from -509 to -726 mV. From the data presented in Table 4.1 it can be seen from the peak separation between the cathodic and anodic potentials (ΔE) and the ratio of the peak cathodic and anodic currents (i_c/i_a) values that these systems exhibit quasi-reversible to irreversible behaviour. The ΔE values of an ideal one electron process is 58 mV and a system of this nature can be considered as reversible. For this study ferrocene had a ΔE value of 110 mV although it is normally expected to display better reversibility with ΔE ranging between 60 and 70 mV. This could be attributed to the history of the glassy carbon electrode. Irreversibility results from slow electron transfer between the molecule of interest and the working electrode. In this situation it is easy to understand how the size of these large molecules, aggregation or hydrogen bonding could all possibly contribute to the observed inefficient or slow electron transfer.

Table 4.1 Electrochemical data for metal-free octa(phenoxy)phthalocyanine derivatives. Solvent used was DMF, with 0.1 mol dm^{-3} tetracthylammonium hexafluorophosphate as the electrolyte. Scan rate 100 mV/s

Compound	$E^{o'}$ /mV (vs. SCE)			ΔE/mV		i_c/i_a	
	E_p(oxidation)	Couple I	Couple II	Couple I	Couple II	Couple I	Couple II
H_2OPPc (**39e**)	372	-726	1006	242	135	3.9	2.5
H_2OMPPc (**39f**)	722	-509	-	209	-	7	-
H_2OCPPc (**39g**)	432	-365	-960	138	162	2.6	2.0
H_2ONPPc (**39h**)	672	-551	-908	199	160	2.4	3.5
H_2OAmPc (**k**)	662	-568	-967	70	180	0.2	1.1
H_2OEPc (**39l**)	622	-648	-922	165	156	1.8	0.9

In a plot of peak current (i_c) against the square root of the scan rate a straight line would indicate a diffusion controlled process. This was observed (Figure 4.4), provided that the electrode is cleaned in between scans since Pc complexes have a tendency to adsorb on to glassy carbon electrodes.

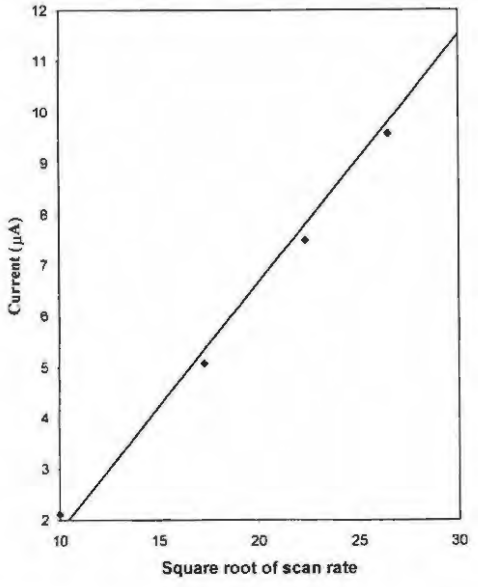

Figure 4.4 Plot of i_c against the square root of the scan rate for couple II of the metal free octa estrone phthalocyanine

4.3.1.2 Metallated phthalocyanine complexes

Zinc phthalocyanine complexes

Figure 4.5 shows a typical cyclic voltammogram of the ZnPc complexes. Typically two reduction couples, Couple I and Couple II, and one oxidation peak were observed. Couple I represents the first reduction $[ZnPc(-2)] \rightarrow [ZnPc(-3)]^{-1}$ and Couple II the second reduction $[ZnPc(-3)]^{-1} \rightarrow [ZnPc(-4)]^{-2}$. Again quasi-reversible to irreversibe behaviour was observed for Couples I and II, as was the case for the metal-free phthalocyanine complexes

and as indicated by the values of ΔE, these values were too large for a reversible system. i_{pa}/i_{pc} also deviated from unity in most cases. Table 4.2 lists the electrochemistry data.

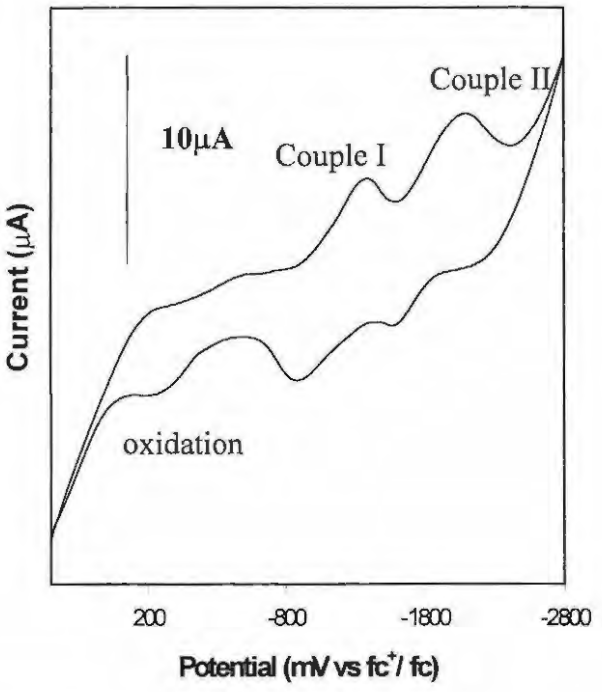

Figure 4.5 Cyclic voltammogram of **40g** in DMSO and scan rate 100 mV/s.

It was observed that the ease of reduction increase in the following order Zn>Ge(IV)>H_2>Sn for the MOPPc complexes [**40e** (-863 mV), **41e** (-733), **39e** (-726), **42e** (-484 mV)]. This order was also observed for the octa estrone complexes (**39l**, **40l-42l**). For the MOMPPc complexes the increasing ease of reduction was almost the same with the following order Zn>Ge>Sn>H_2 [**40f** (-816 mV), **41f** (-730 mV), **42f** (-619 mV), **39f** (-509 mV)].

Table 4.2 Electrochemical data of metallated phthalocyanine derivatives in DMSO unless indicated otherwise. Electrolyte 0.1 mol dm^{-3} tetraethylammonium hexafluorophosphate.

Compound	$E^{o'}$ /mV (vs. SCE)			ΔE/mV		i_c/i_a	
	E_p(oxidation)	Couple I	Couple II	Couple I	Couple II	Couple I	Couple II
ZnOAPc (**40d**)	154	-1123	-	140	140	4.7	3.3
ZnOPPc (**40e**)	531	-863	-1145	162	168	5.9	3.6
ZnOMPPC (**40f**)	592	-816	-1121	445	391	8.3	1.0
ZnOCPPc (**40g**)	236	-1012	-1590	185	198	6.4	>10
ZnONPPc (**40h**)	708	-1030	-1590	146	185	1.1	6.9
ZnOAmPc (**40k**)	271	-1010	-1455	270	151	1.0	1.2
Cl_2GeOPPc (**41e**)	-	-733	-1016	215	166	1.8	3.3
Cl_2GeOMPPc (**41f**)	-	-730	-1102	161	148	1.9	0.8
Cl_2SnOPPc (**42e**)	-	-484	-1019	591	425	1.9	2.3
I_2SnOPPc (**43e**)	-	-549	-1044	553	620	2.0	1.2
Cl_2SnOMPPc (**42f**)	-	-619	-892	180	263	2.6	3.2
ZnOEPc (**40l**)	309	-1132	-	342	-	10	-
Cl_2GeOEPc (**41e**)	-	-828	-1258	375	386	1.1	1.2
Cl_2SnOEPc (**42e**)	-	-532	-914	131	282	0.9	1.0
ZnOCholPc (**40m**)[a]	270	-1089	-1490	180	210	1.5	1.2
Zn(estrone)$_4$Pc (**51**)	410	-1344	-	220	-	4.3	-
(estrone)$_2$SnPc (**53**)	-	-682	-1263	365	394	1.2	0.8

[a] Solvent: Chloroform

By inserting the zinc metal the ring becomes harder to reduce but easier to oxidize for complexes **40f**, **40g** and **40k** than the corresponding non-metallated Pc complexes, **39f**, **39g**, **39k**. This may be due to the added electron density of the metal. This tendency has been observed before with porphyrins[5,6] and was explained by the change in planarity of the molecule on insertion of the metal. Increased planarity of the ring results in better π-conjugation as well as better d-π metal-ring interactions. Crystal structures did indeed reveal increased planarity with increased metal size[7] and hence explained the observed results. In addition it is further explained by the ionic character of the metal

phthalocyanine bond. If the bond has more of an ionic character than a covalent character, the complex may be less stable and consequently harder to reduce.[8] This ionic polarization causes the phthalocyanine ring to possess a more negative charge and is therefore harder to reduce in the presence of the central metal.

Germanium and tin phthalocyanine complexes

Figure 4.6 shows a sample of cyclic voltammograms of ZnPc, GePc and SnPc complexes. No oxidation peaks were observed for any of the GePc and SnPc complexes, Table 4.2, most likely because they occur out of the solvent range. Two reduction couples were, however, observed for these complexes. Reduction in SnPc complexes is expected to occur only at the ring. Thus, the couples in Figure 4.6 and listed in Table 4.2 are assigned to ring based processes, forming $[SnPc(-3)]^{-1}$ and $[SnPc(-4)]^{-2}$ species for Couples I and II respectively. For GePc complexes electrochemical oxidation is also known to occur at the ring, but chemical reduction to Ge(II)Pc is known. Couples I and II for GePc complexes are also assigned to ring based processes forming $[GePc^{-3}]^{-1}$ and $[GePc^{-4}]^{-2}$, Table 4.2.

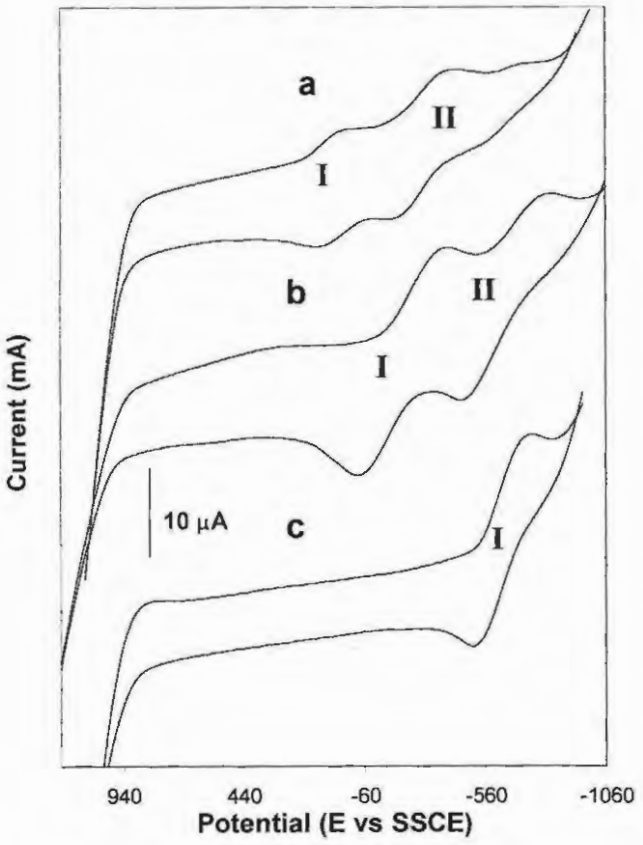

Figure 4.6 Cyclic voltammograms of a) tin (**42l**), b) germanium (**41l**) and c) zinc (**40l**) octa (estrone)phthalocyanines with Couples I and II as indicated.

The $(estrone)_2SnPc$ (**53**) is slightly harder to reduce than the other SnPc complexes. This was also the situation for the $Zn(estrone)_4Pc$ (**51**) complex where the reduction potential for the ZnOEPc (**40l**) was almost 200 mV less negative than for **51**.

4.3.2 Spectroelectrochemistry

4.3.2.1 Zinc phthalocyanine complexes

Electrolysis in an optically transparent thin-layer electrochemical (OTTLE) cell at potentials of the first ring reduction (Couple I) resulted in spectral changes shown in Figure 4.7 for complex **40g**. Since high concentrations have to be used to thin layer

spectroelectrochemical studies, the spectra before electrolysis, Figure 4.7 (i), shows considerable aggregation (as evidenced by the broadness of the Q band spectra). Aggregation is expected at concentrations used for OTTLE. On electrolysis, the Q band decreases in intensity and new broad bands are formed between 500 and 600 nm with a clear isosbestic point at 590 nm. The number of moles of electrons transferred was found to be near unity. The spectral changes shown in Figure 4.7 are characteristic of ring based reduction in phthalocyanines,[9] as is expected for ZnPc complexes. On re-oxidation of the final product in Figure 4.7 b(iii), the Q band was regenerated, but now occurred as a narrow single band, suggesting the presence of mainly the monomeric species following re-oxidation. The monomeric species was probably formed during or following the reduction. Similar spectral changes were observed for the other zinc complexes.

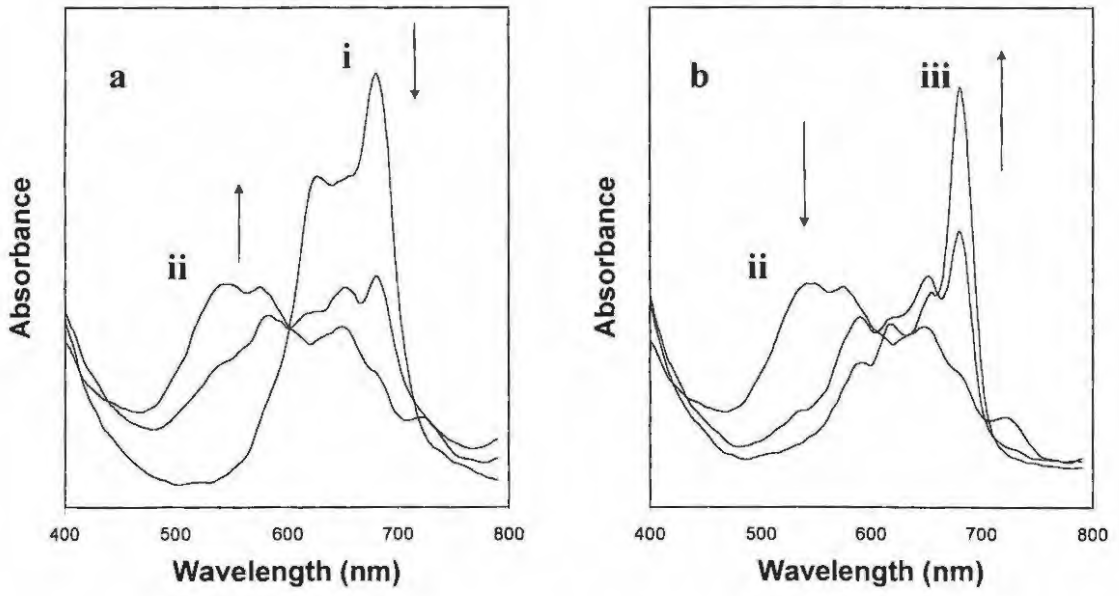

Figure 4.7 Electronic absorption spectral changes observed on a) reduction of **40g** at potentials of first ring reduction, (i) spectra before reduction and (ii) spectra at the end of reduction; b) re-oxidation of the final product (a) at positive potentials, (ii) spectra at the end of reduction in (a) and (iii) spectra following re-oxidation.

4.3.2.2 Germanium and tin phthalocyanine complexes

Application of a negative potential of -1.2 V on a solution of GePc complex resulted in spectral changes shown in Figure 4.8a. These changes are attributed to ring reduction as evidenced by the presence of two peaks between 500 and 600nm. These peaks are typical of ring reduction in MPc complexes.[9]

Upon application of 1.2 V a shift of the Q-band to longer wavelengths as well as a decrease in the absorbance of the spectra was observed (Figure 4.8a). These spectral changes are due to metal based processes, which are characterized by only a shift in the Q-band without a drastic decrease in absorbances or formation of new bands in the 500 to 600 nm region.

The nature of the species formed in Figure 4.8b was further investigated. Chemical reduction and oxidation was done to characterize the species formed. When $NaBH_4$ was used to reduce SnPc, Figure 4.9, spectral changes similar to Figure 4.8 were observed, that is, shift of the Q-band to longer wavelengths. This suggested that the same species may have been formed. Visually this metal reduction is seen as a change in colour from light green to a dark olive green and within seconds to a purple-blue as the ring is also reduced. Addition of chemical oxidants to the final solution in Figure 4.9 regenerated the original green colour.

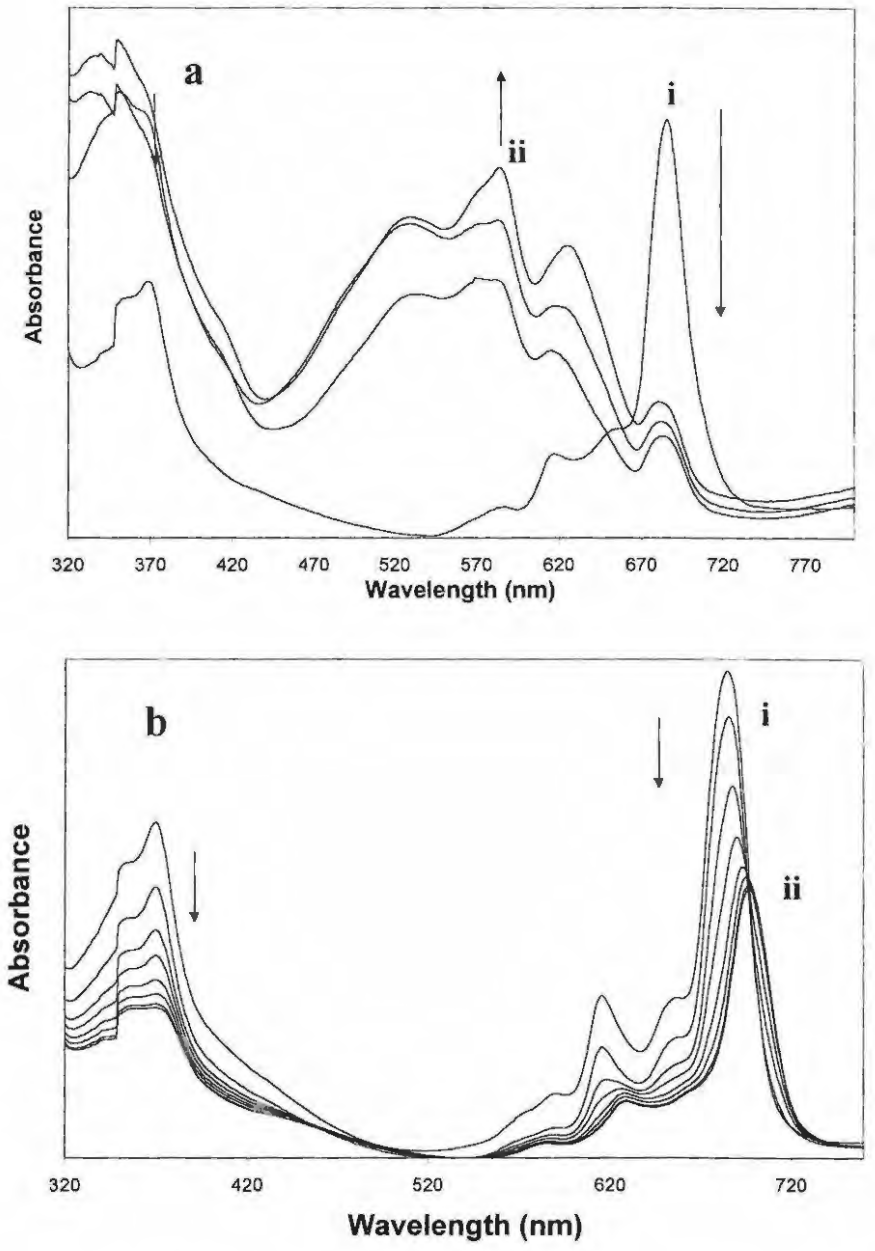

Figure 4.8 Electronic absorption spectra of $Cl_2GeOPPc$ (**41e**) observed (i) before and (ii) after application of a) -1.2 V and b) 1.2 V.

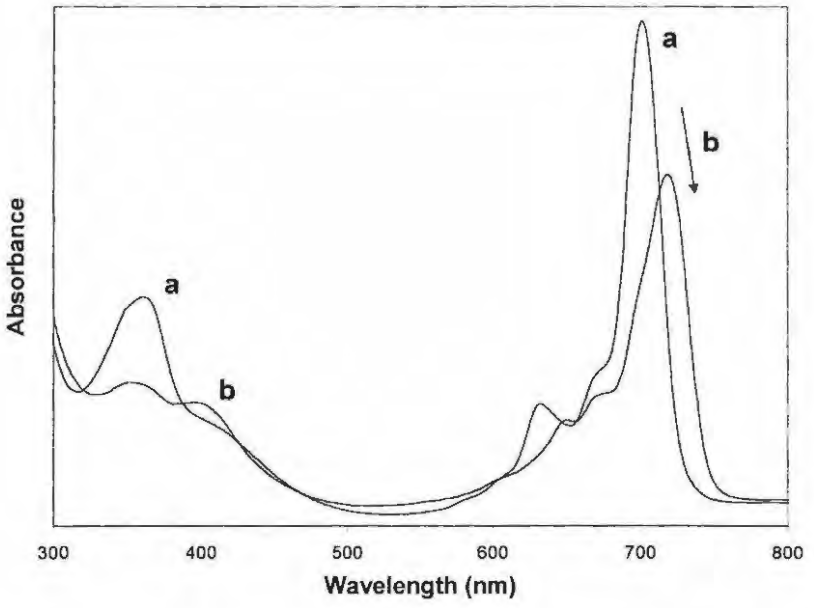

Figure 4.9 Chemical reduction of $I_2SnOPPc$ in DMSO using $NaBH_4$.a) Before and b) after addition of $NaBH_4$.

Work by other groups[10] has shown that reduction of $(Cl)_2Ge(IV)Pc$ with sodium borohydride resulted in a species which did not retain the Pc moiety, and was identified as hydroxygermanium(IV)α,β,γ-triazabenzcorrole (Ge(OH)TBC) shown in Figure 4.10, formed by Pc ring cleavage of the $(Cl)_2GePc$ species. The formation of this species was characterized by a sharp absorption band in the 400 to 450 region. This band was not observed in Figure 4.9. The SnPc complex was found[11] not to show the formation of TBC species upon reduction as was observed for GePc complexes.

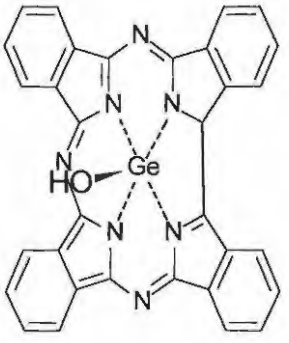

Figure 4.10 Stucture of hydroxygermanium(IV)α,β,γ-triazabenzcorrole (Ge(OH)TBC).

It is clear that ring cleavage does not occur following chemical or electrochemical reduction of GePc or SnPc complexes. The fact that the same spectra are formed by application of a positive potential is surprizing and can not be explained at this stage. The spectra for this species have not been described before.

4.4 Conclusion

The electrochemical behaviour of synthesized compounds has been studied by cyclic voltammetry and spectroelectrochemical methods. It has been found that the redox potentials are shifted significantly to more positive potentials and therefore the oxidation peaks are not always observed. Spectroelectrochemistry revealed that upon application of a positive potential the Sn(IV)Pc and Ge(IV)Pc complexes form species with spectra similar to those observed on chemical reduction, that is, Ge(II)Pc and Sn(II)Pc . Two moles of electrons were obtained on electroreduction. These observations may provide an additional mechanism to cell destruction, that is, cell destruction through singlet oxygen and other radicals as well as electron transfer. From the observations in this chapter it is proposed that the products of the phototransformation of Ge(IV)Pc (Chapter 3) are the corresponding Ge(II)Pc complex.

4.5 References

1. P.T. Kissinger and W.R. Heineman, *J. Chem. Ed.*, **60**, 702 (1983)
2. G.A. Mabbott, *J. Chem. Ed.*, **60**, 698 (1983)
3. A. B. P. Lever, E. R. Milaeva and G. Speier in *Phthalocyanines: Properties and Applications,* C. C. Leznoff and A. B. P. Lever (eds), Vol. 3, VCH, New York (1993)
4. B.L. Wheeler, G. Nagasubramanian, A.J. Bard, L.A. Schechtman, D.R. Dininny and M.E. Kenney, *J. Am. Chem. Soc.*, **106**, 7407 (1984)
5. C.R. Lorenz, D.D. Howard and F. R. Lemke, *J. Electroanal. Chem.*, **415**, 179 (1996)
6. K.M. Kadish, Q. Y. Y. Xu, G. B. Maiya, J. Barbe and R. Guilard, *J. Chem. Soc. Dalton Trans.*, 1531 (1989)
7. K.M. Kane, F.R. Lemke and J.L. Peterson, *Inorg. Chem.*, **34**, 4085 (1995)
8. M. Zerner and M. Gouterman, *Theoret. Chim. Acta (Berlin)*, **4**, 44 (1966)
9. M.J. Stillman in *Phthalocyanines: Properties and applications,* C.C. Leznoff and A.B.P. Lever (eds), Vol.3, VCH, New York (1993)
10. M. Fujiki, H. Tabei and K. Isa, *J. Am. Chem. Soc.* **108**, 1532 (1986)
11. J. Li, L.R. Subramanian and M. Hanack, *Chem. Commun.*, 679 (1997)

Chapter 5

Electrocatalyses

5.1 Introduction

This work reports on the effects of *pH* on the cyclic voltammograms of a series of substituted $CoPc(R)_4$ complexes adsorbed on a glassy carbon electrode (GCE). The structures of the complexes are shown in Schemes 5.1 to 5.4. The thesis examines the effects of the ring substituents on the catalytic behaviour of the substituted CoPc complexes. Cysteine is an amino acid that can be found in most proteins, for example the protein metallothionein contains about 20% cysteine. To contribute towards the development of electrochemical probes for the detection and quantification of certain proteins the electrocatalytic behaviour of the complexes shown in Scheme 5.1 towards the oxidation of cysteine, is examined. Electrocatalytic oxidation of cysteine by adsorbed CoPc and CoTSPc has been studied thoroughly.[1-5] However, the studies on the use of the rest of the substituted CoPc complexes listed in Scheme 5.1 for cysteine oxidation have not been fully explored. GCE modified by electrodeposition of the CoPc complexes is employed for the comparative study of their electrocatalytic activity towards oxidation of cysteine.

A brief discussion will follow on the discussion of the techniques used to modify electrodes for catalyses as well as characterization techniques used to define the properties of these electrodes.

5.1.1 Electrode modification techniques

Electrodes may be modified through various techniques including covalent bond formation, adsorption, polymers and inorganic materials.

The choice of technique depends on the nature of the electrode, the properties of the catalyst and the purpose of the experiment. Gold electrodes are particularly useful in forming what is believed to be a covalent bonds with thiol containing compounds.

Glassy carbon electrodes are also useful in adsorping the catalyst onto the surface through sharing of electron density or coordination to undefined functional groups. Trichlorosilanes have been attached to the hydroxyl groups on carbon electrodes to form a stable siloxy electrode surface. The catalyst is also often incorporated into a polymer film where solubility becomes a limiting factor. The polymer shows increased stability, but maintaining sensitivity may become an added challenge. Inorganic materials such as clays and zeolites have the added benefit of withstanding high temperatures and highly oxidizing environments.

Electrodes are normally allowed to stand in a solution to allow spontaneous adsorption or chemical reactions. A thin coat may be applied through spin-coating or by applying a drop of dilute solution and allowing the solvent to dry. A technique also commonly used is coating through electrochemical deposition. This is done by cycling between two predetermined potentials to allow deposition of the catalyst through electrostatic interaction with the electrode. An increased in current is observed with each cycle and stops increasing after deposition is complete.

5.1.2 Characterization of modified electodes

Since electrodeposition was the technique used to modify the electrode it is important to discuss how the layer on the electrode, is characterized. The area under the reduction or oxidation peak of the catalyst coated onto the electrode is represented by the following equation:[6]

$$Q = nFA\Gamma \qquad \text{.....(5.1)}$$

Where Q = charge, C

n = number of moles of electrons transferred

F = Faraday's constant, 96 485 C/mole

A = area of the electrode, cm^2

Γ = surface coverage, mol cm^{-1}

Q, the charge is determined by calculating the integral of the faradaic current, that is, the area under the oxidation or reduction curve. Once the surface area is determined, the number of layers could be calculated if the dimensions of the molecule are known and the orientation of the molecule on the surface is assumed.

5.2 Results and discussion[‡]

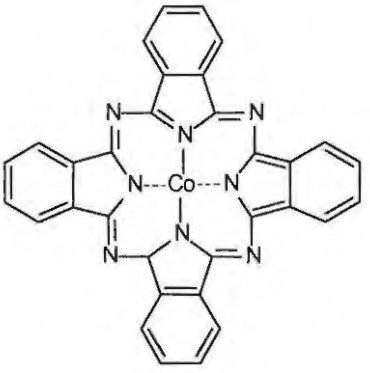

54

Figure 5.1 Cobalt phthalocyanine (CoPc).

The redox peaks for unsubstituted CoPc (Figure 5.1) and other MPc complexes exhibit a strong *pH* dependence when adsorbed onto carbon electrodes and cyclic voltammetry is recorded in buffer only.[7,8] For cobalt(II) and iron(II) tetrasulfonated phthalocyanines, the *pH* dependence of the redox peaks give a slope of 59 mV/pH, indicating a one-electron one-proton process. Slopes ranging from 60 to 64 mV/*pH* were obtained for cobaltetracarboxyphthalocyanine (**62**), cobaltphthalocyanine (**54**) and cobaltoctabutoxy phthalocyanine.[8] For cobaltetraaminophthalocyanine (**59**) a value of 56 mV/*pH* has been reported.[9] The *pH* dependence of potentials has been explained as being due to the uptake of protons or hydroxide by the adsorbed MPc species. This results in lack of reversibility of the couples and a large loss of charge after the first cycle.[8] The loss in current after the first scan may depend on the nature of the buffer employed. Reproducibility of currents at biological *pH* is of importance for the analysis of amino acids, e.g. cysteine (Figure 5.2) and proteins using modified electrodes.

[‡] These results are published as " S. Maree and T. Nyokong, *J. Electroanal. Chem.*, **492,** 120 (2000)"

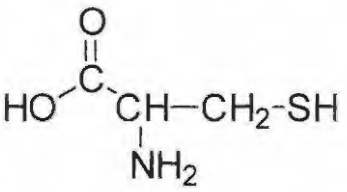

Figure 5.2 Structure of cysteine

5.2.1 Synthesis of cobalt(II) phthalocyanines complexes (Schemes 5.1 to 5.4)

The cobalt(II) phthalocyanine complexes: cobalt(II) tetrasulfophthalocyanine (CoTSPc) (**64**),[10,11] cobalt(II) tetraaminophthalocyanine (CoTAPc) (**59**),[12] cobalt(II) tetranitro-phthalocyanine (CoTNPc) (**58**),[12] cobalt(II) tetracarboxyphthalocyanine (CoTCPc) (**62**)[13] and cobalt(II) tetra-*tert*-butylphthalocyanine (CoTBPc) (**66**)[14] were synthesized and characterized according to published procedures. The complexes gave satisfactory spectroscopic characterization. The synthetic procedures involve the conversion of available substituted phthalimide (**57**), and phthalic anhydride (**60**), phthalic acid (**63**) or phthalonitrile (**65**) to the metal containing phthalocyanine in the presence of cobaltous chloride and urea, using ammonium molybdate as a catalyst. Tert-butyl phthalonitrile (**65**) was heated under reflux in ethylene glycol and $CoCl_2$ to yield CoTBPc (**66**). CoPc (**54**) was purchased from Aldrich and used without further purification.

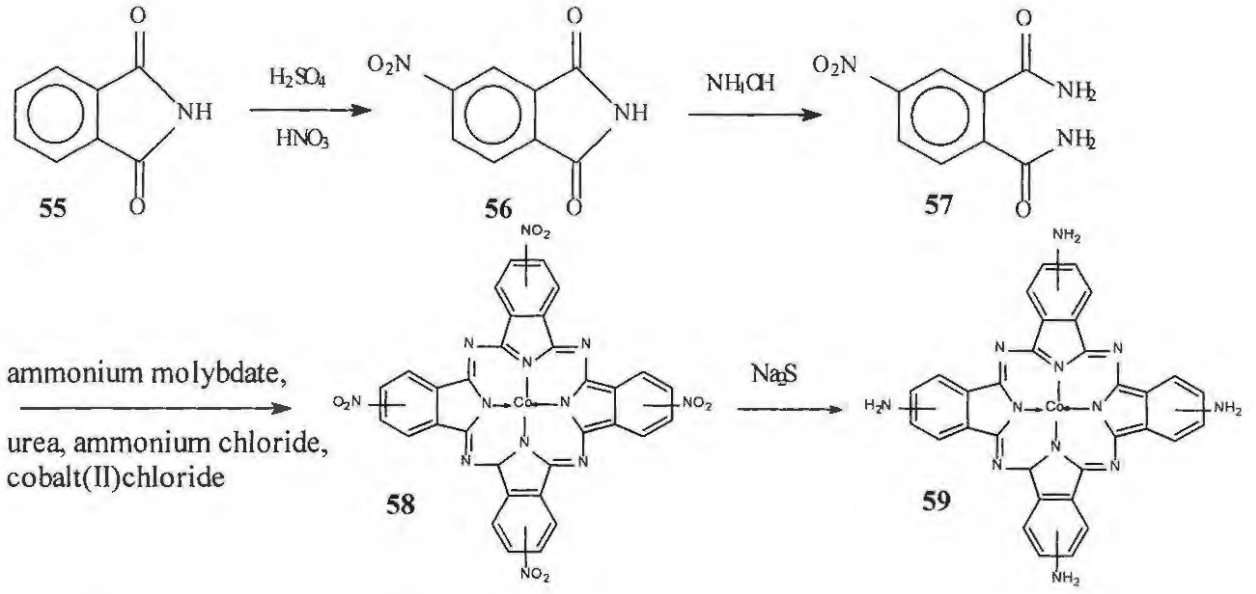

Scheme 5.1 Synthesis of CoTNPc (**58**) and CoTAPc (**59**).

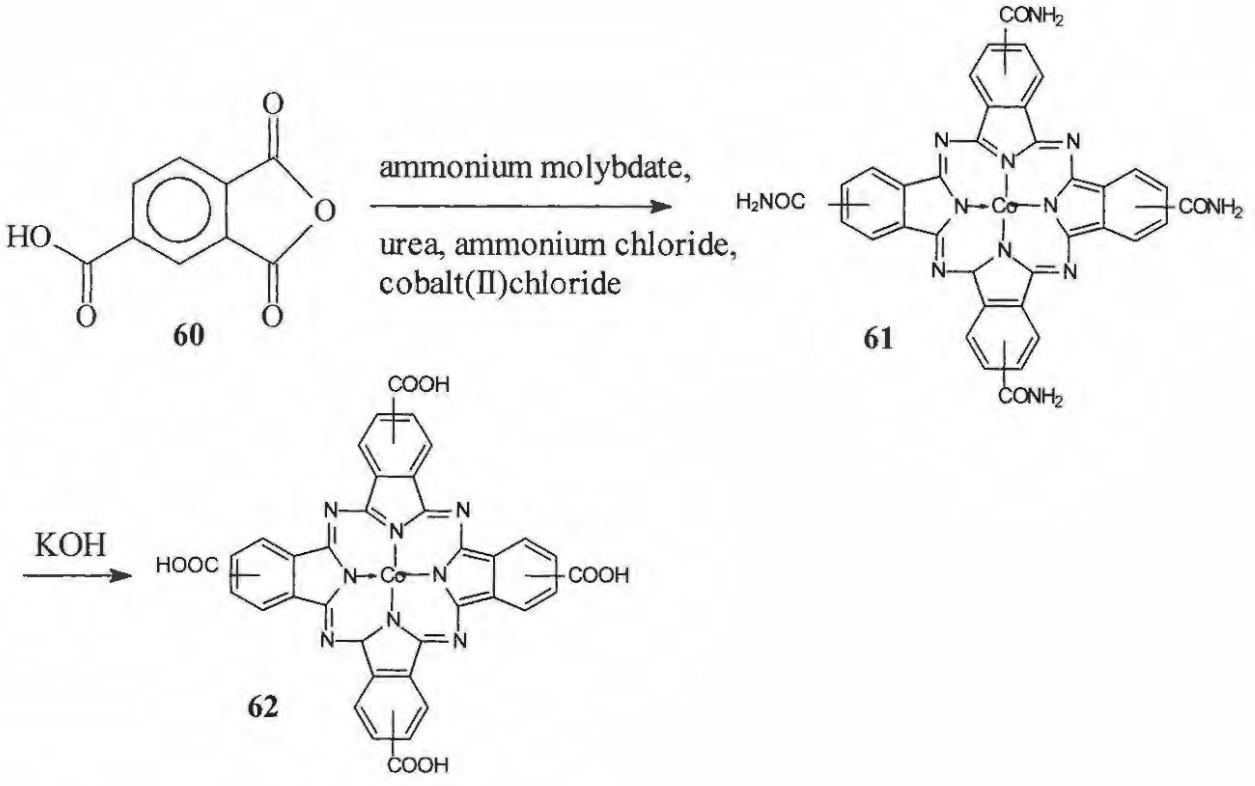

Scheme 5.2 Synthesis of CoTCPc (**62**).

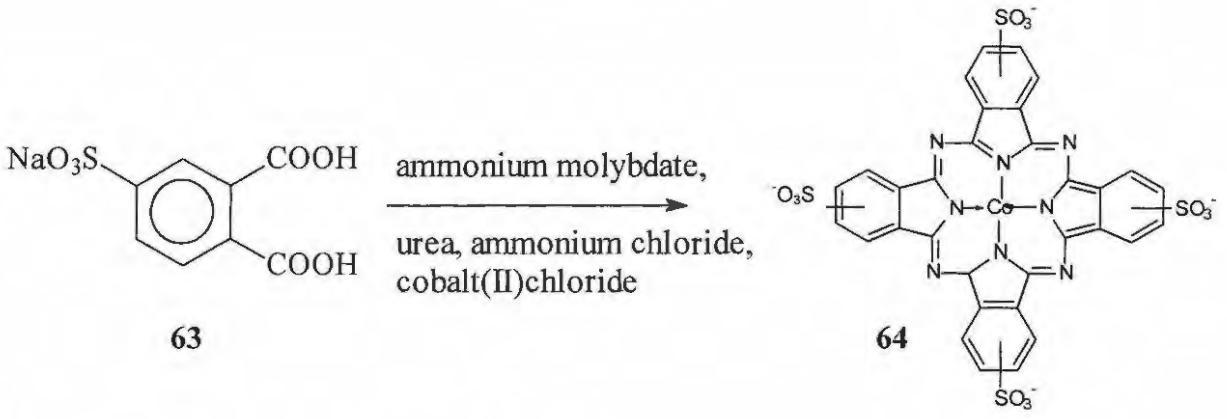

63 64

Scheme 5.3 Synthesis of CoTSPc (**64**)

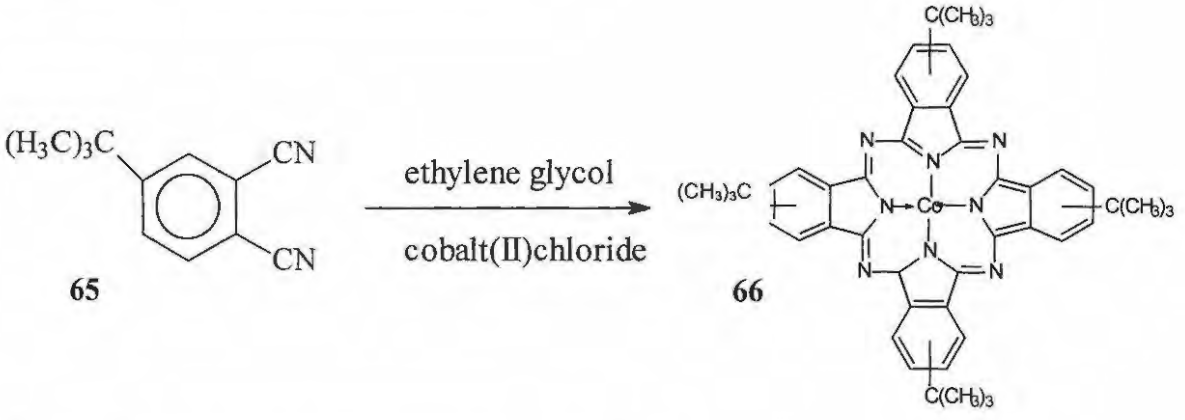

65 66

Scheme 5.4 Synthesis of selected CoTBPc (**66**).

5.2.1.1 Electrode modification

Since the electrocatalytic behaviour of selected phthalocyanines is brought under discussion it was decided to investigate the variables involved in optimal and reproducible electrode modification through electrochemical deposition. These variables include, amongst others, the concentration of the solution from which deposition takes place as well as the deposition scan number. The deposition scan number refers to the number of times it is needed to run through a potential cycle in order to get sufficient deposition.

Effects of concentration on deposition

The charge on the electrode is an indication of the surface coverage obtained during the deposition process and was determined using equation 5.1. In Figure 5.3 it can be seen that the charge and therefore the surface coverage tend to be concentration dependant at CoPc concentrations in the lower (below ~0.0025 mol dm^{-3}) and higher (above ~0.0075 mol dm^{-3}) range.

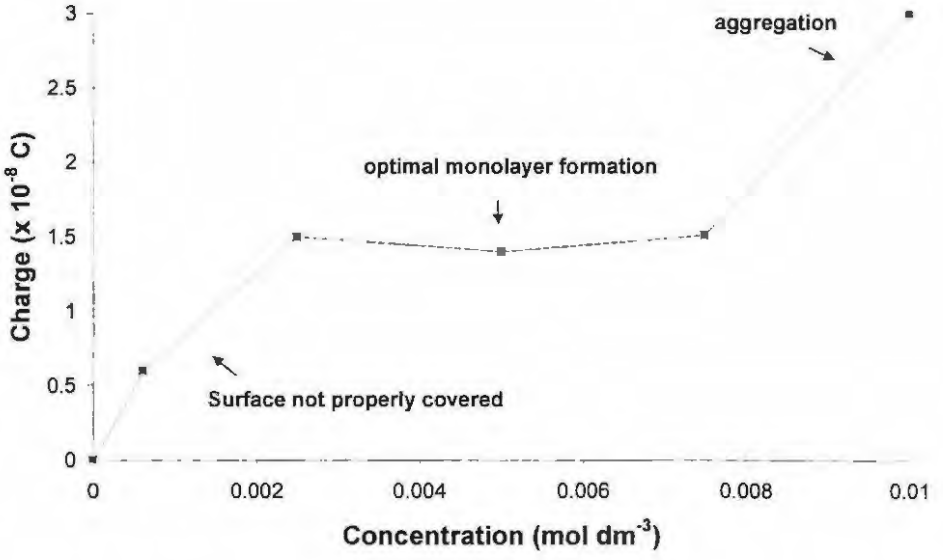

Figure 5.3 Graph of charge versus concentration of CoPc (**54**) in DMF solution from which deposition (10 scans) was performed. The charge was obtained from the peak area in 0.1 mol dm^{-3} Tris buffer solution.

Above 0.0075 mol dm^{-3} aggregation may be involved and below 0.0025 mol dm^{-3} deposition takes place slower because less molecules are in contact with the deposition surface. The degree of surface coverage can therefore be manipulated by changing the concentration used for deposition. It is ideal to work in the concentration range where a monolayer is formed, since improper surface coverage or aggregation effects could influence reproducibility.

Effects of scan number

During the deposition process an increase in peak current with scan number is observed (Figure 5.4). Considering the extent to which this is taking place it can be determined whether it is a simple adsorption process due to ionic attraction between the electrode and the phthalocyanine ring or polymerization of the particular species. If polymerization is taking place the peak current will sharply increase, that is, the first cyclic voltammogram scan would be significantly different from the second and consequent scans. Ionic interaction will show an increase, flatten down and even start decreasing as can be seen in Figure 5.4a.

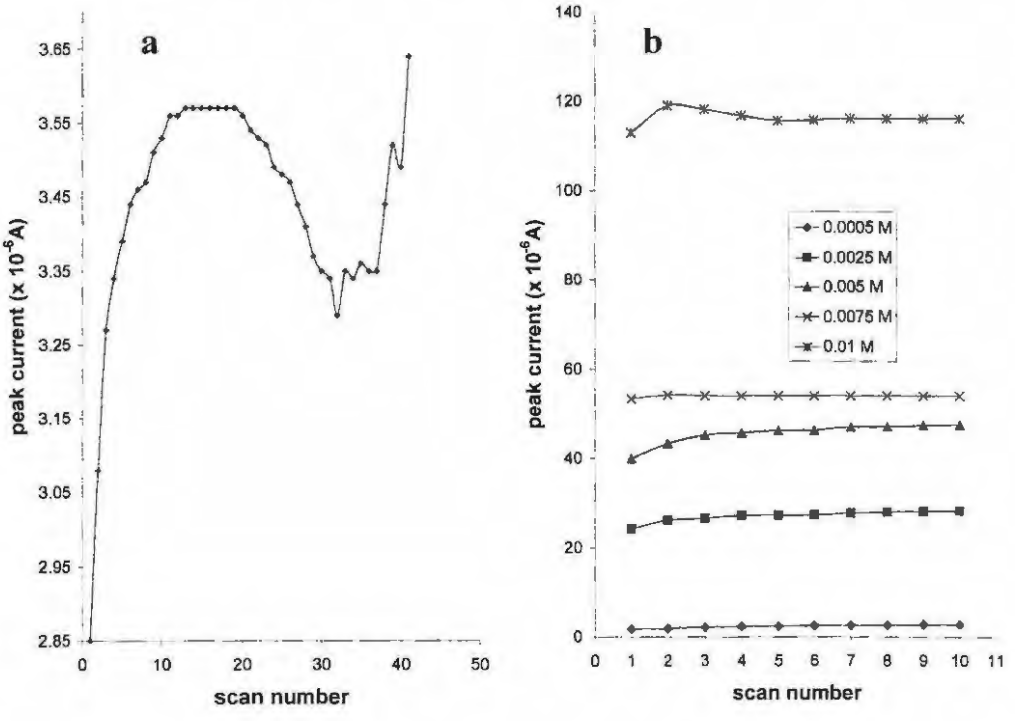

Figure 5.4 A plot of peak current versus scan number representing the deposition process of CoPc in DMF a) [CoPc]=0.0005 M over 40 scans b) over 10 scans.

The decrease in current could either be due to charge build-up or possible degradation of the particular phthalocyanine. After thirty scans in Figure 5.4 deposition becomes erratic and unstable possibly due to either change in the glassy carbon electrode surface or changes in the phthalocyanine structure.

In Figure 5.4b the peak current obtained in the DMF solution at various concentrations over ten scans is shown. As can be expected an increase in peak current is observed with an increase in concentration (0.01 mol dm^{-3} has a peak current of about 115 μA for the first scan where as 0.0005 mol dm^{-3} has a peak current of 2 μA for the first scan). At lower concentrations, e.g. at 0.0005 mol dm^{-3}, the peak current was still increasing gradually after 10 scans where as at 0.0075 mol dm^{-3} the peak current reached a maximum after approximately 2 scans. At higher concentrations (0.01 mol dm^{-3}) a slight increase is observed within the first two scans and then a slight decrease into a stable peak current. This would typically be expected in the case where aggregation and adsorption cause a sudden charge build up that may be released through reorganization into a lower energy orientation of the phthalocyanine molecules on the electrode surface. The conclusion is, therefore, made that optimal reproducible conditions can be found within a concentration range of 0.0025 – 0.0075 mol dm^{-3} using 10 – 20 deposition cycles.

5.2.2 Electrochemical behaviour of the CoPc complexes

Electrochemical behaviour of CoPc complexes has been well studied. In DMF, the first oxidation occurs at the central metal due to the Co^{III}/Co^{II} couple and the first reduction is due

to the Co^{II}/Co^{I} couple.[15] The Co^{III}/Co^{II} is not reversible and this has been attributed to surface adsorption effects.[10,16] Figure 5.5 shows the first scan cyclic voltammograms for all the synthesized complexes. The cyclic voltammograms were recorded only in the range for first metal reduction and first metal oxidation. In all cases, the reduction couple is quasi-reversible, though weak currents were observed for some complexes.

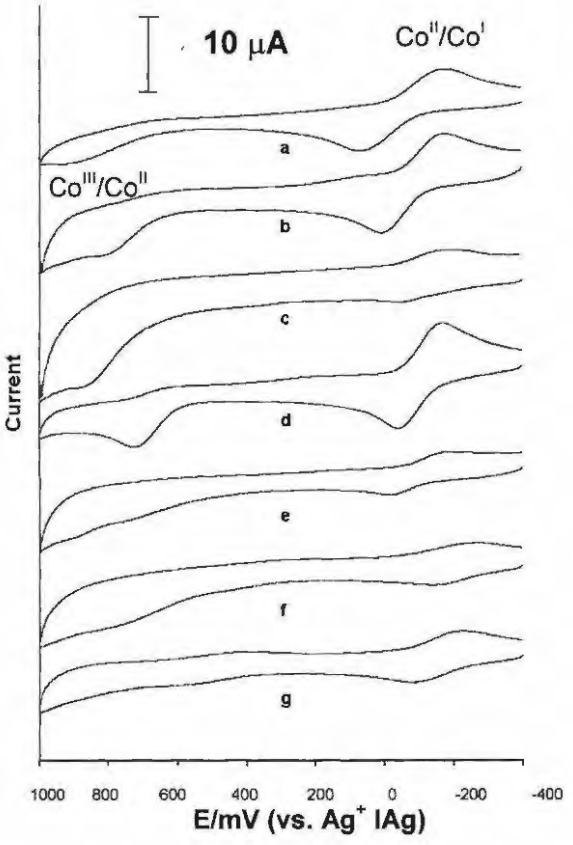

Figure 5.5 Cyclic voltammogram of the $CoPc(R)_4$ complexes in DMF containing TBAHP. Scan rate = 100 mV/sec. (a) CoTSPc (sodium salt), (b) CoPc, (c) CoTCPc, (d) CoTBPc, (e) CoTSPc (acid salt), (f) CoTNPc and (g) CoTAPc.

The peaks become more intense during the second and subsequent scans. In comparison with the literature[15] the reduction couple is assigned to the Co^{II}/Co^{I} couple. The currents for this

couple increased linearly with the square root of the scan rate as expected for a diffusion controlled process. The first oxidation is due to the Co^{III}/Co^{II} process and was irreversible as has been observed before for CoPc complexes. In some cases (e.g. CoTAPc), Figure 5.5g, very weak oxidation currents were obtained.

Table 5.1 lists the potentials for the redox processes of the complexes under discussion. Complexes containing electron-withdrawing groups attached to the phthalocyanine ring are easier to reduce as expected and more difficult to oxidize, e.g. CoTCPc (**62**). The presence of electron-donating groups, e.g. CoTBPc (**66**), results in complexes that are easier to oxidize.

It has been reported that repetitive scanning in a solution containing CoTAPc (**59**) in DMF from 0 to 1.0 V results in a gradual increase in the oxidation currents, due to polymerization of this complex.[15,17] Figure 5.6 shows repetitive cyclic voltammograms for CoTAPc (**59**), CoTNPc (**58**) and the acid salt of CoTSPc (**64**) from DMF solutions and in the presence of the tetrabutylammoniumhexafluorophosphate (TBAHP) electrolyte. A gradual increase in the faradaic current was observed for both the oxidation and reduction processes. As seen in Figure 5.6, the first scan is different from the second and subsequent scans for CoTAPc (**59**), CoTNPc (**58**) and the acid salt of CoTSPc (**60**) as has been observed before[15] for CoTAPc (**59**). The oxidation peaks are broad during the first scan, but improve during the second and subsequent scans.

Table 5.1 Electrochemical data and UV/vis spectroscopic data in DMF for the CoPc complexes and for cysteine oxidation on GCE modified by the CoPc complexes.

Complex	E (mV, vs Ag|AgCl				UV-vis/nm	
	MPc redox processes		Cysteine oxidation		Q-band	Soret-band
	Co^{III}/Co^{II}	Co^{II}/Co^{I}	pH 3.5	pH 9		
CoTCPc (**62**)	880	-30	815	188	678	339
CoTNPc (**58**)	844	-110	742	22	724	366
[CoTSPc]Na (**64a**)	835	8	836	214	672	326
[CoTSPc]H (**64b**)	765	-38	814	144	670	332
CoPc (**54**)	695	-170	665	15	658	326
CoTBPc (**66**)	690	-39	726	121	670	332
CoTAPc (**59**)	650	-66	736	33	714	367

The increase in currents on repetitive scanning of CoTAPc (**59**) was attributed to the formation of polymeric species on the electrode. The fact that for CoTNPc (**58**) and the acid salt of CoTSPc, the first scan was different from the subsequent scans suggests a different species is formed on the electrode and it is suggested that in a similar manner to CoTAPc (**59**), polymeric species are formed and adsorbed onto the electrode during repetitive scanning for CoTNPc (**58**) and the acid salt of CoTSPc (**64b**). Even though the formation of a polymeric species has been reported for CoTNPc (**58**), its structure is not known. It has been suggested [17] that the polymerization process may involve the oxidation of the amino group forming radicals which attack benzene rings of neighbouring molecules. For CoTCPc (**62**) and CoTBPc (**66**), an increase in the currents was observed during the first scan, but decreased gradually with repetitive scanning.

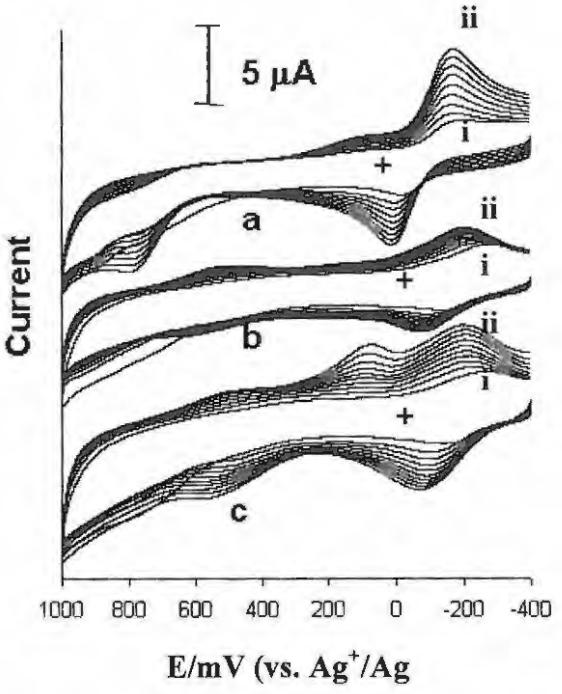

Figure 5.6 Cyclic voltammograms observed on repetitive cycling for (a) CoTAPc, (b) CoTNPc and the acid salt of (c) CoTSPc, in DMF containing TBAHP. Scan rate = 100 mV/sec. (i) fisrt voltammogram and (ii) final voltammogram in all cases.

A purplish-blue coating could be seen on the electrode for some of the complexes following repetitive scanning. The electrodeposition of the sodium salt of CoTSPc onto the glassy carbon electrodes has been described before.[17] In this work surface coverage on the electrode was calculated from the area under the oxidation peaks obtained from cyclic voltammetry, for each of the complexes, when the coated electrode was placed in the blank (buffer only) at *pH* 3.5. The surface coverage was of the order of 10^{-10} mol cm^{-2} for the complexes and was calculated from Equation 5.1.

The potential for the oxidation couple has been shown to shift by 60 mV per *pH* unit for CoTSPc (**64b**) and CoTAPc (**59**)[7,17] over both acid and basic *pH* ranges. A 60 mV/*pH*

dependence was observed for the complexes discussed in this work. It has been reported before that peak currents for FeTSPc adsorbed onto a Ag electrode become broader and the magnitudes of the currents decrease with increase in pH. For the $CoPc(R)_4$ complexes under discussion in this work, the peak currents were at their maximum at low *pH* and decreased with increase in *pH.*

5.2.3 Electrocatalytic oxidation of cysteine

Cysteine is oxidized at high positive potentials on conventional electrodes. Metallophthalocyanine complexes lower the oxidation potential of cysteine to more accessible values when adsorbed onto carbon electrodes.[18,19,20] On CoPc modified electrodes, the oxidation of cysteine in acidic media occurs as a two step electrocatalytic process initiated by electrochemical oxidation of $Co^{II}Pc$ to $Co^{III}Pc$ and completed by the chemical oxidation of cysteine and the regeneration of $Co^{II}Pc$ according to Equations 5.2 to 5.4:

$$Co^{II}Pc \rightarrow Co^{III}Pc + e^- \quad \text{.....(5.2)}$$

$$Co^{III}Pc + RSH \rightarrow Co^{II}Pc + RS^{\cdot +} + H^+ \quad \text{.....(5.3)}$$

$$2\,RS^{+\cdot} \rightarrow RSSR \quad \text{.....(5.4)}$$

where RSH is cysteine and RSSR is cystine.

Thus it is expected that the oxidation potential for cysteine is closely related to the potential of the Co^{III}/Co^{II} couple in CoPc complexes. In alkaline *pH*, the Co^{II}/Co^{I} couple has been implicated in the electrocatalytic process[1], as shown by Equations 5.5 to 5.8:

$$RSH + OH^- \rightarrow RS^- + H_2O \quad \text{.....(5.5)}$$

$$Co^{II}Pc + RS^- \rightarrow [Co^{I}PcSR] \quad \text{.....(5.6)}$$

$$[Co^{I}PcSR] \rightarrow Co^{I}Pc + RS^{\cdot +} \quad \text{.....(5.7)}$$

$$Co^{I}Pc \rightarrow Co^{II}Pc + e^- \quad \text{.....(5.8)}$$

The cyclic voltammetry of cysteine was recorded on electrodes modified with each of the complexes. As an example, Figure 5.7 shows the cyclic voltammograms of adsorbed CoTCPc in the buffer alone (Figure 5.7d) and in the presence of 5×10^{-3} mol dm^{-3} cysteine at *pH* 9 (Figure 5.7a), pH 7 (Figure 5.7b) and *pH* 3.5 (Figure 5.7c) . There is a considerable increase in the oxidation currents in the presence of cysteine as has been observed before when other MPc complexes are employed as adsorbed catalysts for the detection of cysteine.[20,19]

The peak potential for cysteine oxidation at *pH* 3.5 increases with the change in the ring substituent in $CoPc(R)_4$ as follows: $SO_3^- \sim COOH > NO_2 > NH_2 > C(CH_3)_3 > H$. This order is close to the order in the potential for the Co^{III}/Co^{II} couple in CoPc complexes, Table 5.1, in that complexes with a more positive potential for this couple (e.g. CoTCPc) also showed a more positive cysteine oxidation peak. A less positive oxidation potential was observed for complexes containing electron donating ligands, such as CoTBPc.

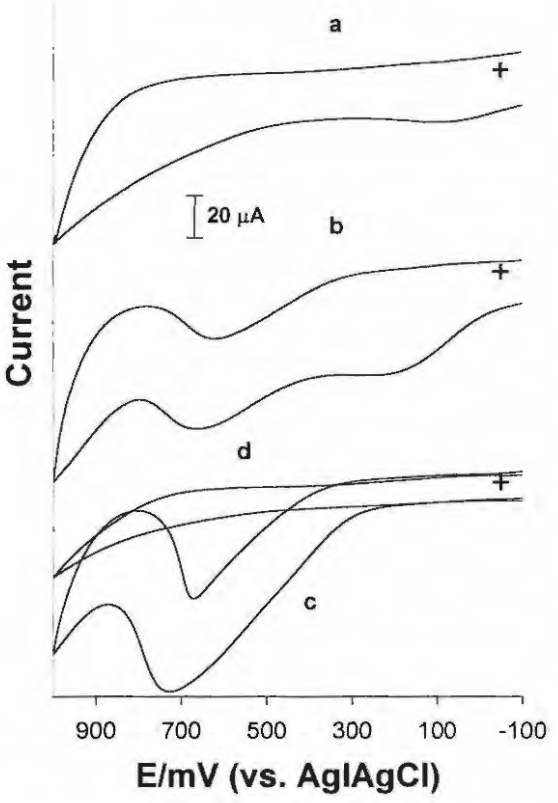

Figure 5.7 Cyclic voltammograms of cysteine on GCE modified with CoTCPc. Cyclic voltammogram of 5 x 10^{-3} mol dm^{-3} cysteine at (a) *pH* 9, (b) *pH* 7 and (c) *pH* 3.5. The cyclic voltgammogram of the modified electrode in buffer only is shown in (d). Scan rate = 100 mV/sec.

The irreversibility of the cysteine oxidation peak and the dip in the current during the return (cathodic scan) are typical of CoPc catalysis of cysteine.[19] It has been suggested before that the dipping in current is due to coordination of the thiol group to the metal center in CoPc. When other MPc complexes such as Mo(O)Pc, OsPc, RhPc and RuPc were employed as electrocatalysts for the analysis of cysteine, the dipping on return is not observed.[20,21] Spectroscopic evidence for the coordination of cysteine following oxidation of the $Co^{II}Pc$ complexes to the $Co^{III}Pc$ species is presented below.

The stability of the modified electrodes towards the analysis of cysteine is of importance. A decrease in catalytic currents for the oxidation of cysteine on CoPc modified carbon electrodes after the first scan has been observed.[2,19,18] The decrease in the currents may be attributed to poisoning of the electrode by adsorption of the oxidation product, cystine. However, it has been reported that the CoPc modified electrode is more stable at very low *pH* (0.05 mol dm^{-3} H_2SO_4) since cystine does not precipitate at this *pH.*[18] A decrease in the activity of the CoPc modified electrode for cysteine catalysis at *pH* 2 has been reported.[2,19] Figure 5.8 shows the variation of peak currents with scan number for the catalytic oxidation of cysteine using GCE modified by the CoPc complexes under *pH* 3.5 and *pH* 8.3 buffer conditions. In all cases a decrease in current is observed after the first scan. The deactivation of the electrode is due to the adsorption of cystine. The current showed an increase again upon rinsing of the electrode in dilute nitric acid. At *pH* 3.5 CoTNPc showed higher currents even after ten scans compared to CoTSPc (acid salt), hence showing that the former is more stable towards cysteine oxidation. The stability of the electrode may be associated with the relative magnitude of the catalytic currents. Considering the magnitudes of the cysteine oxidation currents at *pH* 3.5 and after ten scans, the stability of the electrodes modified with $CoPc(X)_4$ increased according to the ring substituents as follows: $SO_3H < NH_2 < COOH < C(CH_3)_3 < NO_2$ The trend in the stability of the electrode at *pH* 8.3 was slightly different from that at pH 3.5 and was as follows: $NO_2 < NH_2 < SO_3H < C(CH_3)_3 < COOH$. As discussed above, CoTAPc, CoTNPc and the acid salt of CoTSPc form polymeric species on the electrode. These show low catalytic activity in basic media when compared to the rest of the complexes.

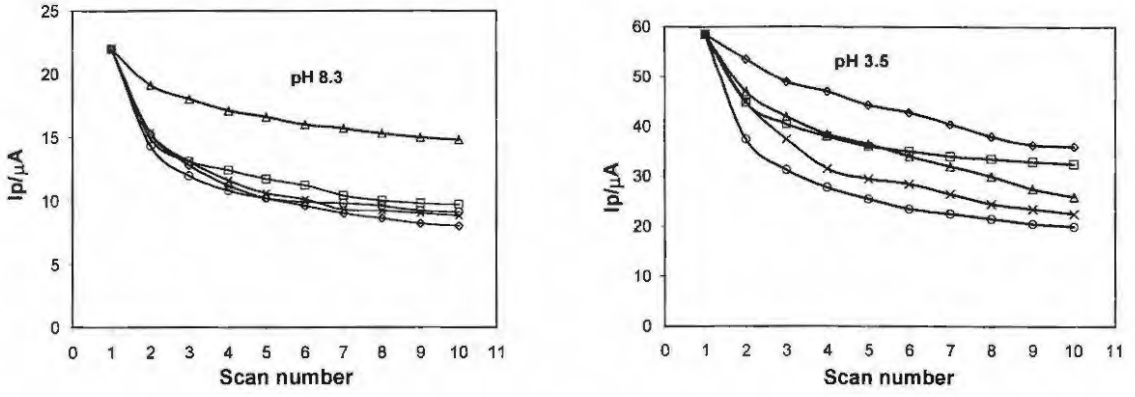

Figure 5.8 Variation of catalytic currents for cysteine oxidation with scan number for the oxidation of cysteine on a GCE modified with the various CoPc complexes. (Δ) CoTCPc (**62**); (□)CoTBPc (**66**); (o) CoTSPc (acid salt) (**64**); (x) CoTAPc, (◇) CoTNPc (**58**). Scan rate = 100 mV/sec. Shown for *pH* 8.3 (left) and *pH* 3.5 (right).

The catalytic oxidation of cysteine was *pH* dependent in that at *pH* 7 two catalytic peaks were observed in the potential range 0.65 - 0.85 V for the first peak and 0 - 0.2 V for the second peak, Figure 5.7. At *pH* 9, the more positive peak disappeared and the less positive peak shifted to even less positive potentials. It has been reported before that in neutral or basic solutions two peaks are observed for the catalytic oxidation of cysteine of CoPc modified electrodes.[2,19] This was attributed to direct cysteine oxidation by the $Co^{II}Pc$ species in basic media,[22] with the formation of a $Co^{I}Pc$ species. It would then be expected that the potential of the less positive cysteine peak will be related to the potential of the Co^{II}/Co^{I} couple in CoPc. The potential of the cysteine catalytic peak at *pH* 9 became less positive depending on the ring substituents as follows: SO_3Na > COOH > $C(CH_3)_3$ > NH_2 > NO_2 > H. This trend follows exactly the trend in the shift of the Co^{II}/Co^{I} couple to more negative potentials for the corresponding CoPc complexes, Table 5.1, hence confirming that the Co^{II}/Co^{I} couple is involved during the catalytic oxidation of cysteine in basic media, by the CoPc species.

The cysteine peak shifted by 29 mV per pH units at *pH'* s less than 7, consistent with a two-electron process. It has been reported that catalytic oxidation of cysteine by copper tetraphenylporphyrin (CuTPP) complexes was more efficient at *pH* = 7.[23] However, in this work a decrease in currents with increase in pH was observed, for both basic and acidic *pH* ranges, Figure 5.9. Considering the first scan only CoTCPc gave higher currents than the rest of the complexes at high *pH* for the same cysteine concentration, Figure 5.8a, suggesting that this complex has a better catalytic activity towards the detection of cysteine under biological *pH'* s.

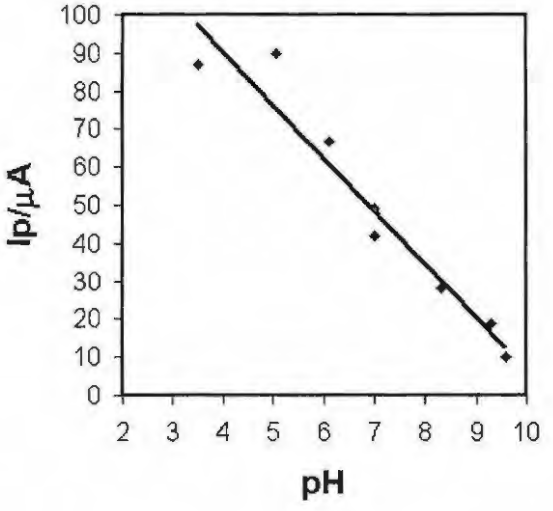

Figure 5.9 Variation of catalytic currents with pH for the oxidation of cysteine on GCE modified with CoTNPc. Scan rate = 100 mV/sec.

5.2.4 Spectroscopic Studies

Spectra of the metallophthalocyanine (MPc) complexes consists of a strong absorption in the visible region called the Q band and a weaker absorption in the UV region called the B or

Soret band as discussed in Chapter 2. The Q and Soret band maxima for the CoPc complexes under discussion in this work are given in Table 5.1. CoTAPc and CoTNPc gave spectra, Table 5.1, which were shifted to longer wavelengths when compared to the rest of the complexes.

It has been suggested that the catalytic oxidation of cysteine on MPc modified electrodes is preceded by coordination of cysteine to the complexes.[20,21] UV/Visible spectroscopy was used to determine if coordination occurs between cysteine and the CoPc complexes under discussion in this paper. Spectral changes were recorded in the solid state by adding solutions of cysteine (pH 3.5) to the CoPc complexes deposited between two glass slides. Spectra were recorded before and after addition of cysteine. There was no change in spectra before and after cysteine addition. However, when the coated glass slide was exposed to bromine fumes, thus oxidation before the cysteine was added, spectral changes shown in Figure 5.10 for CoTAPc (**56**) were observed. Similar spectral changes were observed for the other $CoPc(R)_4$ complexes.

The Q band of the absorbed CoTAPc is observed at 692 nm before exposure (Figure 5.10a) of the slide to bromine fumes. On oxidation of this complex with bromine fumes, a weak peak was observed at 712 nm (Figure 5.10b). Electrochemical oxidation of solid CoPc occurs at the central metal, resulting in a shift of the Q band to longer wavelengths. Thus the spectral changes shown in Figure 5.10 obtained on bromine oxidation of CoPc are consistent with the oxidation of $Co^{II}Pc$ to $Co^{III}Pc$.[24] Addition of cysteine resulted in the shift of the Q band to 706 nm (Figure 5.10c) and not back to the original position for $Co^{II}Pc$ at 692 nm.

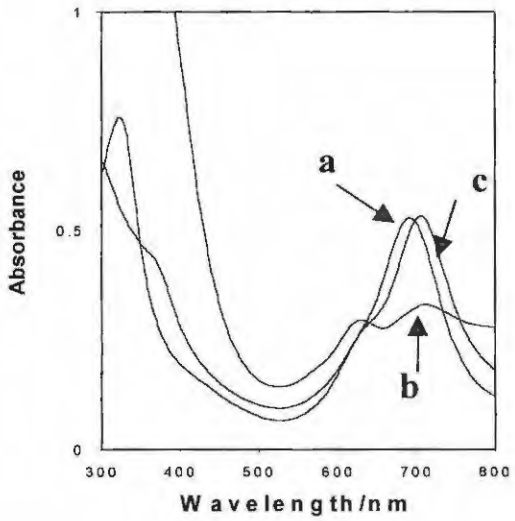

Figure 5.10 Electronic absorption spectra of CoTAPc spin coated onto a glass slide, (a) before and (b) after exposure to bromine fumes. (c) shows the spectra after addition of cysteine at pH 3.5 to the adsorbed CoTAPc.

Spectral changes shown in Figure 5.10 suggest that following addition of cysteine to the chemically oxidized adsorbed Co^{III}TAPc, an electron transfer from cysteine to the Co^{III}TAPc occurs, with the formation of the Co^{II}TAPc species and coordination of cysteine, hence the shift in wavelength from 712 to 706 nm. The electron transfer between Co^{III}Pc species and cysteine has been reported[19] and is shown by Equations 5.2 and 5.3 above. The Co^{II}Pc species formed following the electron transfer, shows a Q band maximum at a different wavelength (706 nm), Figure 5.10c, from the original Co^{II}Pc (692 nm), Figure 5.9a confirming that coordination of cysteine has occurred. Such small shifts in the Q band are typical of axial ligand coordination in MPc complexes.[25] The following mechanism (Equation 5.9 and 5.10) is suggested for the interaction of cysteine with the CoPc species:

$$Co^{II}Pc \xrightarrow{Br_2} Co^{III}Pc + e^- \qquad \text{.....(5.9)}$$

$Co^{III}Pc + RSH \rightarrow (RS^{+\cdot})Co^{II}Pc$ .....(5.10)

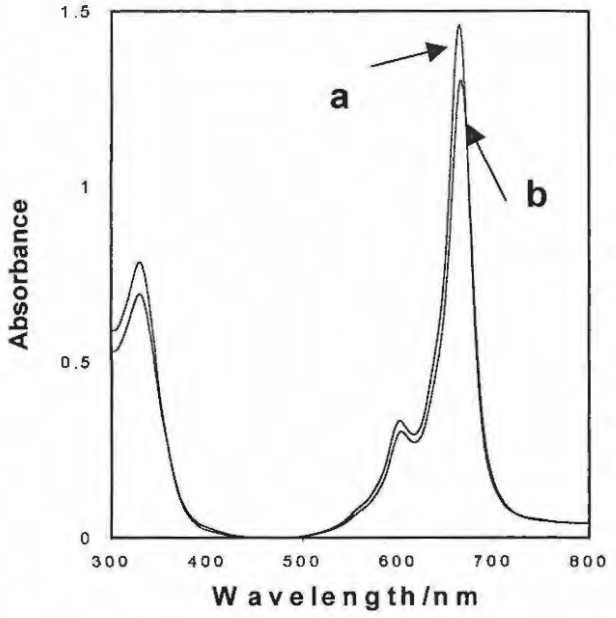

Figure 5.11 Electronic absorption spectra of CoTBPc in DMF (a) before and (b) after addition of cysteine, dissolved in pH 3.5 buffer.

There was no spectroscopic evidence for the coordination of cysteine to the $Co^{II}Pc$ prior to its oxidation with bromine. However, it is important to note that very small shifts (2 nm) towards higher wavelengths were observed on addition of an aqueous cysteine solution to solutions of the $CoPc(R)_4$ complexes in DMF, Figure 5.11, which could be associated with cysteine coordination to the $Co^{II}Pc$ species prior to oxidation to the $Co^{III}Pc$ species. The differences in the behaviour of the $CoPc(R)_4$ complexes, when deposited onto the glass electrode and when in solution, towards the interaction of cysteine could be due to the fact that species in solution are different from those in the solid state.

5.3 Experimental

5.3.1 Synthesis

5.3.1.1 Materials

Phthalimide (**55**), trimelitic anhydride (**60**), 4-sulfophthalic acid (**63**) and 4-tert-butylphthalodinitrile (**65**) were purchased from Aldrich. All solvents were distilled prior to use. ^{1}H NMR (400 MHz) were recorded using the Bruker EMX 400 NMR spectrometer in deuterated DMSO. UV/Visible spectra were recorded using a Varian 500 UV/Vis/NIR spectrophotometer and FTIR spectra (KBr pellets) recorded on a Perkin-Elmer spectrum 2000 FTIR spectrometer.

5.3.1.2 4-Nitrophthalimide (56)[26] (Scheme 5.1)

Fuming nitric acid (30 cm^3) was slowly added to concentrated sulphuric acid (180 cm^3) and the mixture was cooled in an ice bath. When the temperature of the mixed acids reached 12^{0}C phthalimide (**55**) (50.0 g, 0.3 mol) was stirred in as quickly as possible while the temperature was maintained between 10°C and 15°C using an ice-bath. The solution was then allowed to reach room temperature and left to stand overnight. The yellow solution obtained was poured on ice (1.1 kg) while rapidly stirring the solution to yield a beige suspension, which was removed by filtration under reduced pressure. The beige solid was washed with ice-water (6 x 150 cm^3) to yield the 4-nitrophthalimide (**56**) (25.9 g, 40.0%); mp. 197-200°C.

^{1}H NMR (400 MHz, DMSO): δ_H = 8.72 (1H, d, Ar-H), 8.68 (1H, dd, Ar-H), 8.09 (1H, d, Ar-H), 7.96 (1H, s, N-H).

IR (KBr, cm^{-1}): ν = 1780 (s) and 1720 (s) (Co-NH-CO), 1536 (vs) (NO_2 assym.), 1349 (vs) (NO_2 sym.)

5.3.1.3 4-Nitrophthalamide[27] (57) (Scheme 5.1)

4-Nitrophthalimide (**56**) (20 g, 0.1 mol) was stirred in 25 % aqueous ammonia solution (300 cm^3) for 24 hours before a further 100 cm^3 25 % aqueous ammonia solution was added. After 24 hours the yellowish product was filtered off and washed with water (3 x 200 ml) to yield the 4-nitrophthalamide (**57**) (18.7 g, 89 %); mp. 180-183°C.

^{1}H NMR (400 MHz, DMSO): δ_H = 8.42 (1H, d, Ar-H) 8.24 (1H, dd, Ar-H), 7.89 (1H, d, Ar-H).

IR (KBr, cm^{-1}): ν = 3340 (NH_2 str.), 1679 (C=O str.), 1615 (NH_2 def.).

5.3.1.4 Cobalt(II)-2,9,16,23-tetranitrophthalocyanine (58)[28] [CoTNPc] (Scheme 5.1)

4-Nitrophthalimide (**57**) (1.921 g, 10 mmol), cobaltous chloride (0.594 g, 2.5 mmol), ammoniumchloride (0.267 g, 4.9 mmol), ammonium molybdate (0.04 g) and excess urea (3 g) were finely ground and added to nitrobenzene (10 ml) and was heated under reflux for 5 hrs at 185°C ± 5°C after a gradual temperature increase from 25 to 185 °C over 30 minutes. The solid product was filtered and Soxhlet extracted overnight with methanol to remove remaining nitrobenzene. The deep green solid was added to 1M hydrochloric acid (30 ml) saturated with

sodium chloride. This suspension was boiled for 5 minutes and filtered after cooling. After adding the solid to 1M sodium hydroxide (30 ml) containing sodium chloride (11 g) the solution was heated at 90 °C for 30 minutes. The solid was separated by centrifugation and the treatment as above with 1M hydrochloric acid and 1M sodium hydroxide was repeated twice. The green compound was washed with water (100 ml) and dried overnight at 100 °C to yield **58** (75 %). IR (KBr, cm^{-1}): ν = 1538 (NO_2 asym.), 1350 (NO_2 sym.).

UV/Vis (DMSO), λ_{max}(nm) (log ε): 724 (3.93), 651 (3.55), 366 (3.70)

*5.3.1.5 Cobalt(II)-2,9,16,23-tetraaminophthalocyanine (**59**)[27] [CoTAPc] (Scheme 5.1)*

Finely ground cobalt(II)-2,9,16,23-tetranitrophthalocyanine (**58**) (1.4 g, 1.86 mmol) was suspended in water (60 ml), and sodium sulfide nonahydrate (11.1 g, 45 mmol) added and the mixture stirred at 50 °C for 5 hrs. The green product was separated by centrifugation and treated with 1M hydrochloric acid (180 ml). After removal of the solid product by centrifugation, the solid was stirred in 1M sodium hydroxide (120 ml) for 1 hr and centrifuged again. The obtained green product was washed with water (120 ml) and dried overnight at 100 °C to yield **59** (90%).

IR (KBr, cm^{-1}): ν = 3330 (N-H), 1610 (NH_2).

UV/Vis (DMSO), λ_{max}(nm) (log ε): 714 (4.44), 367 (4.35), 292(4.44)

*5.3.1.6 Cobalt(II)-2,9,16,23- tetracarboxyphthalocyanine (**62**)[29] [CoTCPc] (Scheme 5.2)*

A finely grounded mixture of trimeliticanhydride (**60**) (5 g, 0.025 mol), urea (15 g, 0.025 mol), cobaltous chloride (3.57 g, 0.015 mol) and ammonium molybdate (0.5 g, 0.0005 mol)

was added to nitrobenzene (75 ml) and was heated under reflux at an internal temperature of 165°C for 3 hrs. The dark blue-green solid was filtered off and Soxhlet extracted overnight with methanol to remove any nitrobenzene left and dried overnight at 100°C to yield (**61**) (30%). To the amide (**61**) (1.0 g, 1.34 mmol) was added 10% KOH (50 ml) and the mixture refluxed for 5 hours, allowed to cool to room temperarature and centrifuged. The liquid was acidified to precipitate **62**, the solid filtered and washed with water (3 x 50 ml) and dried overnight at 60°C to yield **62** (34%).

IR (KBr, cm^{-1}): ν = 3350 (OH), 1700 (C=O).

UV/Vis (DMSO), λ_{max}(nm) (log ε): 678(3.94), 611(3.31), 339(3.45)

^{1}H NMR (400 MHz, DMSO): δ_H = 8.31 (4H, broad s, Ar-H), 7.77 (8-H, broad s, Ar-H).

*5.3.1.7 Cobalt(II)-2,9,16,23-tetrasulfophthalocyanine (**64**)[30,31] [CoTSPc] (Scheme 5.3)*

A mixture of 4-sulfophthalic acid (**63**) (6g, 0.022 mol), ammonium chloride (654 mg, 0.012 mol), urea (8.1 g, 0.135 mol), ammonium molybdate (93 mg) and cobalt(II) sulfate 7-hydrate (1.26 g, 0.004 mol) were ground together and slowly added to nitrobenzene (5.55 ml) while keeping the internal temperature between 160 – 190°C. This mixture was heated for 6 hrs at 180°C. The solid product was ground and Soxhlet extracted overnight with methanol to remove any nitrobenzene.

The remaining solid was added to 1 N HCl (150 ml) saturated with NaCl. The solution was briefly heated to boiling, cooled to room temperature and filtered. The resulting solid was dissolved in 0.1 N NaOH (100 ml) and heated to 80°C and insoluble purities was immediately

removed by filtration. NaCl (37.5 g) was added to this solution and some of the product precipitated. The slurry was heated and stirred at 80°C until ammonia evolution stopped.

The product was obtained by filtration and the initial reprecipitation process was repeated two additional times. The solid was separated and washed with 80% aqueous ethanol until the filtrate was chloride-free after which it was refluxed for 4 hrs in absolute ethanol. The pure blue product (**64**) was filtered and dried overnight in vacuo over P_2O_5.

IR (KBr, cm^{-1}): ν = 1630, 1190, 1148, 1107, 1031, 703, 644, 598.

UV/Vis (DMSO), λ_{max}(nm) (log ε): 670 (4.30), 606 (3.72), 332 (3.97)

*5.3.1.8 Cobalt(II)-2,9,16,23- tetra-tert-butylphthalocyanine (**66**) [32] [CoTBPc] (Scheme 5.4)*

A mixture of 4-tert-butylphthalodinitrile (**65**) (6.75 g, 0.0365 g), cobaltous chloride (0.75 g, 0.006 mol) and ethylene glycol (90 ml) was heated for 5 hrs at 190 °C After cooling the mixture an equal volume of water was added and the solid collected by filtration and washed with methanol. The crude product was boiled for 2 hrs first with 1 N hydrochloric acid (500 ml) and then 1 N sodium hydroxide. The solid material was washed with water until the filtrate was neutral and then washed with methanol and dried overnight at 100 °C to yield **66**.

IR (KBr, cm^{-1}): 2957, 2904 and 2862 (C-H).

UV/Vis (DMSO), λ_{max}(nm) (log ε): 670(4.81), 606(4.20), 332(4.44)

5.3.2 Electrochemical methods

Electrochemical data were collected with the BioAnalytical Systems (BAS) model 100 B/W electrochemical workstation. Distilled deionized Millipore water was employed for electrochemical studies in aqueous solutions. Tris buffer (0.1 mol dm^{-3}) was employed for electrochemical studies at pH 3.5, 7, 9 and also acted as the electrolyte in aqueous media. A glassy carbon electrode (GCE, 3.0 mm diameter) was used as a working electrode and a platinum wire as an auxiliary electrode. The reference electrode was the Ag | AgCl(3 mol dm^{-3} KCl) .

For electrocatalytic reactions, a glassy carbon electrode was modified with the CoPc complexes by electrodeposition from a 5 x 10^{-3} mol dm^{-3} solution of the CoPc complexes in DMF containing 0.1 mol dm^{-3} TBAHP as an electrolyte. The deposition was carried out by scanning repetitively (10 scans) at 100 mV/sec between -0.4 and 1.0 V vs Ag wire pseudo reference electrode (represented as Ag^{+}/Ag). Prior to coating, the GCE was polished with alumina on a Buehler felt pad, followed by washing with deionised water and rinsing with methanol. Coating of the glass substrates was performed by placing a few drops of DMF solutions of the $CoPc(R)_4$ complexes on a glass slide and allowing the solvent to evaporate for 30 minutes at 80°C.

Electronic spectra were recorded with the Cary 500 UV/Vis/NIR spectrophotometer. Concentrations of CoPc complexes for UV/visible spectroscopic studies were of the order of 10^{-5} mol dm^{-3}. IR spectra (KBr pellets) were recorded with the Perkin Elmer Spectrum 2000 FTIR spectrometer.

5.4 Conclusion

The influence of the ring substituents on MPc complexes have mainly been studied for oxygen reduction. This work shows the redox potential for the oxidation of cysteine is closely related to the $Co^{III}Pc/Co^{II}Pc$ for a series of ring substituted CoPc complexes. Both the potential and the currents for the oxidation of cysteine are affected by the pH of the solution, with higher currents and more positive potentials being observed at low pH for axially non-ligated CoPc complexes. Of all the complexes studied CoTCPc showed better catalytic activity in basic media in that higher currents (first scans) were observed for cysteine oxidation, when compared to the rest of the complexes.

5.5 References

1. J.H. Zagal, *Coord. Chem. Rev.*, **119**, 89 (1992)
2. X. Huang and W.T. Kok, *Anal. Chem.*,**57**, 591 (1985)
3. A. Napier and J.P. Hart, *Electroanalysis*, **8**, 1006 (1996)
4. M. Sekota and T. Nyokong, *Polyhedron*, **16**, 3279 (1997)
5. J. Limson and T. Nyokong, *Electroanalysis*, **9**, 255 (1997)
6. A.J.Bard and L.R. Faulkner, *Electrochemical methods, Fundamentals and applications,* John Wiley and Sons, New York (1980)
7. S. Zecevic, B. Simic-Glavaski, E. Yeager, A.B.P. Lever and P.C. Minor, *J. Electroanal. Chem.*, **196**, 339 (1985)
8. L.D. Rollman and R.T. Iwamoto, *J. Am. Chem. Soc.*, **90**, 1455 (1968)
9. Y.-H. Tse, P. Janda, H. Lam, J. Zang, W.J. Pietro and A.B.P. Lever, *J. Porphyrins and Phthalocyanines*, **1**, 3 (1997)
10. J.H. Weber and D.H. Busch, *Inorg. Chem.*, **4**, 469 (1965)
11. B.N. Achar, G.M. Fohlen, J.A. Parker and J. Keshavayya, *Polyhedron,* **6**, 1463 (1987)
12. N. Kobayashi and Y. Nishiyama, *J. Phys. Chem.*, **89**, 1167 (1985)
13. H. Shirai, A. Maruyama, K. Kobayashi and N. Hojo, *Makromol. Chem.*, **181**, 575 (1980)
14. A.B.P Lever, E.R. Milaeva and G. Speier, in *Phthalocyanines: properties and applications*, **3**, C.C. Leznoff and A.B.P. Lever (eds.), VCH, New York, 1993.
15. H. Li and T.F. Guarr, *J. Chem. Soc., Chem. Comm.*, 833 (1989)
16. T.J. Mafatle and T.Nyokong, *J. Electroanal. Chem.*, **408,** 213 (1996)
17. Y.H. Tse, P. Janda, H. Lam, J. Zang, W.J. Pietro and A.B.P. Lever, *J. Porphyr. Phthalocyanines,* **1**, 3, (1997)
18. J. Limpson and T. Nyokong, *Electroanalysis*, **10**, 988 (1998)
19. M.K. Halbert and R.P. Baldwin, *Anal. Chem.*,**57**, 591 (1985)
20. M. Sekota and T. Nyokong, *Electroanalysis,* **9**, 1257 (1997)
21. M.T. Stankovivh and A.J. Bond, *J. Electroanal. Chem.* **75**, 487 (1977)
22. S.V. Guerra, C.R. Xavier, S. Nakayaki and L.T. Kubota, *Electroanalysis,* **10**, 426 (1998)
23. M.J. Stillman and T. Nyokong, in *Phthalocyanines: Properties and Applications,* C.C. Leznoff and A.B.P. Lever (eds), VCH, New York, 1989.

24. H. Li and T.F. Guarr, *J. Electroanal. Chem.*, **297**, 169 (1991).
25. D. Schlettwein and T. Yoshida, *J. Electranal. Chem.*, **441**, 139 (1998).
26. E.H. Huntress and Shriner, *Org. Synth. Coll. Vol. 2*, 459 (1943)
27. S.W. Oliver and T.D. Thomas, *Heterocycles,* **22**, 2047 (1984)
28. B.N. Achar, G.M. Fohlen, J.A. Parker and J. Keshavayya, *Polyhedron,* **6**, 1463 (1987)
29. N. Kobayashi, H. Lam, W.A. Nevin, C.C. Leznoff and H. Shirai, *J. Am. Chem. Soc.*, **116**, 879 (1994)
30. J.H. Weber and D.H. Busch, *Inorg. Chem.*, **4**, 469 (1965)
31. L.D. Rollman and R.T. Iwamoto, *J. Am. Chem. Soc.*, **90**, 1455 (1968)
32. J. Metz, O. Schneider and M. Hanack, *Inorg. Chem.*, **23**, 1069 (1984)

Overall Conclusion

In conclusion it was shown in this work that both peripheral and axial substituents and the central metal strongly affect the catalytic properties of phthalocyanines. It is important in photodynamic therapy to have complexes that are soluble and having a red-shifted electronic absorption band. By attaching the peripheral and axial groups both these conditions were met. Most of these complexes produced the cytotoxic species, namely singlet oxygen, to satisfaction. By attaching peripheral groups of the specific size and electronegativity, the photostability, potency and imaging properties may be fine-tuned until the desired properties are obtained. This thesis set the basic guidelines to the effect of different substituents (and metals), as well as the behaviour of phthalocyanines containing biologically active compounds, for example cholesterol and estrone, on the photodynamic activity of phthalocyanines. Against this background these complexes could now be studied in a cellular environment, or the information used to develop even more effective sensitizers.

It was also further shown that substituents on the cobalt phthalocyanine as well as the *pH* strongly affect the redox potential of the oxidation of cysteine. It is, however, important to develop electrodes that will show better stability. Since it is suspected that the instability of the electrode results from coordination of cysteine to the cobalt, it may be useful to make use of a strongly coordinating axial ligand to prevent this from happening. The information gathered in this thesis will be useful in designing electrodes for uses at different *pH*'s and potentials.

RHODES UNIVERSITY LIBRARY